Spring 2021 – Epigenetics and Systems Biology
Discussion Session (Environmental Epigenetics)
Michael K. Skinner – Biol 476/576
Week 11 (April 1)

Environmental Epigenetics

Primary Papers

1. Manikkam M, et al., (2012) Plos One 7(2):e31901. (PMID: 22389676)
2. Ben Maamar, et al., (2018) Environmental Epigenetics 26;4(2):dvy010, pp 1-19. (PMID: 29732173)
3. Ben Maamar, et al., (2019) Developmental Biology 445: 280-293. (PMID: 30500333)

Discussion

Student 29 – Ref #1 above

- What are the transgenerational phenotypes?
- How can the epigenetic biomarkers of exposure be used?
- What does the transgenerational actions of multiple environmental exposures suggest?

Student 30 – Ref #2 above

- What is the experimental design?
- What epigenetic technologies and alterations were investigated?
- What is the primary conclusion of the study?

Student 31 – Ref #3 above

- What is the experimental design?
- What were the developmental origins of the sperm epimutations?
- What conclusions on the development of the sperm epimutations are made?

EPIGENETICS
https://doi.org/10.1080/15592294.2020.1853319

Taylor & Francis
Taylor & Francis Group

RESEARCH PAPER

Epigenome-wide association study for glyphosate induced transgenerational sperm DNA methylation and histone retention epigenetic biomarkers for disease

Millissia Ben Maamar, Daniel Beck, Eric E. Nilsson, Deepika Kubsad, and Michael K. Skinner

Center for Reproductive Biology School of Biological Sciences, Washington State University, Pullman, WA, , USA

ABSTRACT

The herbicide glyphosate has been shown to promote the epigenetic transgenerational inheritance of pathology and disease in subsequent great-grand offspring (F3 generation). This generational toxicology suggests the impacts of environmental exposures need to assess subsequent generations. The current study was designed to identify epigenetic biomarkers for glyphosate-induced transgenerational diseases using an epigenome-wide association study (EWAS). Following transient glyphosate exposure of gestating female rats (F0 generation), during the developmental period of gonadal sex determination, the subsequent transgenerational F3 generation, with no direct exposure, were aged to 1 year and animals with specific pathologies identified. The pathologies investigated included prostate disease, kidney disease, obesity, and presence of multiple disease. The sperm were collected from the glyphosate lineage males with only an individual disease and used to identify specific differential DNA methylation regions (DMRs) and the differential histone retention sites (DHRs) associated with that pathology. Unique signatures of DMRs and DHRs for each pathology were identified for the specific diseases. Interestingly, at a lower statistical threshold overlapping sets of DMRs and DHRs were identified that were common for all the pathologies. This is one of the first observations that sperm histone retention can potentially act as a biomarker for specific diseases. The DMR and DHR associated genes were identified and correlated with known pathology specific-associated genes. Observations indicate transgenerational epigenetic biomarkers of disease pathology can be identified in the sperm that appear to assess disease susceptibility. These biomarkers suggest epigenetic diagnostics could potentially be used to facilitate preventative medicine.

ARTICLE HISTORY
Received 13 July 2020
Revised 20 October 2020
Accepted 23 October 2020

KEYWORDS
Glyphosate; sperm; diagnostics; prostate Disease; kidney Disease; obesity; multiple Pathology; ewas

Introduction

Environmental exposures such as toxicants or nutrition can modulate genome activity (e.g. gene expression) and biology through epigenetic processes [1–4]. Epigenetics is defined as 'molecular factors and processes around DNA that regulate genome activity, independent of DNA sequence, and are mitotically stable' [5,6]. Epigenetic processes include DNA methylation, histone modifications, non-coding RNA, chromatin structure, and RNA methylation. Previous observations have shown a variety of environmental factors can promote the epigenetic transgenerational inheritance of disease or phenotypic alterations through epigenetic changes in the germline (sperm or eggs) [1]. The direct exposure of multiple generations, such as the gestating female and fetus, to affect the F0 and F1 generations are termed multigenerational exposures and intergenerational effects [7], while the transmission of epigenetic alterations and phenotypes through the sperm or egg in the absence of continued direct exposure is termed epigenetic transgenerational inheritance [8]. The initial germline transgenerational epigenetic alteration reported involved differential DNA methylation regions (DMRs) [9]. Subsequently, alterations in ncRNA were observed [10], and injection of altered sperm ncRNA into eggs transgenerationally propagated a behavioural alteration observed [11]. Histone alterations in sperm associated with histone retention regions (DHRs) have also been observed transgenerationally [12,13]. Recently, the concurrent transgenerational alterations in DMRs, DHRs, and ncRNA have been observed in sperm [13,14]. Therefore,

CONTACT Michael K. Skinner skinner@wsu.edu Center for Reproductive Biology, School of Biological Sciences, Washington State University Pullman, WA 99164-4236, USA

the integrated actions of all the epigenetic processes appear to be involved in the epigenetic transgenerational inheritance phenomenon. The alterations of the DMRs in sperm have been previously associated with toxicant-induced transgenerational diseases and pathologies [15–17]. The current study further investigates these epigenetic biomarkers and association with disease susceptibility.

Glyphosate is one of the most commonly used herbicides in agriculture worldwide [18,19]. Monsanto, St. Louis Missouri, commercialized glyphosate in the 1970s which is now used extensively in corn, soy, and canola crops [18]. Annual increases in glyphosate use have been observed in most agricultural crops, as well as in public lawn and garden use. The USA Environmental Protection Agency (EPA) has designated glyphosate as 'safe' for direct exposure toxicity. The European Food Safety Authority (EFSA) has stated there is a low acute toxicity observed by oral, dermal, or inhalation routes. The International Agency for Research on Cancer (IARC) has expressed a concern regarding cancer following glyphosate exposure [20]. General public exposure is primarily assumed to be from food consumption of crops that have had application of glyphosate, due to the ability of the plants to take up the compound [19]. The No Observational Adverse Effect Level (NOAEL) is 50 mg/kg per day dose [21]. Exposures of 50–500 mg/kg per day have been reported [22]. The relatively rapid half-life of ~5–10 hours in mammals and minimal direct exposure toxicity observed supports the regulatory agency determinations.

Recently we have demonstrated that a low-level glyphosate direct exposure, below the NOAEL dose, has no effect on the pathologies of the directly exposed individuals using a mammalian rat model [23], supporting previous studies that direct exposure toxicity of glyphosate is minimal [24,25]. When the exposed gestating female F0 generation and F1 generation offspring were examined later in life, they both were found to have negligible detectable alteration in pathology from the control vehicle exposed population [23]. However, the subsequent F2 generation grand offspring and F3 generation great-grand offspring did have a significant increase in the frequency of pathology and disease [23]. The direct actions of glyphosate on the F0 generation gestating female and F1 generation offspring were not found to promote major pathology, but generational toxicology on the F2 and F3 generations were observed [23]. The effects observed in the F1 generation were alterations in puberty and weaning weights in males and females [23]. The altered pathology in the F2 generation males involved increases in testis and kidney disease, altered pubertal onset, increased obesity, and the presence of multiple disease [23]. The F2 generation female altered pathology included increased ovarian disease, mammary tumors, altered pubertal onset, obesity, premature birth abnormalities, and the presence of multiple diseases [23]. The glyphosate-induced transgenerational disease in the F3 generation pathology in males included prostate disease, obesity, weaning weight alterations, and increased multiple disease frequency [23]. Transgenerational F3 generation pathology in females included ovarian disease, kidney disease, parturition abnormalities, obesity, and increased presence of multiple diseases [23]. All these transgenerational pathologies observed are relevant to human populations that have observed generational increases in these diseases, including ovarian disease, kidney disease, prostate disease, testis disease, altered pubertal onset, obesity, parturition abnormalities, and the presence of multiple diseases [1]. Therefore, the previous observations demonstrate negligible disease in the direct-exposed generations, but significant disease in subsequent generations, termed generational toxicology [1], that is mediated through glyphosate-induced epigenetic transgenerational inheritance mechanisms.

Previous studies with the agricultural fungicide vinclozolin [17,26], pesticide DDT (dichlorodiphenyl-trichloroethane) [16], and herbicide atrazine [15] have shown the ability of these toxicants to induce the epigenetic transgenerational inheritance of disease, and these pathologies are associated with potential epigenetic biomarker signatures of DMRs. The individual animals with specific pathologies in these transgenerational model systems were associated with unique epigenetic (i.e. DMRs) signatures for each of the different toxicant exposures [1,15,16].

A transgenerational disease DMR biomarker signature was identified for the majority of transgenerational pathologies observed. Therefore, the concept that an epigenetic biomarker for a specific disease induced by a variety of the toxicants transgenerationally has been established [15,16].

The current study extends these previous analyses to include the potential that both DMRs and differential histone retention sites (DHRs) can also be used as transgenerational disease biomarkers. This is one of the first reports of the potential that sperm DHRs may act as disease biomarkers. In addition, the assessment of potential overlapping DMR and DHR biomarkers between different diseases or pathologies was determined. Glyphosate induced epigenetic transgenerational sperm DMR and DHR biomarkers for specific disease were identified. How the various disease biomarkers overlap were investigated to assess the underlying potential epigenetic alterations associated with the transgenerational disease. Observations provide insight into the role of environmental epigenetics and transgenerational inheritance in disease etiology, with a focus on generational toxicology.

Materials and methods summary

Animal studies and breeding

Outbred Sprague Dawley SD male and female rats were fed a standard diet with water ad lib and mated. Gestating female rats were exposed to glyphosate and offspring bred for three generations in the absence of exposure. The breeding strategy and details are described in the Supplemental Methods. The F3 generation was aged to 1 year and pathologies assessed, as described in the Supplemental Methods. Sperm were isolated and used for epigenetic analysis and correlated to individuals' disease, as described in the Supplemental Methods. All experimental protocols for the procedures with rats were pre-approved by the Washington State University Animal Care and Use Committee (protocol IACUC # 2568), and all methods were performed in accordance with the relevant guidelines and regulations.

Epigenetic analysis, statistics and bioinformatics

DNA was isolated from the purified sperm, as previously described [13] in the Supplemental Methods. Methylated DNA immunoprecipitation (MeDIP) and differential histone retention with H3 histone chromatin immunoprecipitation (H3-ChIP), followed by next-generation sequencing (MeDIP-Seq) and (H3-ChIP-Seq) was performed. MeDIP-Seq and H3-ChIP-Seq, sequencing libraries, next-generation sequencing quality control, and bioinformatics analysis were performed, as described in the Supplemental Methods. Epimutation gene associations and analysis are also described in the Supplemental Methods. All molecular data have been deposited into the public database at NCBI (GEO # GSE118557 and GSE152678), and R code computational tools are available at GitHub (https://github.com/skinnerlab/MeDIP-seq) and www.skinner.wsu.edu.

Results

Animal breeding

Sprague Dawley gestating female rats (F0 generation) at 90 days of age were exposed in order to study the transgenerational effects of glyphosate. Previously we have identified inbreeding depression of transgenerational epigenetics [27], so prefer an outbred line of rats to optimize the epigenetic transgenerational inheritance of pathologies. The pregnant rats were transiently exposed (25 mg/kg body weight glyphosate daily) between days 8–14 of gestation during fetal gonadal sex determination when germ cell epigenetic programming occurs. Twenty-five mg/kg/day is half the No Observable Adverse Effect Level (NOAEL) exposure of 50 mg/kg/day [28]. Glyphosate has a rapid metabolism turnover of 5–10-h half-life, such that the concentration will decrease by approximately 75–90% daily during the transient exposure period. The 2–4 half-lives that occur each 24-h period indicates that after 7 days of exposure less than 50 mg/kg/daily, the exposures NOAEL, would be present. The offspring F1 generation rats (directly exposed *in utero*) were aged to 90 days of age and bred within the lineage to generate the grand-offspring F2 generation (directly exposed through the F1 generation germline), which were then bred

at 90 days of age to generate the F3 generation (not directly exposed so transgenerational). The control lineage used F0 gestating rats exposed to the vehicle control dimethyl sulphoxide (DMSO) or phosphate-buffered saline (PBS). All the lineages were aged to 1 year and euthanized for pathology and sperm epigenetic analysis. At each generation, five litters were obtained with no sibling or cousin breeding to prevent any inbreeding artifacts in the control or glyphosate lineages. Due to the lack of any inbreeding, the potential frequency of genetic segregation is minimal in the F3 generation and was not observed with sibling comparisons. As previously described and to prevent litter bias, at each generation between 6 and 8 unrelated founder gestating females from different litters were bred, and five litters were obtained and culled early in postnatal development to 10 pups per litter with animals of each sex from each litter used to generate 25–50 individuals of each sex for each generation for analysis [23]. Similar numbers of males and females were used from each litter to avoid any litter bias. Additional details of the breeding strategy are presented in the Supplemental Methods. All protocols and studies were approved by the Washington State University Animal Care and Use Committee (protocol IACUC # 2568).

Pathology analysis

In our previous study, pathology calls were made by assessing histology sections of testis, kidney, prostate, and gonadal adipocytes [23]. The complete histological sections were analysed by two different observers blinded to the exposure. In the event of a discrepancy, a third observer blinded to the exposure was also used. The pathology parameters identified were as previously described [15–17,23]. For the testis pathology, the abnormalities quantified were atrophy of seminiferous tubules, vacuoles within seminiferous tubules, and sloughing of cellular debris into the tubular lumen (maturation arrest). For prostate pathology, the abnormalities quantified were atrophy of prostatic epithelium, vacuoles within the prostatic epithelium, and prostatic epithelial hyperplasia. For kidney pathology, the abnormalities quantified were reduced glomerular size, thickening of the Bowman's capsule, and renal cysts. The age of puberty onset was determined. Obesity was assessed with an increase in adipocyte size (area), body mass index (BMI) and abdominal adiposity [16]. In all cases the number of abnormalities in an animal's tissue was compared with the mean number of abnormalities in the control group to determine if that tissue was diseased, as described in the Supplemental Methods. For the F3 generation glyphosate lineage male pathology, the individual animals are listed and a (+) indicates presence of disease and (-) absence of disease (Table 1). The F3 generation control lineage male pathology, the individuals are listed similarly (Supplemental Table S1). Only the individuals with a single disease for a specific pathology were used for that pathology, except in the case of the multiple category disease when animals with two of more diseases were used. This allows a more accurate association with disease and eliminates the confounding presence of other disease or co-morbidities. The control lineage did not have sufficient numbers of animals with a specific disease, Supplemental Table S1, so were not analysed further. Although the F3 generation males had a testis disease group, two individuals had only testis disease, so too few for further analysis. The other disease had n = 4 individuals for kidney disease, n = 7 with prostate disease, n = 13 for obesity, and n = 10 for multiple (≥2) disease, Table 1. The disease animals were compared to animals with no disease n = 8, Table 1. The limited number of individuals needs to be considered in data interpretation and statistical analysis. In contrast to previous analyses using DDT or vinclozolin sperm biomarkers for disease, when all animals with a specific disease were analysed independent of co-morbidities [16,17], the current study sought to optimize disease specific biomarker assessment.

Sperm DNA methylation analysis

Transgenerational inheritance of pathology and disease requires the germline (sperm or egg) to transmit epigenetic information between generations [1]. Purified sperm were collected from the control and glyphosate lineage F3 generation males for epigenetic analysis, as described in the Supplemental Methods. Potential differential DNA

Table 1. F3 generation glyphosate lineage male pathology. The individual animals for the glyphosate lineage males are listed and a (+) indicates presence of disease and (-) absence of disease. The animals with shaded (+) were used for the epigenetic analysis due to the presence of only one disease, except the multiple (≥2) disease.

	Puberty	Testis	Prostate	Kidney	Tumor	Lean	Obese	Multiple Disease	Total Disease
ID									
Gly-1		-	-	-	-	-	+	-	**1**
Gly-2		-	-	-	-	-	+	-	**1**
Gly-3		-	+	-	-	-	-	-	**1**
Gly-4		+	-	-	-	-	-	-	**1**
Gly-5	-	-	-	-	-	-	+	-	**1**
Gly-6	-	+	-	+	-	-	+	+	**3**
Gly-7	-	-	-	-	-	-	+	-	**1**
Gly-8	-	-	-	+	-	-	-	-	**1**
Gly-9	-	-	+	-	-	-	-	-	**1**
Gly-10	-	-	-	-	-	-	-	-	**0**
Gly-11	-	-	-	-	-	-	-	-	**0**
Gly-12	-	-	-	-	-	-	+	-	**1**
Gly-13	-	+	+	-	-	-	-	+	**2**
Gly-14	-	-	-	+	-	-	-	-	**1**
Gly-15	-	-	+	-	-	-	-	-	**1**
Gly-16	-	-	-	-	-	-	+	-	**1**
Gly-17	-	-	-	+	-	-	-	-	**1**
Gly-18	-	-	-	-	-	-	-	-	**0**
Gly-19	-	+	-	+	-	-	+	+	**3**
Gly-20	-	+	+	+	-	-	-	+	**3**
Gly-21	-	+	-	+	-	-	+	+	**3**
Gly-22						-	+	-	**1**
Gly-23		-	-	-	-	-	+	-	**1**
Gly-24	-	-	-	+	-	-	-	-	**1**
Gly-25	-	+	-	+	-	-	-	+	**2**
Gly-26		-	-	-	-	-	+	-	**1**
Gly-27	-	-	-	-	-	-	-	-	**0**
Gly-28	-	-	+	+	-	-	+	+	**3**
Gly-29	-	-	-	-	-	-	+	-	**1**
Gly-30	-	-	+	-	-	-	+	+	**2**
Gly-31	-	-	+	-	-	-	+	+	**2**
Gly-32	-	-	-	-	-	-	-	-	**0**
Gly-33	-	+	-	-	-	-	-	-	**1**
Gly-34	-	-	-	-	-	-	-	-	**0**
Gly-35	-	-	-	-	-	-	+	-	**1**
Gly-36	-	-	+	-	-	-	-	-	**1**
Gly-37		-	-	-	-	-	-	-	**0**
Gly-38	-	-	-	-	-	-	-	-	**0**
Gly-39	-	-	-	-	-	-	+	-	**1**
Gly-40	-	-	+	-	+	-	-	+	**2**
Gly-41	-	-	+	-	-	-	-	-	**1**
Gly-42	-	-	+	-	-	-	-	-	**1**
Gly-43	-	-	-	-	-	-	+	-	**1**
Gly-44	-	-	-	+	-	-	-	-	**1**
Gly-45	-	-	+	-	-	-	-	-	**1**
Affected	**0**	**8**	**13**	**11**	**1**	**0**	**19**	**10**	
Population	**37**	**44**	**44**	**44**	**44**	**45**	**45**	**45**	

methylation regions (DMRs) in the sperm were identified using a comparison between the control and the glyphosate lineage (Figure 1a). Within the glyphosate lineage, individuals with a given disease (prostate, kidney, obesity, multiple disease (≥2)) were compared to non-diseased animals from the glyphosate lineage to define disease-specific DMRs (Figure 1b–E).

DNA from the sonicated purified sperm was isolated, fragmented and the methylated DNA immunoprecipitated using a methyl-cytosine antibody (MeDIP). The MeDIP DNA fragments were then sequenced for an MeDIP-Seq analysis, as described in the Supplemental Methods [12,13,29]. The MeDIP-Seq analysis was used since >90% of the genome has low CpG density regions, so can assess >90% of the genome-wide DNA methylation. The sperm DMR numbers are presented in Figure 1 for various edgeR statistical p-value cut-off threshold values, and a stringent

DMR Identification

a Glyphosate versus Control DMRs

p-value	All Window	Multiple Window
0.001	6457	183
1e-04	1395	43
1e-05	**340**	**11**
1e-06	93	6
1e-07	39	0

Significant windows	1	2	3	4
Number of DMR	329	7	3	1

b Prostate Disease DMR Biomarkers

p-value	All Window	Multiple Window
0.001	1623	12
1e-04	**242**	**2**
1e-05	33	1
1e-06	7	1
1e-07	2	1

Significant windows	1	2
Number of DMR	240	2

c Kidney Disease DMR Biomarkers

p-value	All Window	Multiple Window
0.001	1220	4
1e-04	**180**	**1**
1e-05	23	1
1e-06	3	0
1e-07	2	0

Significant windows	1	2
Number of DMR	179	1

d Obesity Disease DMR Biomarkers

p-value	All Window	Multiple Window
0.001	1582	7
1e-04	**250**	**1**
1e-05	45	0
1e-06	9	0
1e-07	2	0

Significant windows	1	2
Number of DMR	249	1

e Multiple Disease DMR Biomarkers

p-value	All Window	Multiple Window
0.001	2076	87
1e-04	**345**	**31**
1e-05	75	4
1e-06	17	1
1e-07	3	0

Significant windows	1	2	3	5
Number of DMR	314	20	10	1

f DMR Overlap

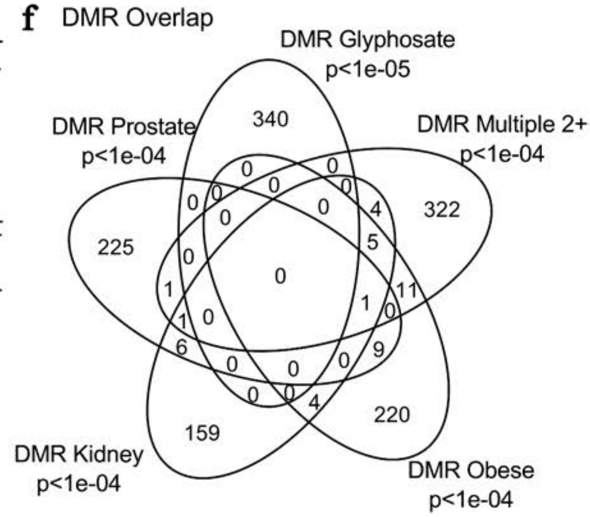

Figure 1. DMR identification and numbers. The number of DMRs found using different p-value cut-off thresholds. The All Window column shows all DMRs. The Multiple Window column shows the number of DMRs containing at least two significant windows (1 kb each). The number of DMRs with the number of significant windows (1 kb per window) at an edgeR p-value threshold bolded for DMR. (a) Glyphosate versus control DMRs; (b) Prostate disease DMRs; (c) Kidney disease DMRs; (d) Obesity disease DMRs; and (e) Multiple disease DMRs. (f) Venn diagram DMR overlap of each data set with edgeR p-value indicated. The bolded edgeR p-value was used for all subsequent data analysis.

p-value of $p < 1e{-}05$ (control versus glyphosate) or $p < 1e{-}04$ (diseased versus non-diseased) were selected as the threshold for subsequent analyses, as previously described [23]. The total number of DMRs for the control versus glyphosate is 340 with 11 of them having multiple neighboring 1000 bp windows (Figure 1a and Supplemental Table S2). The previously reported transgenerational F3 generation sperm glyphosate versus control lineage DMRs used three pools of different animals to identify the glyphosate-induced sperm DNA alterations [23]. The current study used individual animal sperm analysis to identify the glyphosate-induced transgenerational F3 generation DMRs (Figure 1a). A comparison of these two studies demonstrates the 340 DMRs with a $p < 1e{-}05$ has an overlap of 129 DMRs with the previous DMRs at $p < 0.05$. Therefore, a 38%

overlap was observed at this reduced statistical threshold. We feel this is a reasonable degree of overlap due to the original study [23] using three pooled sets of samples compared to individual animal analysis in the current study. The current study of individual animal analysis has higher statistical power due to the larger sample size compared to the previous pooled analysis with n = 3 [23].

The animals with a specific disease were compared to non-disease animals to identify the disease-specific sperm DMRs. Previous studies have demonstrated this statistical threshold is optimal for disease-specific epigenetic biomarkers [15–-15–17,26]. The group of animals with prostate disease had 242 DMRs at p < 1e-04 with two multiple windows (i.e., 1 kb each) detected, (Figure 1b). The kidney disease group was found to have 180 total DMRs with 1 of these having multiple neighboring windows (Figure 1c). The obesity disease group had 250 DMRs at p < 1e-04 with 1 of these having multiple neighboring windows (Figure 1d). The multiple disease group had 345 DMRs at p < 1e-04 with 31 of them having multiple neighboring 1000 bp windows, Figure 1e. Using a log-fold-change analysis of individual DMRs, approximately 50% had an increase in DNA methylation with the rest a decrease in DNA methylation, Supplemental Tables S2-S6. Therefore, the different diseases were found to have altered DNA methylation in the F3 generation sperm. Interestingly, negligible overlap was observed between these different DMRs at a statistical threshold of p < 1e-04, (figfigure 1f). Observations indicate glyphosate can promote germline epigenetic alterations in DNA methylation with predominantly disease specific DMRs with an edgeR p < 1e-04 threshold (Supplemental Tables S2 – S6).

The DMRs chromosomal locations are presented in Figure 2 where arrowheads indicate DMR locations, and black boxes the DMR clusters. All chromosomes had DMRs for glyphosate versus control, but the prostate, kidney, obesity and multiple disease DMR biomarkers were not on the Y or mitochondrial DNA (MT). Therefore, the DMRs were genome-wide and identified on nearly all chromosomes. These DMR chromosomal signatures are potential sperm biomarkers for disease. The CpG density of the DMRs and the DMRs length are shown in Supplemental Figure S1. The CpG density of the DMRs for all the comparisons was 1–5 CpG per 100 bp being predominant, (Supplemental Figure S1). This is characteristic of a low-density CpG deserts [30] which was previously reported with other transgenerational DMRs. The length of the DMRs for each disease biomarker and glyphosate versus control were 1–4 kb with 1 kb length being predominant, Supplemental Figure S1. Generally, the DMRs are 1 kb in size with around 10 CpGs, as previously reported [30]. A principal component analysis (PCA) for the different DMR genomic site comparisons (glyphosate versus control, prostate disease biomarker, kidney disease biomarker, obesity disease biomarker and multiple disease biomarker) demonstrated clustered DMR principal component separation of the control versus glyphosate, and the prostate, kidney, obesity and multiple diseased versus non-diseased (Supplemental Figure S2).

Sperm histone retention analysis

Previous observations have demonstrated that differential histone retention in sperm also appears to have a role in epigenetic transgenerational inheritance [12]. Similarly to the DMRs, the differential histone retention regions (DHRs) in the sperm were identified using a comparison between the control and the glyphosate lineage (Figure 3a and Supplemental Table S7). Within the same glyphosate lineage animals with a given disease (prostate, kidney, obesity, multiple disease (≥ 2)) versus non-diseased animals were assessed to identify DHRs (Figure 3b–E and Supplemental Tables S8–S11). Interestingly, a high number of DHRs (836) was found at edgeR p < 1e-05 in the glyphosate versus control comparison, Figure 3a. A smaller number of DHRs were detected at p < 1e-04 in the disease biomarkers (prostate, kidney, obesity and multiple diseases), (Figure 3b–E). Similar to the DMR analysis, an overlap of these disease specific DHRs at edgeR p < 1e-04 revealed minimal overlap (figure 3f). The chromosomal locations of these DHRs are presented in Figure 4. The different DHRs appear to be genome-wide for the glyphosate versus

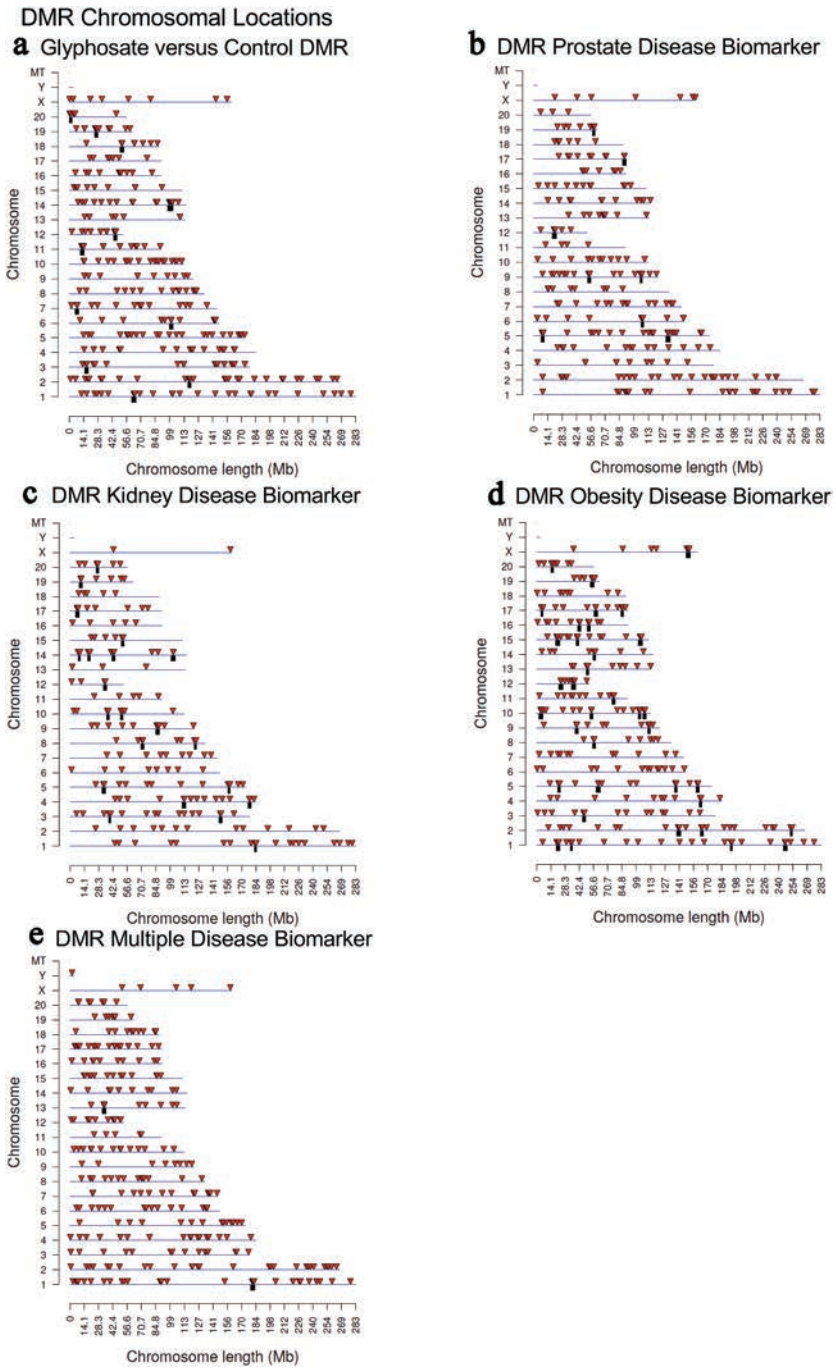

Figure 2. DMR chromosomal locations. The DMR locations on the individual chromosomes is represented with an arrowhead and a cluster of DMRs with a black box. All DMRs containing at least one significant window at the select (bold) edgeR p-value threshold are shown. The chromosome number and size of the chromosome (megabase) are presented. (a) Glyphosate versus control DMRs; (b) Prostate disease DMRs; (c) Kidney disease DMRs; (d) Obesity disease DMRs; and (e) Multiple disease DMRs.

control comparison, but are more specific over the genome for prostate, kidney, obesity and multiple diseases.

The DHRs CpG density and length of DHRs are presented in (Supplemental Figure S3). The CpG density of the DHRs for all the comparisons was 1–5 CpG per 1000 bp being predominant, Supplemental Figure S3. The length of the DHRs for each disease biomarker and glyphosate versus control were 1–3 kb with 1 kb length being predominant except for the glyphosate versus control showing DHRs length from 1 to 10 kb with 1 and 2 kb length being predominant, Supplemental Figure S3. Generally, the DHRs are 1 kb in size

DHR Identification

a Glyphosate versus Control DHRs

p-value	All Window	Multiple Window
0.001	35739	4779
1e-04	6189	280
1e-05	**836**	**12**
1e-06	124	5
1e-07	21	5

Significant windows	1	2	3	5	8
Number of DMR	824	9	1	1	1

b Prostate Disease DHR Biomarkers

p-value	All Window	Multiple Window
0.001	490	2
1e-04	**42**	**0**
1e-05	7	0
1e-06	2	0
1e-07	0	0

Significant windows	1
Number of DMR	42

c Kidney Disease DHR Biomarkers

p-value	All Window	Multiple Window
0.001	658	5
1e-04	**70**	**0**
1e-05	7	0
1e-06	0	0
1e-07	0	0

Significant windows	1
Number of DMR	70

d Obesity Disease DHR Biomarkers

p-value	All Window	Multiple Window
0.001	417	0
1e-04	**36**	**0**
1e-05	6	0
1e-06	0	0
1e-07	0	0

Significant windows	1
Number of DMR	36

e Multiple Disease DHR Biomarkers

p-value	All Window	Multiple Window
0.001	1338	8
1e-04	**109**	**0**
1e-05	14	0
1e-06	2	0
1e-07	0	0

Significant windows	1
Number of DMR	109

f DHR Overlap

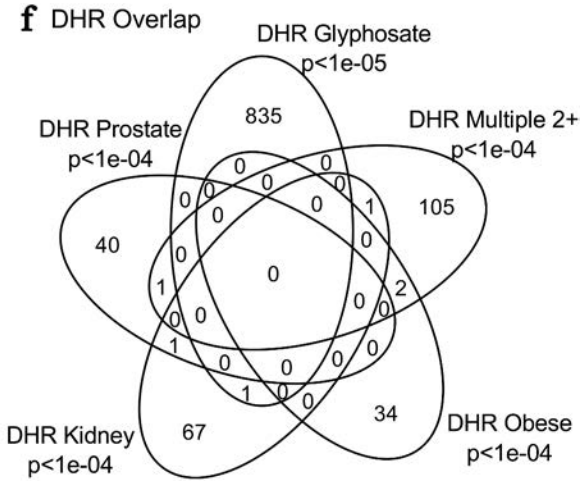

Figure 3. DHR identification and numbers. The number of DHRs found using different edgeR p-value cut-off thresholds. The All Window column shows all DHRs. The Multiple Window column shows the number of DHRs containing at least two significant windows (1 kb each). The number of DHRs with the number of significant windows (1 kb per window) at a bolded p-value threshold is presented. (a) Glyphosate versus control DHRs; (b) Prostate disease DHRs; (c) Kidney disease DHRs; (d) Obesity disease DHRs; and (e) Multiple disease DHRs. (f) Venn diagram DHR overlap for each data set with p-value indicated.

with around 10 CpGs as previously reported [30]. A PCA of the different DMR genomic site comparisons (glyphosate versus control, prostate disease biomarker, kidney disease biomarker, obesity disease biomarker and multiple disease biomarker) for the DHRs revealed a clustered separation of the diseases versus non-disease, (Supplemental Figure S4). This helps confirm the edgeR analysis is identifying differential disease sites.

Epimutation comparison analysis

A relatively stringent edgeR p-value for the DMRs or DHRs is used for the identification of these disease specific epimutations, as previously described [15–17,26]. A reduced statistical threshold of $p < 0.05$ was used to compare and further evaluate the potential overlap of the DMRs or DHRs between the glyphosate versus control and

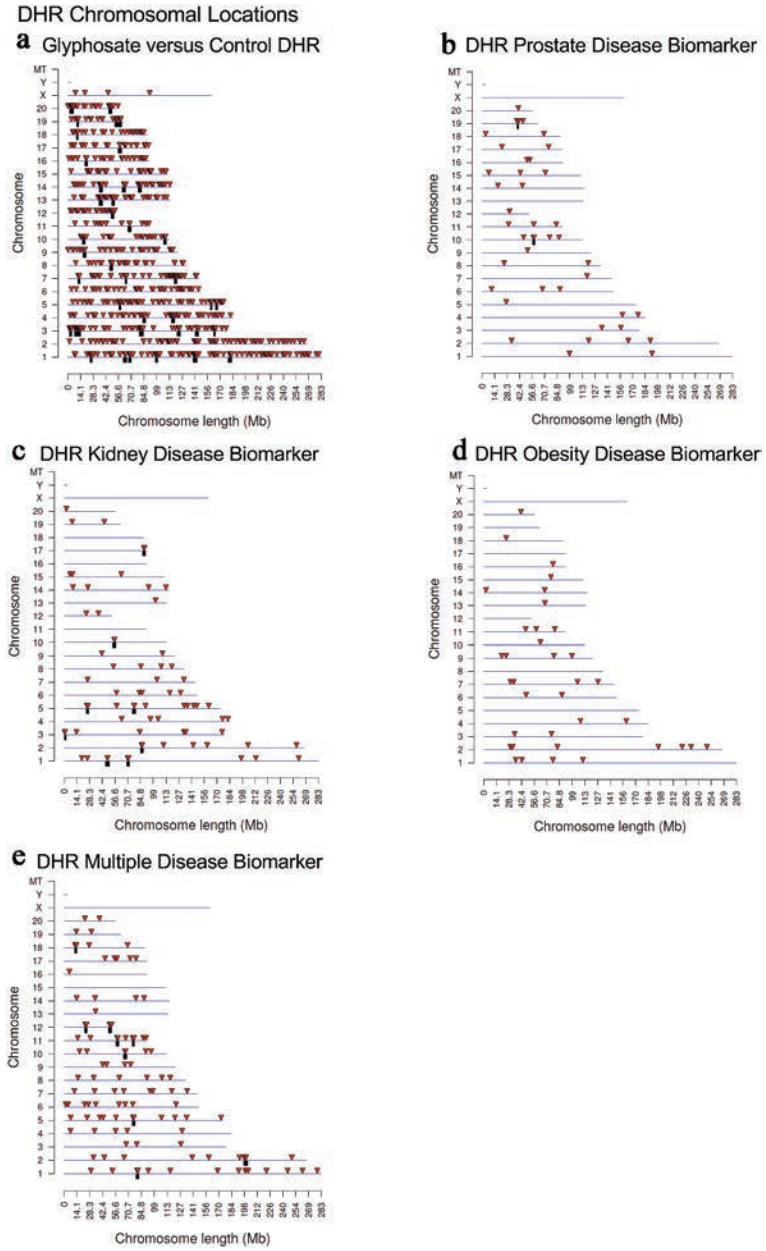

Figure 4. DHR chromosomal locations. The DHR locations on the individual chromosomes is represented with an arrowhead and a cluster of DHRs with a black box. All DHRs containing at least one significant window at the edgeR p-value threshold selected (bold) are shown. The chromosome number and size (megabase) are presented. (a) Glyphosate versus control DHRs; (b) Prostate disease DHRs; (c) Kidney disease DHRs; (d) Obesity disease DHRs; and (e) Multiple disease DHRs.

the different disease biomarkers when compared to the higher edgeR p < 1e-04 statistical threshold DMRs. By lowering the stringency to a p-value of <0.05 for the comparison (i.e. extended overlap) the procedure allows for the identification of more potential overlaps between the glyphosate versus control, and the prostate, kidney, obesity and multiple disease comparisons. The relatively high statistical threshold is used as the epigenetic site definition. A comparison of the p < 1e-04 for the DMRs, with each potential comparison at p < 0.05, Figure 5, demonstrates a much higher overlap between the prostate DMRs and the kidney DMRs (37.2%) and obesity DMRs (59.5%) (Figure 5a). The extended overlap between the DMRs for the different pathologies generally was minimally 30% and as high as 70%, as indicated with highlighted horizontal row comparisons. Interestingly, minimal overlap was observed between the DMRs and DHRs (<10%), except for

p<0.05 / p<1e-04	DMR Glyphosate	DMR Prostate	DMR Kidney	DMR Obese	DMR Multiple 2+	DMR Multiple 3+
DMR Glyphosate	340 (100.00%)	16 (4.71%)	16 (4.71%)	16 (4.71%)	27 (7.94%)	28 (8.24%)
DMR Prostate	29 (11.98%)	242 (100.00%)	90 (37.19%)	144 (59.50%)	115 (47.52%)	97 (40.08%)
DMR Kidney	13 (7.22%)	82 (45.56%)	180 (100.00%)	102 (56.67%)	100 (55.56%)	79 (43.89%)
DMR Obese	15 (6.00%)	131 (52.40%)	118 (47.20%)	250 (100.00%)	176 (70.40%)	167 (66.80%)
DMR Multiple 2+	48 (13.91%)	133 (38.55%)	130 (37.68%)	204 (59.13%)	345 (100.00%)	340 (98.55%)
DMR Multiple 3+	38 (11.45%)	111 (33.43%)	127 (38.25%)	166 (50.00%)	309 (93.07%)	332 (100.00%)
DHR Glyphosate	217 (25.96%)	97 (11.60%)	95 (11.36%)	104 (12.44%)	113 (13.52%)	113 (13.52%)
DHR Prostate	2 (4.76%)	0 (0.00%)	3 (7.14%)	1 (2.38%)	1 (2.38%)	0 (0.00%)
DHR Kidney	5 (7.14%)	5 (7.14%)	7 (10.00%)	3 (4.29%)	6 (8.57%)	5 (7.14%)
DHR Obese	0 (0.00%)	2 (5.56%)	0 (0.00%)	2 (5.56%)	2 (5.56%)	2 (5.56%)
DHR Multiple 2+	10 (9.17%)	4 (3.67%)	3 (2.75%)	3 (2.75%)	5 (4.59%)	3 (2.75%)
DHR Multiple 3+	3 (21.43%)	0 (0.00%)	3 (21.43%)	1 (7.14%)	6 (42.86%)	6 (42.86%)

p<0.05 / p<1e-04	DHR Glyphosate	DHR Prostate	DHR Kidney	DHR Obese	DHR Multiple 2+	DHR Multiple 3+
DMR Glyphosate	149 (43.82%)	22 (6.47%)	16 (4.71%)	13 (3.82%)	36 (10.59%)	1 (0.29%)
DMR Prostate	62 (25.62%)	6 (2.48%)	13 (5.37%)	5 (2.07%)	7 (2.89%)	4 (1.65%)
DMR Kidney	42 (23.33%)	6 (3.33%)	12 (6.67%)	4 (2.22%)	9 (5.00%)	7 (3.89%)
DMR Obese	67 (26.80%)	8 (3.20%)	12 (4.80%)	6 (2.40%)	13 (5.20%)	3 (1.20%)
DMR Multiple 2+	152 (44.06%)	8 (2.32%)	17 (4.93%)	10 (2.90%)	12 (3.48%)	6 (1.74%)
DMR Multiple 3+	129 (38.86%)	12 (3.61%)	15 (4.52%)	12 (3.61%)	22 (6.63%)	18 (5.42%)
DHR Glyphosate	836 (100.00%)	137 (16.39%)	115 (13.76%)	34 (4.07%)	223 (26.67%)	34 (4.07%)
DHR Prostate	8 (19.05%)	42 (100.00%)	18 (42.86%)	20 (47.62%)	32 (76.19%)	15 (35.71%)
DHR Kidney	16 (22.86%)	26 (37.14%)	70 (100.00%)	27 (38.57%)	36 (51.43%)	14 (20.00%)
DHR Obese	4 (11.11%)	21 (58.33%)	17 (47.22%)	36 (100.00%)	22 (61.11%)	10 (27.78%)
DHR Multiple 2+	30 (27.52%)	50 (45.87%)	43 (39.45%)	56 (51.38%)	109 (100.00%)	108 (99.08%)
DHR Multiple 3+	2 (14.29%)	6 (42.86%)	5 (35.71%)	4 (28.57%)	13 (92.86%)	14 (100.00%)

Figure 5. Extended overlap disease DMRs and DHRs. The p-value data set at p < 1e-04 for disease-specific and p < 1e-05 for exposure specific are compared to the p < 0.05 data to identify potential overlap between the different pathologies with DMR or DHR number and percentage of the total presented. The grey highlight is the expanded 100% overlap and yellow highlight overlaps >25%.

the glyphosate versus control comparisons with >25% overlap, (Figure 5). An additional comparison was made between individuals with ≥2 or ≥3 different pathologies. The overlap between these ≥2 and ≥3 multiple diseases was greater than 90% (Figure 5). Therefore, there was not an increase of DMR or DHR with ≥3 pathologies, and similar DMR and DHR sites were identified. Observations suggest having an increased amount of disease/pathology does not appear to correlate with an increased number of epigenetic alterations. No further analysis of the ≥3 pathology DMR data was performed.

The same reduced statistical edgeR threshold extended overlap was used for the DHRs in Figure 5b. Similarly to the DMRs, a comparison of the p < 1e-04 for the DHRs, with each potential comparison at p< 0.05, (Figure 5b), shows a much higher overlap between the prostate DHRs and the kidney DHRs (42.9%) and obesity DHRs (47.6%) and multiple disease DHRs (76.2%) (Figure 5b). Although very few overlaps are observed between the DMRs and DHRs (Figure 5b), observations indicate that a subset of DMRs and DHRs appear to be common among diseases for a specific disease comparison. Analysis of the

DMR or DHR overlaps for sites that are common between the different pathologies identified lists for both, Supplemental Table S12. The lists of DMR and DHR in common with all pathologies identify those with associated genes. Interestingly, when the common DMR and DHR sites for a specific disease comparison were identified and then compared between all the diseases, negligible overlap was observed (Figures 1F and 3f). Therefore, there are common DMRs within a specific disease comparisons, but these common DMR sets are primarily disease specific, (Supplemental Figure S5).

Epimutation gene associations

The list of DMRs and DHRs for all the epigenetic alterations identified are presented in Supplemental Tables S2–S11. Epimutation gene associations used DMR or DHR identified within 10 kb of a gene so as to include proximal and distal promoter elements. The minority of DMR or DHR, less than 20%, have epimutations associated with genes. Therefore, the majority are intergenic and not within 10 kb of a gene. The DMR and DHR associated genes found were categorized into relevant functional categories for the glyphosate versus control, and for each set of disease biomarkers (Figure 6). The associated gene categories listed for the Tables S2-S11 used DAVID and Panther public databases with direct experimental gene functional links, as described in the Supplemental Methods. The common GO terms with gene associations are based on literature search correlations between genes and function, which have accuracy issues, even with updated bioinformatics procedures [31], and so were not used in the current study. The top 10 gene categories containing multiple genes are presented for DMRs (Figure 6a) and DHRs (Figure 6b). Epimutations were found predominantly in the signalling, metabolism, transcription, receptor and cytoskeleton categories for both DMRs and DHRs (Figure 6). The number of epimutations was higher for the DMRs compared to the DHRs. The highest represented gene categories typically involve the gene categories with the highest number of associated genes, such as metabolism. No statistical analysis was performed to determine over-represented gene category associations. This analysis was simply done to determine that the general gene category associations expected were observed.

The disease-specific DMR-associated genes, Supplemental Figure S2-S6, were analysed using a Pathway Studio gene database and network tool to identify associated gene processes (Figures 7 and 8). Not surprisingly, the disease-specific DMR-associated genes predominantly corresponded with the associated disease for prostate disease, kidney disease, and obesity (Figure 7). Some additional associated disease groups were also identified. Interestingly, the multiple (≥2) disease epimutation biomarker DMR-associated genes were found to be correlated with all the major prostate, kidney, and obesity processes (Figure 8). The individual gene processes and shared gene processes are identified (Figure 8). The epimutation gene associations with previously identified disease-linked genes helps validate the observations and biomarkers. Statistical analysis of over-representation of DMR-associated genes with diseases as performed by Pathway Studio software (Elsevier, Inc. 2020) revealed that for prostate disease DMR-associated genes (Figure 7a) the disease term Benign Prostatic Hypertrophy was enriched ($p = 0.048$). For obesity disease DMR-associated genes (Figure 7c) the term Obesity was enriched ($p = 0.046$). For the multiple disease DMR-associated genes (Figure 8) the disease terms Obesity ($p = 0.004$), Polycystic Kidney Disease ($p = 0.0008$), and Prostatic Adenocarcinoma ($p = 0.008$) were significantly enriched.

Discussion

A previous study by our laboratory demonstrated the ability of one of the most commonly used agricultural herbicides, glyphosate, to promote the epigenetic transgenerational inheritance of pathology [23]. Negligible pathology was observed in the F0 or F1 generations from direct exposure, but a significant increase in pathology and disease was observed in the grand offspring F2 generation and great-grand offspring F3 generation [23]. This is termed generational toxicology, and appears to develop through the epigenetic transgenerational inheritance of germline epimutation alterations

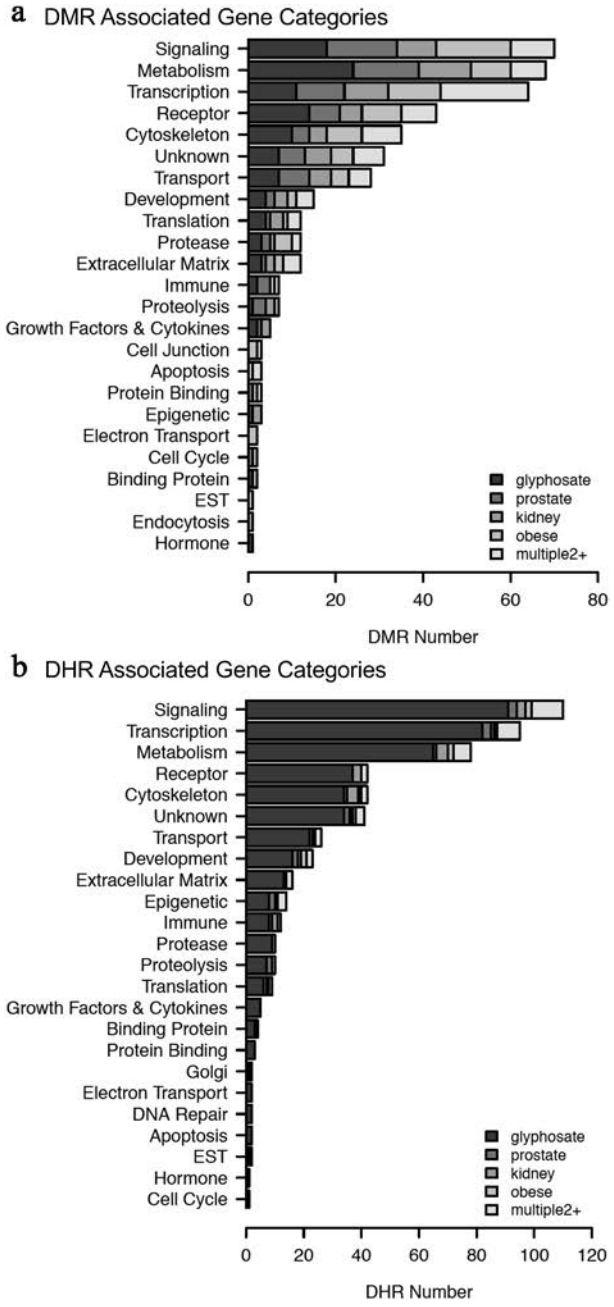

Figure 6. Associated gene categories. (a) DMR-associated gene categories. (b) DHR associated gene categories. The different gene categories and number DMR or DHR presented with color index insert. No statistical analysis was performed for over-represented genes, but sample correlations provided for each gene category.

that include imprinted-like gene characteristics and are transmitted to subsequent generations [1,32]. The current study used groups of individuals with a single pathology to identify potential epigenetic biomarkers for disease. The pathologies observed with sufficient numbers of animals include prostate disease, kidney disease, obesity, and multiple disease with individuals with ≥2 different pathologies. These are relevant pathologies for humans in that prostate disease is one of the most prominent pathologies in human males [33]. Prostate disease impacts 50% of the males over the age of 50 years and 100% of the males over 70 years in the USA. Kidney disease is also a prominent disease in ageing population. Obesity is dramatically increasing in the population for both males and females with greater than 30% of the males in the USA [34] and Europe. Although genetic mutations with GWAS have been associated with these human pathologies, the percentage of the disease populations with the genetic mutation association is generally less than 1% of the disease population.

In contrast, altered epigenetic sites termed epimutations appear to have a much higher frequency and appear in the majority of individuals with the disease [15–17]. The current study supports this observation with the majority of individuals with the disease having the pathology epimutation biomarkers. For the transgenerational F3 generation males, the number of differential DNA methylation regions (DMRs) identified for each disease was generally over 200 for the individual disease at edgeR $p < 1e\text{-}04$ threshold. Negligible overlap was observed between the different prostate, kidney, obesity, or multiple disease pathologies DMR biomarkers, Figure 1. Interestingly, at a reduced comparison statistical threshold, a 30–50% overlap was observed among the different comparisons for specific disease DMR biomarker sets, Figure 5. Therefore, potential pathology specific epigenetic biomarkers were identified, but individual comparison overlapping sets of DMRs at a reduced threshold are present. The DMR gene associations demonstrate correlation with previously known genes linked to the respective pathologies, and the multiple diseases with the majority of the pathologies. Observations suggest subsets of epimutations common between the pathologies are minimal, while a unique set of pathology-specific biomarkers are present that may provide the disease-specific susceptibility.

In addition to the DMR pathology biomarkers, the novel observation was made that sperm differential histone retention regions (DHRs) are also observed with the different pathologies. The

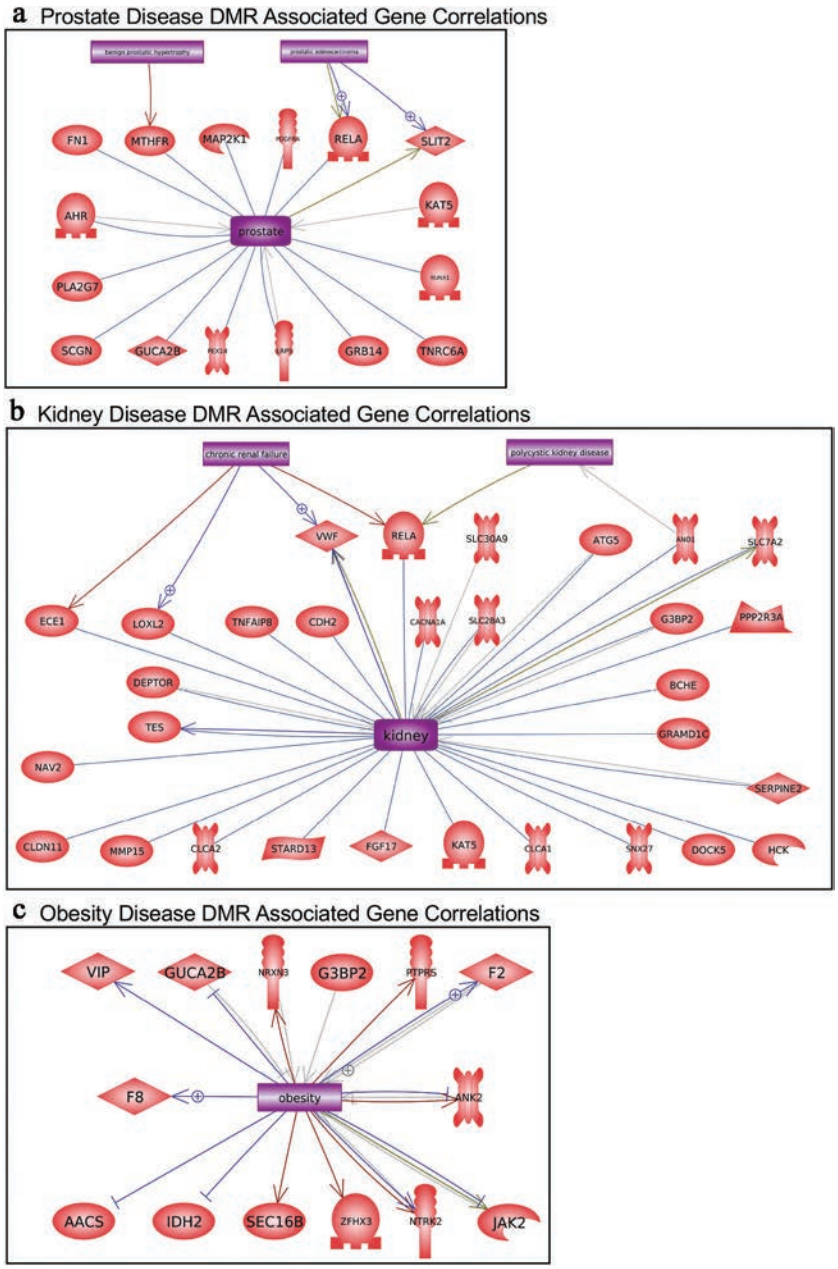

Figure 7. DMR-associated genes within the pathology biomarker DMR set for each individual pathology. The physiologic and pathology process is listed with direct gene links. (a) Prostate disease, (b) kidney disease, and (c) obesity.

number of DHRs were less than the number of DMRs and the DHRs were also found to have disease specificity, Figure 3. The histones in sperm are replaced by protamines to compact DNA into the head of the sperm [35] at the later stage of spermatogenesis in the testis following meiosis. However, specific histone retention sites are observed and found to be conserved [12]. Recently we identified environmental toxicant-induced epigenetic transgenerational inheritance of differential histone retention regions (DHRs) [13,14]. The current study demonstrates glyphosate appears to promote the epigenetic transgenerational inheritance of DHRs in sperm. These sperm DHRs also appear to provide epigenetic biomarkers for disease, and this is one of the first observations of DHRs as potential biomarkers for disease. An overlap at edgeR $p < 1e\text{-}04$ demonstrated limited overlap of DHRs between the different pathologies, but at a reduced threshold comparison overlap demonstrated a 25–75% overlap between the pathologies, Figure 5. Negligible

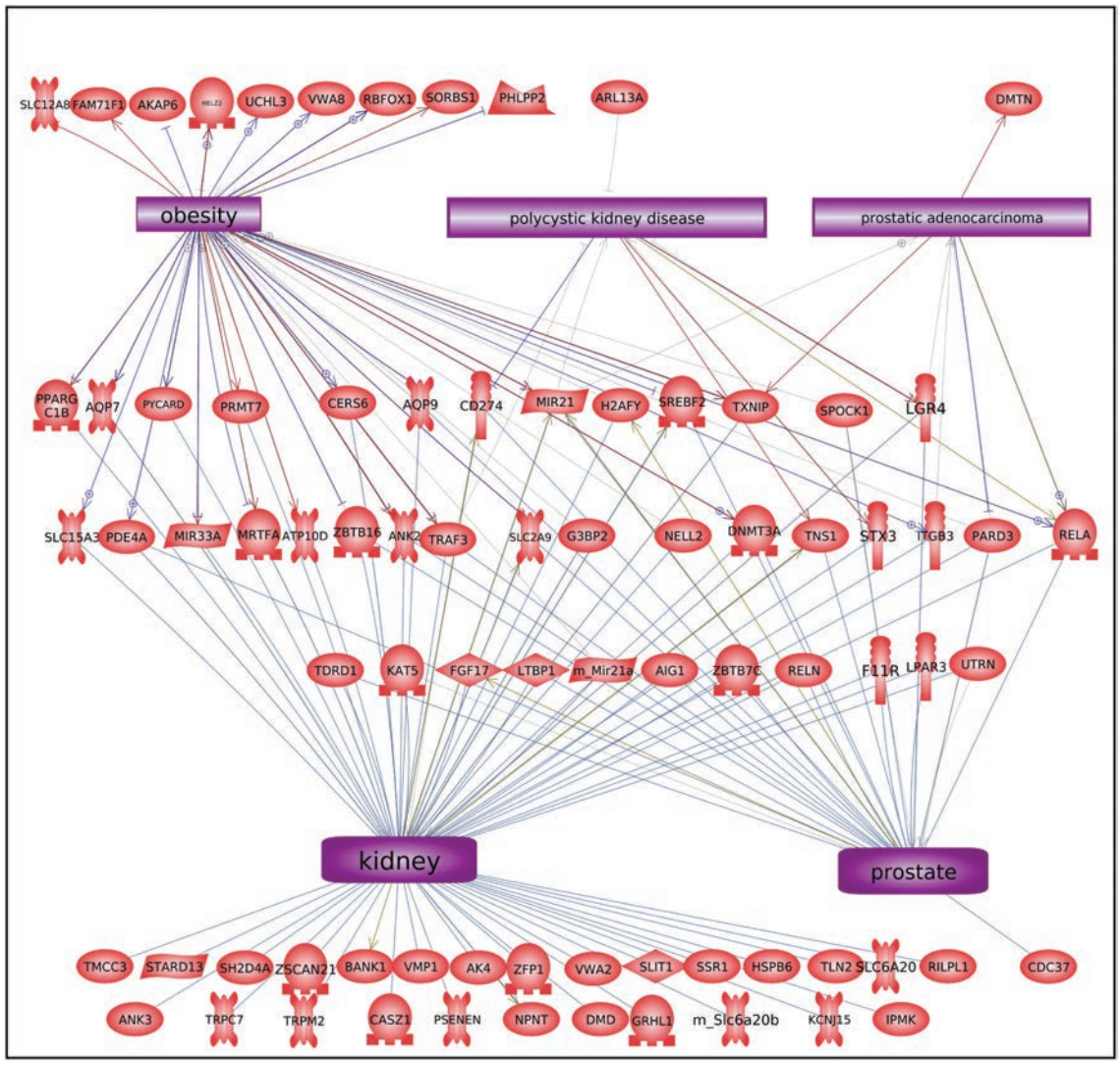

Figure 8. DMR-associated genes within the pathology biomarker DMR set for multiple disease pathology. The physiologic and pathology process is listed with direct gene links.

overlap was observed between the DMRs and DHRs at each of the edgeR statistical thresholds. Observations demonstrate the sperm DHRs also appear to provide potential epigenetic biomarkers for disease. The combination of DMRs and DHRs is anticipated to facilitate pathology diagnosis.

A limitation of the current study was the low numbers of animals with a specific individual disease. The edgeR analysis is optimal for the identification of individual DMR or DHR and used a high stringency threshold. Although an edgeR p-value was used to identify and analyse both the disease biomarker DMRs and DHRs [15–17,26], analysis for multiple testing error for false discovery rate (FDR) only provided a $p < 0.05$ for the exposure versus control comparison with a larger number of individuals. The FDR values for the disease biomarkers were >0.1. Previous studies have demonstrated limitation in FDR analysis with low sample numbers due to the presumptions in the multiple testing parameters [36–41]. Although several corrections for this limitation of FDR have been designed to correct FDR for low sample number limitations, we feel the edgeR value is more useful, due to its use in the identification of the individual epimutations. Therefore, the low sample number is a limitation in the current analysis. Potential higher variability in the data needs to be considered even though higher edgeR values were used, but this does not

address multiple testing corrections. Future studies will need to use higher n-values and/or improved analysis techniques to reduce this analysis limitation [36–41].

The presence of the glyphosate-induced transgenerational DMRs in sperm for specific pathologies suggests potential epigenetic biomarkers may be used to assess paternal transmission of disease susceptibility to the offspring. Such an epigenetic biomarker could potentially be used as a preconception diagnostic to determine the susceptibility of disease for the subsequent generations, but future studies are required to investigate this possibility. The knowledge that a disease susceptibility exists would allow potential preventative lifestyle change and therapeutics to be used and/or developed. Therefore, future generation health care could be transitioned to a preventative medicine strategy versus the reactionary medicine used today. The current study provides associated pathology with epigenetic biomarkers of both DMRs and DHRs. Further analysis is needed to determine the use of these biomarkers for early life disease susceptibility biomarkers, prior to the onset of diseases. The previous studies suggest this may be possible [-15–17], but formal preventative diagnostics have not been developed. Therefore, the current study used glyphosate induction of transgenerational disease as a proof of concept such environmental biomarkers can be identified and potentially used as diagnostics for disease susceptibility in the future. Since epigenetic biomarkers have a high frequency of association with individuals, the incorporation of epigenetic diagnostics into medicine is anticipated to facilitate preventative medicine and disease management.

Availability of Data and Materials

All molecular data have been deposited into the public database at NCBI (GEO # GSE118557 and GSE152678), and R code computational tools are available at GitHub (https://github.com/skinnerlab/MeDIP-seq) and www.skinner.wsu.edu.

Ethics approval

All experimental protocols for the procedures with rats were pre-approved by the Washington State University Animal Care and Use Committee (protocol IACUC # 2568), and all methods were performed in accordance with the relevant guidelines and regulations.

Consent for Publication

Not applicable.

Acknowledgments

We acknowledge Dr. Ingrid Sadler-Riggleman, Ms. Michelle Pappalardo, and Mr. Ryan Thompson for technical assistance. We acknowledge Ms. Amanda Quilty for editing and Ms. Heather Johnson for assistance in preparation of the manuscript. We thank the Genomics Core laboratory at WSU Spokane for sequencing data. This study was supported by John Templeton Foundation (50183 and 61174) (https://templeton.org/) grants to MKS and NIH (ES012974) (https://www.nih.gov/) grant to MKS. The funders had no role in study design, data collection and analysis, decision to publish, or preparation of the manuscript.

Author contributions

MBM Molecular analysis, data analysis, wrote and edited manuscript.

DB Bioinformatic analysis, data analysis, edited manuscript.

EN Animal studies, cell isolations, data analysis, edited manuscript.

DK Animal breeding and care, data analysis, edited manuscript.

MKS Conceived, oversight, obtained funding, data analysis, wrote and edited manuscript.

Disclosure of Interest

The authors report no conflict of interest.

ORCID

Eric E. Nilsson http://orcid.org/0000-0001-8894-4054

References

[1] Nilsson E, Sadler-Riggleman I, Skinner MK. Environmentally induced epigenetic transgenerational inheritance of disease. Environ Epigenet. 2018;4(2):1–13.

[2] Soubry A. Epigenetic inheritance and evolution: a paternal perspective on dietary influences. Prog Biophys Mol Biol. 2015;118(1–2):79–85.

[3] Vaiserman AM, Koliada AK, Jirtle RL. Non-genomic transmission of longevity between generations:

potential mechanisms and evidence across species. Epigenetics Chromatin. 2017;10(1):38.
[4] Legoff L, D'Cruz SC, Tevosian S, et al. Transgenerational inheritance of environmentally induced epigenetic alterations during mammalian development. Cells. 2019;8(12):1559.
[5] Waterland RA. Epigenetic mechanisms and gastrointestinal development. J Pediatr. 2006;149(5 Suppl): S137–42.
[6] Skinner MK, Guerrero-Bosagna C. Environmental signals and transgenerational epigenetics. Epigenomics. 2009;1(1):111–117.
[7] Skinner MK. What is an epigenetic transgenerational phenotype? F3 or F2. Reprod Toxicol. 2008;25(1):2–6.
[8] Skinner MK. Environmental epigenetic transgenerational inheritance and somatic epigenetic mitotic stability. Epigenetics. 2011;6(7):838–842.
[9] Anway MD, Cupp AS, Uzumcu M, et al. Epigenetic transgenerational actions of endocrine disruptors and male fertility. Science. 2005;308(5727):1466–1469.
[10] Klastrup LK, Bak ST, Nielsen AL. The influence of paternal diet on sncRNA-mediated epigenetic inheritance. Mol Genet Genomics. 2019;294(1):1–11.
[11] Gapp K, Jawaid A, Sarkies P, et al. Implication of sperm RNAs in transgenerational inheritance of the effects of early trauma in mice. Nat Neurosci. 2014;17 (5):667–669. .
[12] Ben Maamar M, Sadler-Riggleman I, Beck D, et al. Epigenetic transgenerational inheritance of altered sperm histone retention sites. Sci Rep. 2018;8(1):1–10.
[13] Ben Maamar M, Sadler-Riggleman I, Beck D, et al. Alterations in sperm DNA methylation, non-coding RNA expression, and histone retention mediate vinclozolin-induced epigenetic transgenerational inheritance of disease. Environ Epigenet. 2018;4(2): dvy010. .
[14] Skinner MK, Ben Maamar M, Sadler-Riggleman I, et al. Alterations in sperm DNA methylation, non-coding RNA and histone retention associate with DDT-induced epigenetic transgenerational inheritance of disease. Epigenetics Chromatin. 2018;11(1):1–24. .
[15] McBirney M, King SE, Pappalardo M, et al. Atrazine induced epigenetic transgenerational inheritance of disease, lean phenotype and sperm epimutation pathology biomarkers. PloS One. 2017;12(9):e0184306. .
[16] King SE, McBirney M, Beck D, et al. Sperm epimutation biomarkers of obesity and pathologies following DDT induced epigenetic transgenerational inheritance of disease. Environ Epigenet. 2019;5(2):dvz008.
[17] Nilsson E, King SE, McBirney M, et al. Vinclozolin induced epigenetic transgenerational inheritance of pathologies and sperm epimutation biomarkers for specific diseases. PloS One. 2018;13(8):e0202662. .
[18] Benbrook CM. Trends in glyphosate herbicide use in the United States and globally. Environ Sci Eur. 2016;28(1):3.
[19] Myers JP, Antoniou MN, Blumberg B, et al. Concerns over use of glyphosate-based herbicides and risks associated with exposures: a consensus statement. Environ Health. 2016;15:19.
[20] Davoren MJ, Schiestl RH. Glyphosate-based herbicides and cancer risk: a post-IARC decision review of potential mechanisms, policy and avenues of research. Carcinogenesis. 2018;39(10):1207–1215.
[21] ATSDR. Toxicological profile for glyphosate. U.S. Department of Health and Human Services, Public Health Service, Agency for Toxic Substances and Disease Registry. ATSDR.; 2019.
[22] Mesnage R, Defarge N, Spiroux de Vendomois J, et al. Potential toxic effects of glyphosate and its commercial formulations below regulatory limits. Food Chem Toxicol. 2015;84:133–153.
[23] Kubsad D, Nilsson EE, King SE, et al. Assessment of glyphosate induced epigenetic transgenerational inheritance of pathologies and sperm epimutations: generational toxicology. Sci Rep. 2019;9(1):6372.
[24] Mertens M, Hoss S, Neumann G, et al. Glyphosate, a chelating agent-relevant for ecological risk assessment? Environ Sci Pollut Res Int. 2018;25(6):5298–5317.
[25] Van Bruggen AHC, He MM, Shin K, et al. Environmental and health effects of the herbicide glyphosate. Sci Total Environ. 2018;616–617:255–268.
[26] Stouder C, Paoloni-Giacobino A. Transgenerational effects of the endocrine disruptor vinclozolin on the methylation pattern of imprinted genes in the mouse sperm. Reproduction. 2010;139(2):373–379.
[27] Guerrero-Bosagna C, Covert T, Haque MM, et al. Epigenetic transgenerational inheritance of vinclozolin induced mouse adult onset disease and associated sperm epigenome biomarkers. Reprod Toxicol. 2012;34(4):694–707. .
[28] Euorpean Food Safety Authority E. Conclusion on the peer review of the pesticide risk assessment of the active substance glyphosate. Efsa J. 2015;13(11):4302.
[29] Guerrero-Bosagna C, Settles M, Lucker B, et al. Epigenetic transgenerational actions of vinclozolin on promoter regions of the sperm epigenome. PloS One. 2010;5(9):e13100.
[30] Skinner MK, Guerrero-Bosagna C. Role of CpG deserts in the epigenetic transgenerational inheritance of differential DNA methylation regions. BMC Genomics. 2014;15(1):692.
[31] Minneci F, Piovesan D, Cozzetto D, et al. FFPred 2.0: improved homology-independent prediction of gene ontology terms for eukaryotic protein sequences. PloS One. 2013;8(5):e63754.
[32] Ben Maamar M, King SE, Nilsson E, et al. Epigenetic transgenerational inheritance of parent-of-origin allelic transmission of outcross pathology and sperm epimutations. Dev Biol. 2020;458(1):106–119.
[33] Rawla P. Epidemiology of prostate cancer. World J Oncol. 2019;10(2):63–89.

[34] Hales CM, Carroll MD, Fryar CD, et al. Prevalence of obesity among adults and youth: United States, 2015–2016. Hyattsville, MD: National Center for Health Statistics; 2017.
[35] Rathke C, Baarends WM, Awe S, et al. Chromatin dynamics during spermiogenesis. Biochim Biophys Acta. 2014;1839(3):155–168.
[36] Devlin B, Roeder K, Wasserman L. Analysis of multilocus models of association. Genet Epidemiol. 2003;25(1):36–47.
[37] Higdon R, van Belle G, Kolker E. A note on the false discovery rate and inconsistent comparisons between experiments. Bioinformatics. 2008;24(10):1225–1228.
[38] Yang H, Churchill G. Estimating p-values in small microarray experiments. Bioinformatics. 2007;23 (1):38–43.
[39] Bretz F, Landgrebe J, Brunner E. Multiplicity issues in microarray experiments. Methods Inf Med. 2005;44 (3):431–437.
[40] Jung SH. Sample size and power calculation for molecular biology studies. Methods Mol Biol. 2010;620:203–218.
[41] Nilsson R, Bjorkegren J, Tegner J. On reliable discovery of molecular signatures. BMC Bioinformatics. 2009;10:38.

Epigenetics & Chromatin

RESEARCH Open Access

Integration of sperm ncRNA-directed DNA methylation and DNA methylation-directed histone retention in epigenetic transgenerational inheritance

Daniel Beck, Millissia Ben Maamar and Michael K. Skinner*

Abstract

Background: Environmentally induced epigenetic transgenerational inheritance of pathology and phenotypic variation has been demonstrated in all organisms investigated from plants to humans. This non-genetic form of inheritance is mediated through epigenetic alterations in the sperm and/or egg to subsequent generations. Although the combined regulation of differential DNA methylated regions (DMR), non-coding RNA (ncRNA), and differential histone retention (DHR) have been shown to occur, the integration of these different epigenetic processes remains to be elucidated. The current study was designed to examine the integration of the different epigenetic processes.

Results: A rat model of transiently exposed F0 generation gestating females to the agricultural fungicide vinclozolin or pesticide DDT (dichloro-diphenyl-trichloroethane) was used to acquire the sperm from adult males in the subsequent F1 generation offspring, F2 generation grand offspring, and F3 generation great-grand offspring. The F1 generation sperm ncRNA had substantial overlap with the F1, F2 and F3 generation DMRs, suggesting a potential role for RNA-directed DNA methylation. The DMRs also had significant overlap with the DHRs, suggesting potential DNA methylation-directed histone retention. In addition, a high percentage of DMRs induced in the F1 generation sperm were maintained in subsequent generations.

Conclusions: Many of the DMRs, ncRNA, and DHRs were colocalized to the same chromosomal location regions. Observations suggest an integration of DMRs, ncRNA, and DHRs in part involve RNA-directed DNA methylation and DNA methylation-directed histone retention in epigenetic transgenerational inheritance.

Keywords: Epigenetics, ncRNA, DNA methylation, Histone, Transgenerational, Sperm, Non-genetic inheritance, Review

Background

Over the past two decades numerous studies have demonstrated a non-genetic form of inheritance termed epigenetic transgenerational inheritance that is mediated by germline alterations in epigenetic processes [1–3]. One of the first observations involved the environmental agricultural toxicant vinclozolin, which is one of the most commonly used agricultural fungicides, to induce the epigenetic transgenerational inheritance of testis pathology and DNA methylation alterations [1]. Similar observations with a wide variety of environmental toxicants, from dioxin to DDT (dichloro-diphenyl-trichloroethane), have identified similar epigenetic inheritance impacts on a variety of different disease conditions [3–5]. The transgenerational phenotypic manifestations of vinclozolin and DDT include the induction of testis, prostate,

*Correspondence: skinner@wsu.edu
Center for Reproductive Biology, School of Biological Sciences, Washington State University, Pullman, WA 99164-4236, USA

kidney, and ovary pathology, as well as obesity [3]. An early observation in mice identified a traumatic stress-induced impact on the epigenetic transgenerational inheritance of behavioral abnormalities [6, 7]. Interestingly, the injection of eggs with the ncRNA from stressed individual male sperm promoted the same transgenerational phenotypes [6]. Subsequent studies have supported a role of either DNA methylation or ncRNA in the germline-mediated epigenetic transgenerational inheritance [3, 8]. This epigenetic transgenerational inheritance phenomenon has been shown to be induced by environmental chemicals, nutrition, stress and trauma abnormalities in rodents and humans [3, 7, 9], as well as a wide variety of environmental stresses in plants [10, 11], insects [12, 13], worms [14], fish [15–17], birds [18, 19], and a variety of mammals such as pigs and humans [20–22]. A number of physiological impacts have been observed including pathologies in the brain, reproductive organs, kidney, immunity, obesity, and infertility [1–3]. The environmentally induced epigenetic transgenerational inheritance phenomenon has been well established, and has significant impacts on disease etiology [2, 3] and other areas of biology such as evolution [23].

Although most previous investigations have focused on an individual epigenetic process such as DNA methylation [3, 4, 10] or ncRNA [6, 8], few have examined multiple processes. Our previous studies demonstrated in both vinclozolin and DDT-induced epigenetic transgenerational inheritance of pathology that the transgenerational F3 generation sperm had coordinately altered differential DNA methylation regions (DMRs), expression of non-coding RNAs (ncRNAs), differential histone retention sites (DHRs), and histone modifications [24, 25]. These observations suggest potential interactions between the different epigenetic processes, but this remains to be elucidated during the epigenetic inheritance phenomenon. Previous studies have demonstrated a role for ncRNA in RNA-directed DNA methylation in a number of different systems [26–28]. The ncRNA can help localize the DNA methylation site and facilitate subsequent chromatin remodeling processes. Therefore, the integration of ncRNA and DNA methylation has been established. Histone modifications can also be modified dramatically by ncRNA and chromatin remodeling in order to transition from euchromatin-active gene expression sites to heterochromatin-inactive sites of DNA [29]. Although information is available on histone retention in sperm and its impacts on the embryo [30, 31], the potential role of different epigenetic processes in histone retention has not been reported. Recently, a role for environmental exposures (e.g., vinclozolin and DDT) to promote transgenerational epigenetic inheritance of sperm histone retention has been observed [24, 25, 32]. The current study investigates the potential integration of DNA methylation, ncRNA, and histone alterations in the epigenetic transgenerational inheritance phenomenon.

Previous analyses of the concurrent expression of the epigenetic processes between the F1, F2, and F3 generations with a stringent statistical threshold have demonstrated negligible overlap between the different generations or between the epigenetic processes [24, 25]. The current study used an extended overlap analysis with a less stringent statistical threshold and found overlaps between the generations and epigenetic marks. The potential integration of the different epigenetic processes and generational conservation was identified.

Results

The experimental design involved F0 generation gestating outbred Sprague Dawley female rats at 120 days of age being exposed during embryonic days 8–14 (E8–E14) transiently to vinclozolin (100 mg/kg body weight/day), or DDT (25 mg/kg body weight/day), or vehicle dimethyl sulfoxide (DMSO) control, as previously described [24, 25]. The F1 generation offspring were obtained and aged to 90 days of age then bred within the lineage (control, vinclozolin, or DDT) in order to generate the F2 generation grand offspring. Afterward, the F2 generation was similarly bred to generate the transgenerational F3 generation great-grand offspring within the lineage. At each generation or lineage no sibling or cousin breeding was used to avoid any inbreeding artifacts [1, 3]. Litter bias was avoided by culling litters to 10 (approximately 5 females and 5 males), and then only one or two males and females from each litter being used for breeding within the lineage, as previously described. All males were aged to 120 days and sacrificed for sperm collection for molecular analysis, as described for previous reported studies [24, 25]. The number of individual animals investigated at each generation for sperm collection and molecular analysis was approximately 10–17 males, so $n = 10–17$ for animals with three different pools of 4–6 animals for each generation and epimutation analysis. The sperm collected were used to isolate RNA, DNA, and chromatin for analysis of ncRNA, DNA methylation, histone retention, and histone modification, as described in previous studies [24, 25], (Fig. 1). The molecular data from these previous studies (GEO # GSE109775, GSE106125, and NCIB SRA: PRJNA430483 largeRNA (control and DTT), PRJNA430740 smallRNA) were analyzed to explore data further bioinformatically.

The sperm DMRs, ncRNA (both small sncRNA and large lncRNA), and DHRs were analyzed in each sample, as previously described [24, 25], for the vinclozolin and DDT F1, F2 and F3 generation sperm samples. The numbers and overlaps of DMRs, ncRNA, and DHRs for

(See figure on next page.)

Fig. 1 Generational epimutation overlap at high stringent statistical threshold. **a** F1 generation vinclozolin lineage DMR ($p < 1e{-}06$), DHR ($p < 1e{-}06$), and ncRNA ($p < 1e{-}04$). **b** F1 generation DDT lineage DMR ($p < 1e{-}06$), DHR ($p < 1e{-}06$), and ncRNA ($p < 1e{-}04$). **c** F2 generation vinclozolin lineage DMR ($p < 1e{-}06$), DHR ($p < 1e{-}06$), and ncRNA ($p < 1e{-}04$). **d** F2 generation DDT lineage DMR ($p < 1e{-}06$), DHR ($p < 1e{-}06$), and ncRNA ($p < 1e{-}04$). **e** F3 generation vinclozolin lineage DMR ($p < 1e{-}06$), DHR ($p < 1e{-}06$), and ncRNA ($p < 1e{-}04$). **f** F3 generation DDT lineage DMR ($p < 1e{-}06$), DHR ($p < 1e{-}06$), and ncRNA ($p < 1e{-}04$)

each generation with a high stringency threshold are presented as previously reported in (Fig. 1). The overlaps with a Venn diagram for the transgenerational F3 generation for the different epigenetic marks is negligible with the high stringency threshold, (Fig. 1e, f), for each exposure, as previously identified [24, 25]. The F1 and F2 generations also were primarily distinct among the epimutations, (Fig. 1a–d). Although the different epigenetic alterations are present at each generation for both exposure lineages, the overlaps with a stringent statistical threshold were negligible, suggesting distinct functions and a lack of integration, as previously suggested [24, 25].

Interestingly, when a comparison of one epimutation at a high stringency was made to the others at $p < 0.05$, a number of genomic locations were identified with the different types of epimutations present. The chromosomal locations of these altered epigenetic marks (i.e., epimutations) are presented in (Fig. 2) and in (Additional file 1: Tables S1–S6) for each generation for both vinclozolin and DDT lineage sperm samples. The color-coded labels identify the DMR, ncRNA, and DHRs throughout the genomes with common chromosomal locations for each generation. Only those sites significant at high stringency (color code index) with one epimutation analysis that overlap with the other epimutations at $p < 0.05$ are shown, (Fig. 2). Specific epimutation chromosomal locations, statistical p-values, and gene associations are presented in (Additional file 1: Tables S1–S6). In the F1 and F2 generations only the alterations in ncRNAs and DMRs were found, as previously described [24, 25]. Therefore, the overlaps were primarily between the ncRNA and DMR in the F1 and F2 generations, (Fig. 2a–d). The DHRs developed in the transgenerational F3 generation, as previously described [24, 25]. In the F1 and F2 generations the ncRNA was predominantly the high statistically significant epimutation and overlap with DMR at the $p < 0.05$, (Fig. 2a–c), with a mix of ncRNA and DMR in the DDT lineage F2 generation, (Fig. 2d). The transgenerational F3 generation also had a mix of ncRNA and DMR at a high statistical significance, as well as a number of DHR, (Fig. 2e, f). Therefore, chromosomal locations with multiple epimutations are identified with ncRNA being predominant in the F1 and F2 generations with the high statistical threshold, and DMRs being more predominant in the F3 generation with a mix of the various epimutations, (Fig. 2 and Additional file 1: Tables S1–S6).

An extended overlap analysis was performed with both the DDT and vinclozolin lineage data using a less stringent statistical threshold for the comparisons, (Fig. 3). The more stringent statistical threshold epigenetic data sets (DMRs $p < 1e{-}06$, ncRNA $p < 1e{-}04$, and DHRs $p < 1e{-}06$) were compared between the generations and the epigenetic marks with a $p < 0.05$ statistical threshold. This optimized the potential to identify overlaps compared to the more stringent thresholds used in (Fig. 1). The rows present the more stringent threshold DMRs, ncRNA, and DHRs for the F1, F2, and F3 generations. The columns present the corresponding $p < 0.05$ threshold overlaps with the higher p-value threshold data sets. Examination of the horizontal rows, as expected, show 100% overlap (i.e., shaded) for the same data set and the number of associated epigenetic marks and percentage (%) overlap with the left margin value. This extended overlap allows the two different threshold stringencies to be compared and to determine additional overlap observations, (Fig. 3). Similar trends in the overlaps are observed for both the DDT and vinclozolin data sets. One of the initial observations was that the F1 generation ncRNA had a high percentage overlap with the F3 generation DMR, (Fig. 3 and Additional file 1: Tables S1 and S2). Similar observations are made with the F1 and F2 generations. For the F1 generation, DDT ncRNA had over a 20% overlap observed with the F1, F2, and F3 generation DMRs, while vinclozolin F1 generation ncRNA had approximately 35% overlap with the F1, F2, and F3 generation DMRs, (Figs. 3 and 4a, b). The lists of overlapping ncRNA and DMR sites are presented in (Additional file 1: Tables S1 and S2). The F2 and F3 generation ncRNA were similar with the overlap with the DDT generation DMRs of approximately 20%, but reduced to 10–15% with the vinclozolin DMRs, (Fig. 3). Therefore, some ncRNAs were common between the generations, and had overlap with the DMRs that ranged between 8–35% overlap for the vinclozolin DMRs and 15–20% overlap for DDT DMRs. The potential that the ncRNA may promote RNA-directed DNA methylation is suggested. The Venn diagrams presented in (Fig. 4a, b) support those overlaps and the epigenetic ncRNA and DMR overlaps are listed in (Additional file 1: Tables S1 and S2).

The next observation was that the F1, F2, and F3 generation DMRs had a 20–48% overlap with the F3 generation DHRs for the DDT and vinclozolin lineages, (Fig. 3).

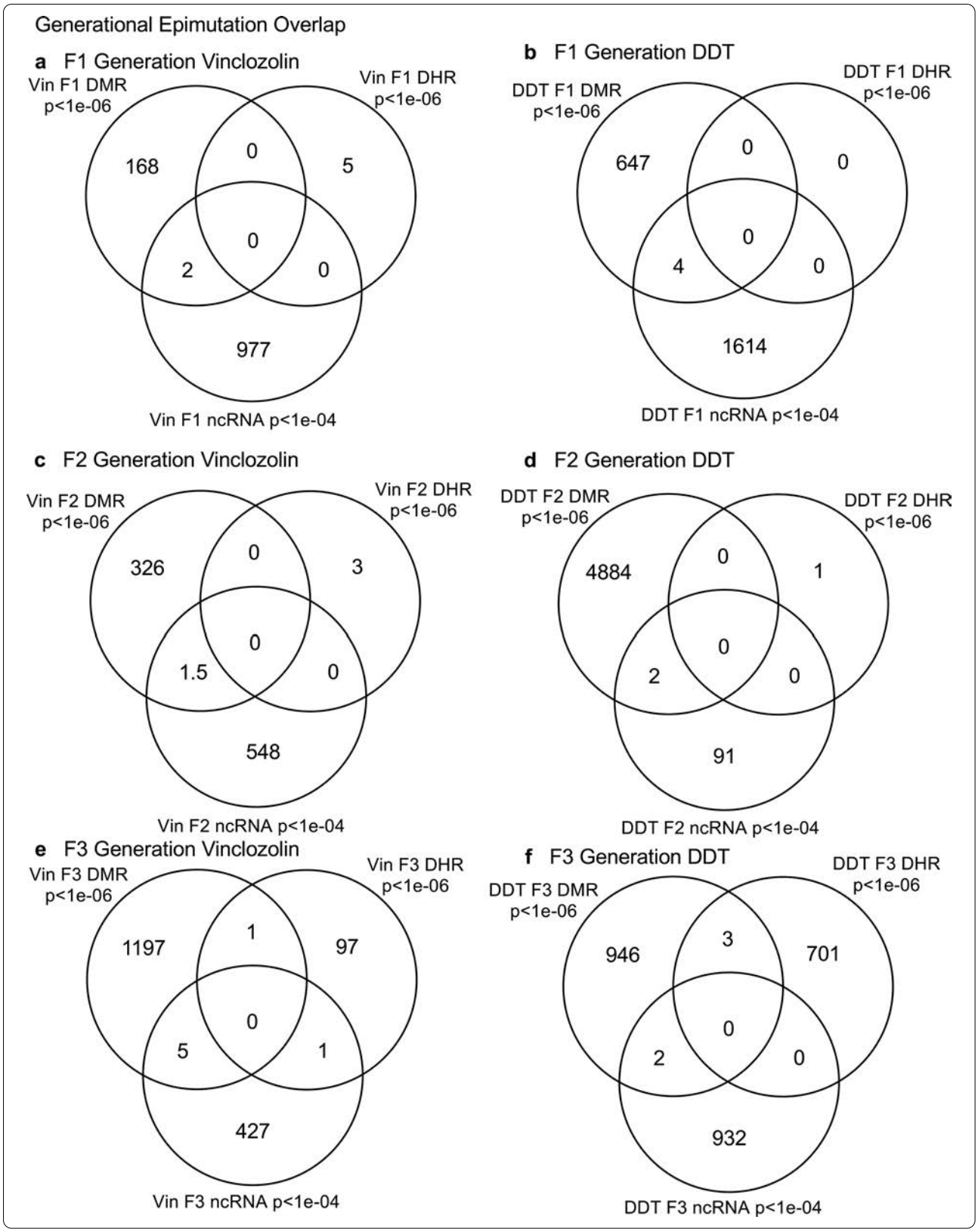
Generational Epimutation Overlap
a F1 Generation Vinclozolin
Vin F1 DMR p<1e-06
Vin F1 DHR p<1e-06
Vin F1 ncRNA p<1e-04
168
0
5
0
2
0
977
b F1 Generation DDT
DDT F1 DMR p<1e-06
DDT F1 DHR p<1e-06
DDT F1 ncRNA p<1e-04
647
0
0
0
4
0
1614
c F2 Generation Vinclozolin
Vin F2 DMR p<1e-06
Vin F2 DHR p<1e-06
Vin F2 ncRNA p<1e-04
326
0
3
0
1.5
0
548
d F2 Generation DDT
DDT F2 DMR p<1e-06
DDT F2 DHR p<1e-06
DDT F2 ncRNA p<1e-04
4884
0
1
0
2
0
91
e F3 Generation Vinclozolin
Vin F3 DMR p<1e-06
Vin F3 DHR p<1e-06
Vin F3 ncRNA p<1e-04
1197
1
97
0
5
1
427
f F3 Generation DDT
DDT F3 DMR p<1e-06
DDT F3 DHR p<1e-06
DDT F3 ncRNA p<1e-04
946
3
701
0
2
0
932

(See figure on next page.)

Fig. 2 Chromosomal colocalization of overlap epimutations. The overlap of one epimutation at high statistical stringency (DMR $p < 1e{-}06$, DHR $p < 1e{-}06$, or ncRNA $p < 1e{-}04$) overlap with others at $p < 0.05$. The epimutation at high stringency is identified with color and marked as indicated by the inset legend. The chromosomal number and size (megabase) are presented. **a** F1 generation vinclozolin lineage ncRNA and DMR. **b** F1 generation DDT lineage ncRNA and DMR. **c** F2 generation vinclozolin lineage ncRNA and DMR. **d** F2 generation DDT lineage ncRNA and DMR. **e** F3 generation vinclozolin lineage DMR, DHR and ncRNA. **f** F3 generation DDT lineage DMR, DHR and ncRNA

Interestingly, the F3 generation DHRs had a 23–47% overlap with the F1, F2, and F3 generation DMRs for both exposure lineages. The Venn diagram overlaps in (Fig. 4c, d) support these DMR and DHR overlaps and suggests DMRs may help guide DHR formation transgenerationally. The overlapping F3 generation DMRs and DHRs are presented in (Additional file 1: Tables S3 and S4).

An interesting observation was the overlap between the F1, F2, and F3 generation DMRs for both DDT and vinclozolin exposures, (Figs. 3 and 4e, f). The highest overlap for the DDT F1 generation DMRs was the F2 generation DMRs with a 71% overlap, and for the vinclozolin F2 generation DMRs with the F3 generation DMRs with a 73% overlap. The highest for the F3 generation DMRs was 79% overlap with the vinclozolin F2 DMRs. Generally, a 25–50% overlap existed between the F1, F2, and F3 generation DMRs for both exposures, (Fig. 3). A Venn diagram supports this observation and demonstrates approximately 25% overlap for the vinclozolin DMRs and 35% overlap for the DDT DMRs, (Fig. 4e, f). Lists of these overlapping DMRs are presented in (Additional file 1: Tables S5 and S6). Therefore, a percentage (25–35%) of the F1 generation individual DMRs were retained transgenerationally.

Generally, the F3 generation epigenetic alterations had more overlap among each other and with the other generations for both exposures. A Venn diagram analysis was used to identify the epigenetic sites with overlapping DMRs, ncRNA, and DHRs, (Fig. 4). The overlapping F3 generation epigenetic sites were approximately 25% for vinclozolin and DDT lineages. A permutation analysis was performed to demonstrate this is significantly greater than the random overlap observed, with a p value of $p \leq 0.05$ for both 1 kb and 10 kb overlapping sites. Several sites were randomly selected and are mapped to identify the overlapping chromosomal locations of the DMR, ncRNA, and DHR, (Fig. 5). The actual statistical significance of the overlapping epimutations in these examples includes: (Fig. 5a) (ncRNA $p < 1e{-}04$, DHR $p < 0.03$, and DMR $p < 0.005$); (Fig. 5b) (ncRNA $p < 1e{-}04$, DHR $p < 0.001$, and DMR $p < 0.0004$); (Fig. 5c) (DHR $p < 1e{-}08$, ncRNA $p < 0.005$, and DMR $p < 0.04$); and (Fig. 5d) (ncRNA $p < 1e{-}06$, DMR $p < 1e{-}04$, and DHR $p < 1e{-}05$). The potential that RNA-directed DNA methylation and DMR-directed histone retention is involved is reviewed in the "Discussion" section.

All the previous analyses and overlaps presented were based on a direct overlapping chromosomal location for the ncRNA, DMR and DHR. The question was addressed if a greater number of sites exist with epimutations that were in the same region but not directly overlapped. A 5 kb distance on either side of the epimutations was used to have a 10 kb window for the potential overlapping region. An extended overlap using this 10 kb window was used with the same data that will identify sites that directly overlap and those nearby within the 10 kb window, Fig. 6. The level of overlap with a 10 kb window identified the same overlaps presented and discussed, but the level of overlap was in the 80–99% range, (Fig. 6). Both the vinclozolin and DDT lineage had the same high level of overlap with most being > 90% range, with a permutation analysis p value of $p < 0.001$. Using this 10 kb window the majority of ncRNA, DMRs and DHRs overlapped between the generations and epimutations. This supported all the previous observations and demonstrated a significant level of epimutation overlap. Since approximately 90% of the F3 generation DMRs overlapped with the F3 generation DHRs and F1 generation ncRNA, the conserved F3 generation DMRs, (Additional file 1: Table S5 and S6), were used in a Pathway Studio analysis to link DMR associated genes with cellular processes and pathologies, (Additional file 1: S1 and S2). A large number of the DMR and epimutation associated genes linked to various transgenerational pathologies previously observed, including kidney disease, mammary tumors, immune abnormalities, prostate disease, metabolic disease, or behavioral abnormalities [3, 33, 34].

Discussion

Previous studies have demonstrated the concurrent presence of DMRs, ncRNA, and DHRs in sperm following DDT or vinclozolin exposure of F0 generation gestating females during gonadal sex determination [24, 25]. These data were obtained and reported at a stringent statistical threshold selection and demonstrated negligible overlap at each generation, (Fig. 1) [24, 25]. The current study was designed to further investigate the potential integration of the different epigenetic processes between the F1, F2, and F3 generations. An approach was taken to compare the more stringent statistical threshold values for DMRs, ncRNAs, and DHRs with the less stringent $p < 0.05$ threshold between the different epigenetic processes

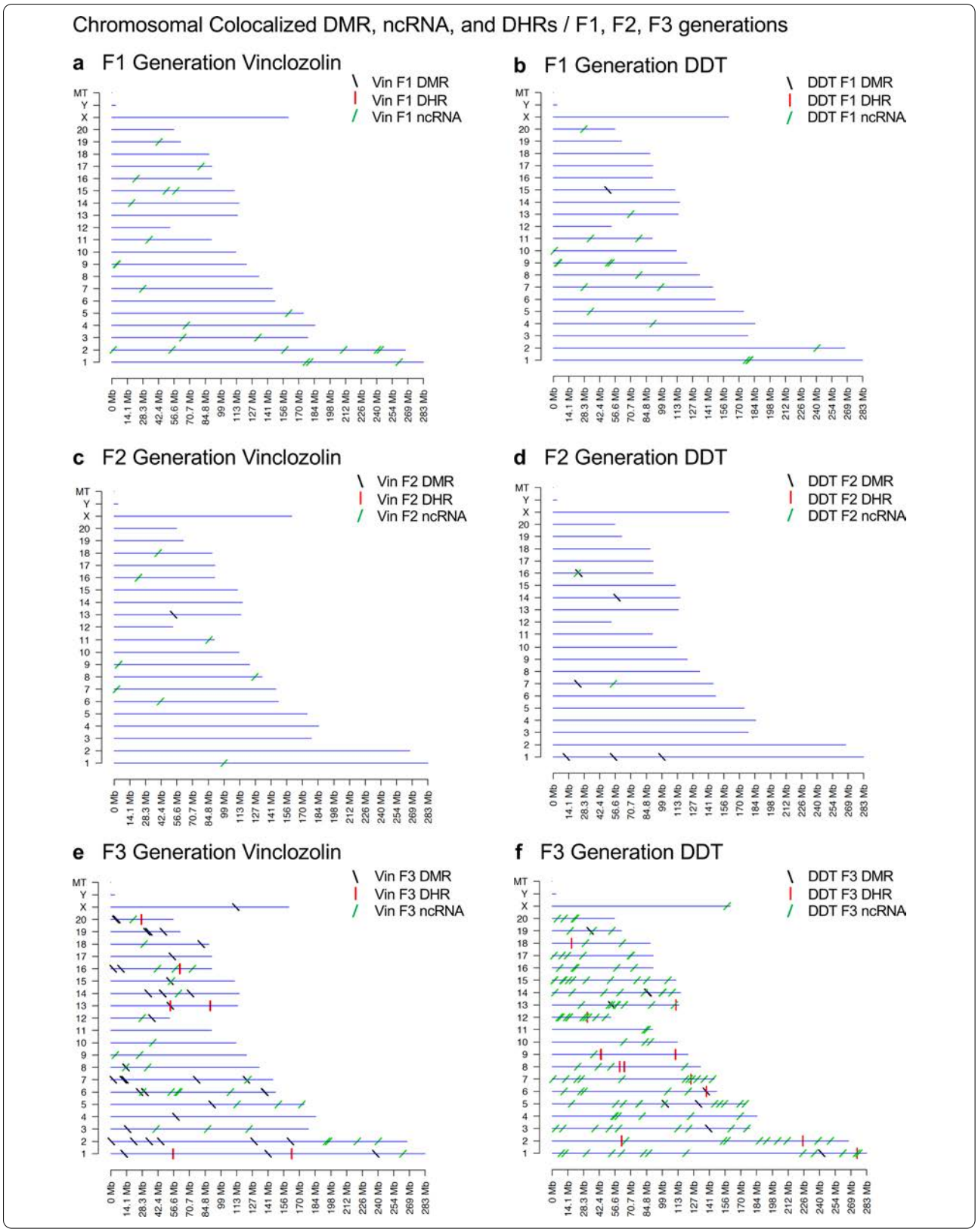
Chromosomal Colocalized DMR, ncRNA, and DHRs / F1, F2, F3 generations
a F1 Generation Vinclozolin
Vin F1 DMR
Vin F1 DHR
Vin F1 ncRNA
b F1 Generation DDT
DDT F1 DMR
DDT F1 DHR
DDT F1 ncRNA
c F2 Generation Vinclozolin
Vin F2 DMR
Vin F2 DHR
Vin F2 ncRNA
d F2 Generation DDT
DDT F2 DMR
DDT F2 DHR
DDT F2 ncRNA
e F3 Generation Vinclozolin
Vin F3 DMR
Vin F3 DHR
Vin F3 ncRNA
f F3 Generation DDT
DDT F3 DMR
DDT F3 DHR
DDT F3 ncRNA
MT Y X 20 19 18 17 16 15 14 13 12 11 10 9 8 7 6 5 4 3 2 1
0 Mb 14.1 Mb 28.3 Mb 42.4 Mb 56.6 Mb 70.7 Mb 84.8 Mb 99 Mb 113 Mb 127 Mb 141 Mb 156 Mb 170 Mb 184 Mb 198 Mb 212 Mb 226 Mb 240 Mb 254 Mb 269 Mb 283 Mb

Extended Epimutation Overlap

a Vinclozolin Epimutations

p>.05 / p<1e-5	F1.DMR	F1.DHR	F1.ncRNA	F2.DMR	F2.DHR	F2.ncRNA	F3.DMR	F3.DHR	F3.ncRNA
F1.DMR	170 (100.00%)	1 (0.59%)	10 (5.88%)	63 (37.06%)	4 (2.35%)	2 (1.18%)	80 (47.06%)	34 (20.00%)	6 (3.53%)
F1.DHR	2 (40.00%)	5 (100.00%)	0 (0.00%)	3 (60.00%)	2 (40.00%)	0 (0.00%)	1 (20.00%)	1 (20.00%)	0 (0.00%)
F1.ncRNA	326 (33.30%)	27 (2.76%)	979 (100.00%)	352 (35.96%)	26 (2.66%)	94 (9.60%)	362 (36.98%)	378 (38.61%)	52 (5.31%)
F2.DMR	155 (47.40%)	31 (9.48%)	14 (4.28%)	327 (100.00%)	21 (6.42%)	7 (2.14%)	241 (73.70%)	118 (36.09%)	15 (4.59%)
F2.DHR	1 (33.33%)	1 (33.33%)	0 (0.00%)	1 (33.33%)	3 (100.00%)	0 (0.00%)	1 (33.33%)	0 (0.00%)	0 (0.00%)
F2.ncRNA	47 (8.55%)	18 (3.27%)	42 (7.64%)	68 (12.36%)	15 (2.73%)	549 (99.82%)	67 (12.18%)	71 (12.91%)	35 (6.36%)
F3.DMR	576 (47.88%)	57 (4.74%)	116 (9.64%)	950 (78.97%)	57 (4.74%)	27 (2.24%)	1203 (100.00%)	359 (29.84%)	64 (5.32%)
F3.DHR	23 (23.23%)	22 (22.22%)	8 (8.08%)	34 (34.34%)	17 (17.17%)	4 (4.04%)	41 (41.41%)	99 (100.00%)	10 (10.10%)
F3.ncRNA	61 (14.06%)	6 (1.38%)	38 (8.76%)	78 (17.97%)	10 (2.30%)	26 (5.99%)	81 (18.66%)	73 (16.82%)	434 (100.00%)

b DDT Epimutations

p>.05 / p<1e-5	F1.DMR	F1.DHR	F1.ncRNA	F2.DMR	F2.DHR	F2.ncRNA	F3.DMR	F3.DHR	F3.ncRNA
F1.DMR	651 (100.0%)	48 (7.4%)	43 (6.6%)	463 (71.1%)	37 (5.7%)	14 (2.2%)	332 (51.0%)	315 (48.4%)	51 (7.8%)
F1.DHR	0 (0.0%)	0 (100.0%)	0 (0.0%)	0 (0.0%)	0 (0.0%)	0 (0.0%)	0 (0.0%)	0 (0.0%)	0 (0.0%)
F1.ncRNA	365 (22.6%)	27 (1.7%)	1614 (99.8%)	432 (26.7%)	22 (1.4%)	76 (4.7%)	344 (21.3%)	608 (37.6%)	97 (6.0%)
F2.DMR	3719 (76.1%)	229 (4.7%)	278 (5.7%)	4886 (100.0%)	208 (4.3%)	91 (1.9%)	2790 (57.1%)	2041 (41.8%)	266 (5.4%)
F2.DHR	0 (0.0%)	0 (0.0%)	0 (0.0%)	0 (0.0%)	1 (100.0%)	0 (0.0%)	0 (0.0%)	0 (0.0%)	0 (0.0%)
F2.ncRNA	22 (23.4%)	4 (4.3%)	14 (14.9%)	26 (27.7%)	2 (2.1%)	94 (100.0%)	19 (20.2%)	39 (41.5%)	17 (18.1%)
F3.DMR	256 (26.9%)	25 (2.6%)	37 (3.9%)	351 (36.9%)	27 (2.8%)	18 (1.9%)	951 (100.0%)	213 (22.4%)	30 (3.2%)
F3.DHR	334 (47.4%)	22 (3.1%)	38 (5.4%)	319 (45.3%)	17 (2.4%)	11 (1.6%)	240 (34.1%)	704 (100.0%)	36 (5.1%)
F3.ncRNA	243 (26.0%)	28 (3.0%)	135 (14.5%)	335 (35.9%)	18 (1.9%)	127 (13.6%)	199 (21.3%)	338 (36.2%)	928 (99.4%)

Fig. 3 Extended epimutation overlap. The epimutations at high stringency (DMR $p < 1e{-}06$, DHR $p < 1e{-}06$, and ncRNA $p < 1e{-}04$) in rows were compared to epimutations at $p < 0.05$ in columns. The number of overlap epimutations and percentage of the total are presented for each overlap. As anticipated, 100% overlap was observed for the same generation and epimutation indicated by shaded box. **a** Vinclozolin lineage epimutation and **b** DDT lineage epimutation overlap

(See figure on next page.)

Fig. 4 Epimutation overlaps. Generational DMR overlap with F1 generation ncRNA $p < 0.05$. A Venn diagram overlap of F1, F2, and F3 generation DMR ($p < 1e{-}06$) with F1 generation ncRNA ($p < 0.05$). **a** Vinclozolin lineage DMR and ncRNA overlap. **b** DDT lineage DMR and ncRNA overlap. Generational DMR overlap with F3 generation DHR $p < 0.05$. A Venn diagram overlap of F1, F2, and F3 generation DMR ($p < 1e{-}06$) with F3 generation DHR ($p < 0.05$). **c** Vinclozolin lineage DMR and DHR overlap. **d** DDT lineage DMR and DHR overlap. Generational DMR overlap. A Venn diagram overlap of F1 generation DMR ($p < 1e{-}06$) with F2 and F3 generation DMR ($p < 0.05$). **e** Vinclozolin lineage DMR overlap. **f** DDT lineage DMR overlap

and generations. This extended overlap approach generated a number of observations to suggest an integration between generations for the epigenetic transgenerational inheritance phenomenon.

An interesting observation from the extended overlap of DMRs demonstrated that approximately 40–50% of the F1 generation sperm DMRs were retained and also present in the F2 and transgenerational F3 generations,

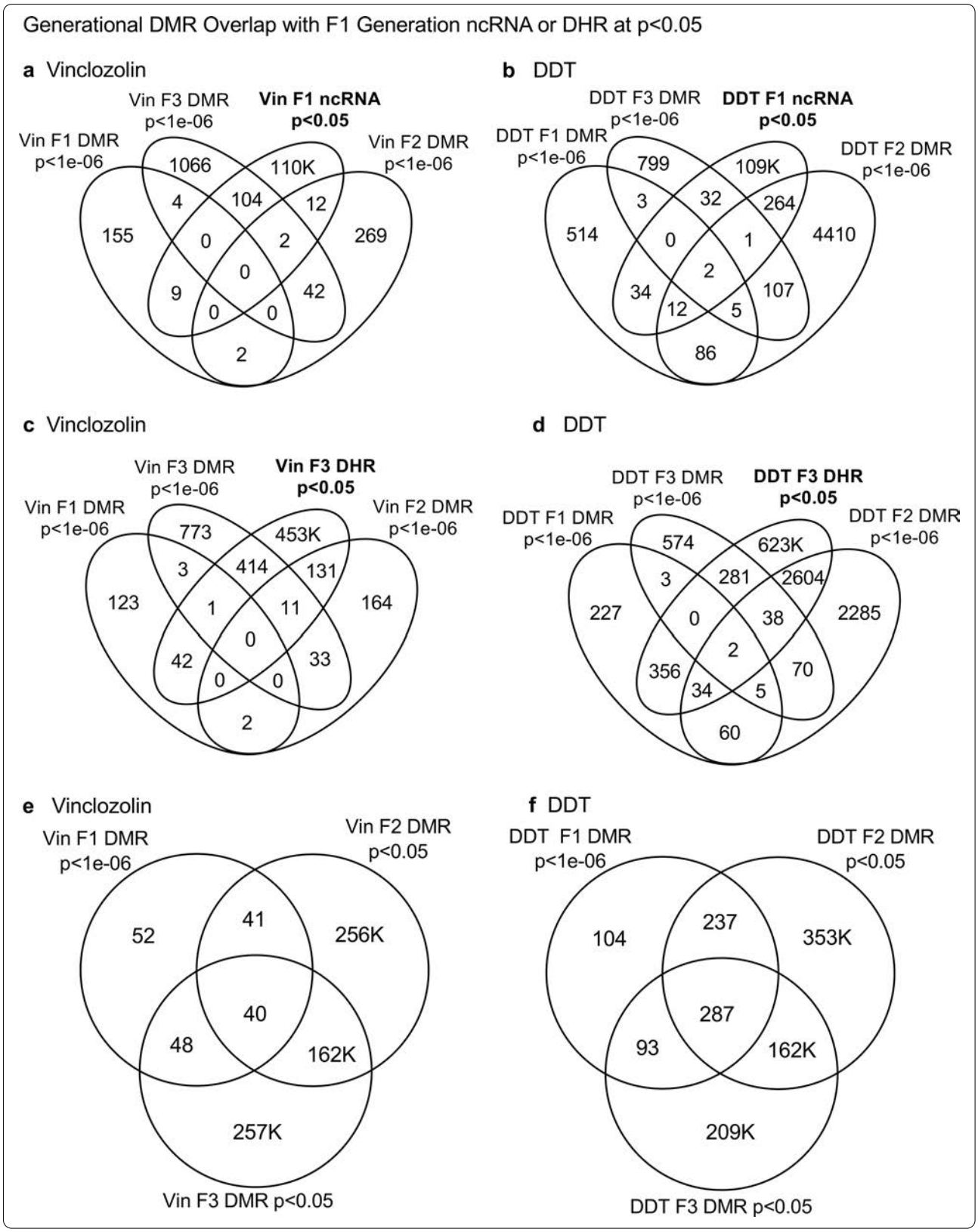
Generational DMR Overlap with F1 Generation ncRNA or DHR at p<0.05
a Vinclozolin
Vin F3 DMR p<1e-06
Vin F1 ncRNA p<0.05
Vin F1 DMR p<1e-06
Vin F2 DMR p<1e-06
1066
110K
4
104
12
155
0
2
269
0
9
42
0
0
2
b DDT
DDT F3 DMR p<1e-06
DDT F1 ncRNA p<0.05
DDT F1 DMR p<1e-06
DDT F2 DMR p<1e-06
799
109K
3
32
264
514
0
1
4410
2
34
107
12
5
86
c Vinclozolin
Vin F3 DMR p<1e-06
Vin F3 DHR p<0.05
Vin F1 DMR p<1e-06
Vin F2 DMR p<1e-06
773
453K
3
414
131
123
1
11
164
0
42
33
0
0
2
d DDT
DDT F3 DMR p<1e-06
DDT F3 DHR p<0.05
DDT F1 DMR p<1e-06
DDT F2 DMR p<1e-06
574
623K
3
281
2604
227
0
38
2285
2
356
70
34
5
60
e Vinclozolin
Vin F1 DMR p<1e-06
Vin F2 DMR p<0.05
52
41
256K
40
48
162K
257K
Vin F3 DMR p<0.05
f DDT
DDT F1 DMR p<1e-06
DDT F2 DMR p<0.05
104
237
353K
287
93
162K
209K
DDT F3 DMR p<0.05

Fig. 5 Genomic colocalization of DMR, DHR and ncRNA. The genomic and colocalized DMR, DHR and ncRNA presented. The region size (bp), genes present, and localization of DMR, DHR and ncRNA identified. The various examples include **a** nc-005100.4, **b** nc-005104.4, **c** nc-005111.4, and **d** nc-005113.4 from the NCBI Rattus norvegicus release 106 in 2016

(Figs. 3 and 4e, f). This was 88–97% of the DMRs when 10 kb windows were used, (Fig. 6). A permutation analysis demonstrated this was significant ($p < 0.001$) and not due to random associations. The list of conserved F1 generation DMRs in subsequent generations is presented in (Additional file 1: Tables S5 and S6, and those DMRs with gene associations suggest approximately 50% of these conserved DMRs were associated with genes. Many of these genes had associations with a variety of pathologies, Additional file 1: Figures S1 and S2). Therefore, a percentage of the F1 generation sperm DMRs were programmed and then conserved in subsequent generations. Although a majority of the F1 generation sperm DMRs were conserved generationally, there were minimal similarities between the different generations for ncRNAs, (Figs. 3 and 6). The DHRs were primarily present in the F3 generation sperm, so not conservation between generations, (Fig. 3.) In contrast, when a 10 kb region is considered

Extended 10 kb Window Epimutation Overlap

a Vinclozolin Epimutations (10 kb)

p>.05 / p<1e-5	F1.DMR	F1.DHR	F1.ncRNA	F2.DMR	F2.DHR	F2.ncRNA	F3.DMR	F3.DHR	F3.ncRNA
F1.DMR	170 (100.0%)	25 (14.7%)	17 (10.0%)	150 (88.2%)	21 (12.4%)	8 (4.7%)	155 (91.2%)	151 (88.8%)	7 (4.1%)
F1.DHR	5 (100.0%)	5 (100.0%)	0 (0.0%)	4 (80.0%)	4 (80.0%)	0 (0.0%)	5 (100.0%)	5 (100.0%)	0 (0.0%)
F1.ncRNA	831 (84.9%)	89 (9.1%)	979 (100.0%)	892 (91.1%)	73 (7.5%)	308 (31.5%)	891 (91.0%)	879 (89.8%)	74 (7.6%)
F2.DMR	283 (86.5%)	68 (20.8%)	23 (7.0%)	327 (100.0%)	54 (16.5%)	12 (3.7%)	312 (95.4%)	294 (89.9%)	15 (4.6%)
F2.DHR	2 (66.7%)	3 (100.0%)	0 (0.0%)	3 (100.0%)	3 (100.0%)	0 (0.0%)	3 (100.0%)	3 (100.0%)	0 (0.0%)
F2.ncRNA	403 (73.3%)	74 (13.5%)	119 (21.6%)	471 (85.6%)	68 (12.4%)	549 (99.8%)	456 (82.9%)	487 (88.5%)	55 (10.0%)
F3.DMR	1092 (90.8%)	129 (10.7%)	155 (12.9%)	1171 (97.3%)	104 (8.6%)	47 (3.9%)	1203 (100.0%)	1060 (88.1%)	74 (6.2%)
F3.DHR	84 (84.8%)	45 (45.5%)	11 (11.1%)	86 (86.9%)	37 (37.4%)	8 (8.1%)	87 (87.9%)	99 (100.0%)	11 (11.1%)
F3.ncRNA	352 (81.1%)	75 (17.3%)	89 (20.5%)	370 (85.3%)	59 (13.6%)	91 (21.0%)	372 (85.7%)	378 (87.1%)	434 (100.0%)

b DDT Epimutations (10 kb)

p>.05 / p<1e-5	F1.DMR	F1.DHR	F1.ncRNA	F2.DMR	F2.DHR	F2.ncRNA	F3.DMR	F3.DHR	F3.ncRNA
F1.DMR	651 (100.0%)	102 (15.7%)	56 (8.6%)	637 (97.8%)	93 (14.3%)	24 (3.7%)	599 (92.0%)	643 (98.8%)	59 (9.1%)
F1.DHR	0 (0.0%)	0 (100%)	0 (0.0%)	0 (0.0%)	0 (0.0%)	0 (0.0%)	0 (0.0%)	0 (0.0%)	0 (0.0%)
F1.ncRNA	1438 (88.9%)	155 (9.6%)	1614 (99.8%)	1529 (94.5%)	128 (7.9%)	178 (11.0%)	1349 (83.4%)	1577 (97.5%)	193 (11.9%)
F2.DMR	4735 (96.9%)	590 (12.1%)	440 (9.0%)	4886 (100.0%)	520 (10.6%)	139 (2.8%)	4471 (91.5%)	4764 (97.5%)	327 (6.7%)
F2.DHR	1 (100.0%)	1 (100.0%)	0 (0.0%)	1 (100.0%)	1 (100.0%)	0 (0.0%)	1 (100.0%)	0 (0.0%)	0 (0.0%)
F2.ncRNA	88 (93.6%)	14 (14.9%)	28 (29.8%)	89 (94.7%)	9 (9.6%)	94 (100.0%)	79 (84.0%)	92 (97.9%)	30 (31.9%)
F3.DMR	801 (84.2%)	121 (12.7%)	64 (6.7%)	859 (90.3%)	119 (12.5%)	26 (2.7%)	951 (100.0%)	872 (91.7%)	37 (3.9%)
F3.DHR	638 (90.6%)	72 (10.2%)	58 (8.2%)	660 (93.8%)	55 (7.8%)	17 (2.4%)	596 (84.7%)	704 (100.0%)	40 (5.7%)
F3.ncRNA	822 (88.0%)	134 (14.3%)	257 (27.5%)	871 (93.3%)	106 (11.3%)	202 (21.6%)	790 (84.6%)	894 (95.7%)	928 (99.4%)

Fig. 6 Extended epimutation overlap within a 10-kb region. The epimutations at high stringency (DMR $p < 1e{-}06$, DHR $p < 1e{-}06$, and ncRNA $p < 1e{-}04$) in rows were compared to epimutations at $p < 0.05$ in columns. The number of overlap epimutations and percentage of the total are presented for each overlap. As anticipated, 100% overlap was observed for the same generation and epimutation indicated by shaded box. **a** Vinclozolin lineage epimutation and **b** DDT lineage epimutation overlap

approximately 40% of the F3 generation DHRs are present in the F1 and F2 generations, (Fig. 6). The potential role of these DMRs for guided transgenerational histone retention is discussed below.

The second interesting observation was the overlap of the F1 generation sperm ncRNA with the F1, F2, and F3 generation DMRs. Over 20% in DDT and 35% in vinclozolin F1 generation ncRNA overlapped with the F1, F2, and F3 generation DMRs, (Figs. 3 and 4 and Additional file 1: Tables S1 and S2). Observations suggest the potential role of ncRNA-directed DNA methylation in the direct exposure F1 generation and transgenerational F3 generation. Previous literature has established a role for RNA-directed DNA methylation in a number of biological and cellular systems [26–28]. This involves the ability of the ncRNA to recruit or direct chromatin remodeling proteins and proteins such as DNA methyltransferase to guide the DNA methylation at a chromosomal site, which has been established in a variety of different organisms and developmental processes

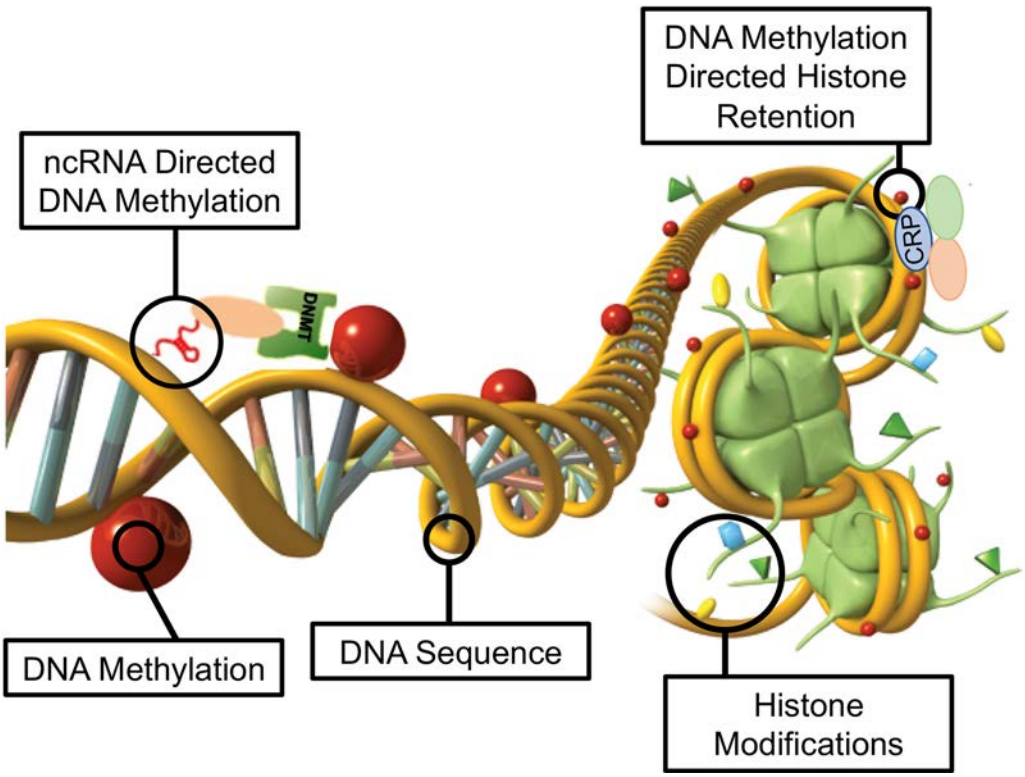

Fig. 7 Diagram of ncRNA-directed DNA methylation and DNA methylation-directed histone retention. The red dot identifies DNA methylation, green histone the nucleosome with modifications in histone tails indicated. The ncRNA association with cofactors and DNA methyltransferase (DNMT) promoting DNA methylation (red dot) for RNA-directed DNA methylation. The DNA methylation (red dot) association with chromatin remodeling proteins (CRP) to promote histone retention is indicated

[26–28]. Observations suggest ncRNA-directed DNA methylation may have a role in the epigenetic transgenerational inheritance phenomenon. Although the F1 generation ncRNA have the highest overlap with the F3 generation DMRs, overlaps are also observed with the F1 and F2 generation ncRNA with the various generation DMRs, (Fig. 3). When a 10 kb region overlap is considered, the F1 generation ncRNAs have a 91% overlap with the F2 and F3 generation DMRs, (Fig. 6). The overlaps of the ncRNA and DMRs suggest ncRNA-directed DNA methylation has a potential role in the epigenetic transgenerational inheritance process, (Fig. 7). A combination of F1 generation direct exposure alterations in ncRNA and subsequent transgenerational F3 generation actions on DNA methylation appears to be involved. The colocalized epigenetic sites with ncRNA and DNA methylation support this proposal, (Fig. 5). Although the molecular process of RNA-directed DNA methylation has been established [26–28], and suggested in generational impacts in plants and humans [35, 36], the current study only demonstrates the strong correlations of the ncRNA and DMRs. Future studies are needed to provide more molecular insights and validation of the ncRNA-directed DNA methylation in the epigenetic transgenerational phenomenon.

Another interesting observation was the overlap of the transgenerational F3 generation DMRs with the DHRs. Although negligible DHRs are present in the F1 or F2 generations, the F3 generation has DHRs that overlap with F1 and F2 generation DMRs, (Fig. 3). For the DDT DMRs there was a range of 35–50% overlap and for vinclozolin DMRs, a 23–41% overlap. Considering a 10 kb region overlap, the F3 generation DHRs had an 85–95% overlap with the DMRs at all the generations, (Fig. 6). The permutation analysis demonstrated this number of 10 kb region overlaps is not due to random associations ($p < 0.001$). The literature for spermatid exchange of histones for protamines to condense the DNA into the head of the sperm is well established in most organisms investigated [37–39]. Although the vast majority of the sperm DNA has associated protamines, a percentage of the histones are retained, which varies between 5–10% of the DNA in different mammalian species [40]. Previously, we found histone retention was significantly increased in the transgenerational F3 generation sperm with the presence of new retention sites [24, 25, 32]. Therefore,

an additional epigenetic mechanism influenced during the epigenetic transgenerational inheritance process involves altered histone retention [32]. Previous literature has described the transition proteins and processes of the replacement of histones for protamines [41, 42], but the role of epigenetic processes such as DNA methylation have not been considered. Our previous observations suggest a role for this process in epigenetic inheritance [24, 25]. The current study indicates a potential role for DNA methylation in guiding or directing histone retention,(Figs. 3 and 6). Previous studies have demonstrated a critical role for DNA methylation in the actions of chromatin remodeling proteins [41–43]. So, DNA methylation could alter the associated proteins and secondary structure of DNA that is an aspect of the process of histone retention. Although further investigation of the molecular processes is required in future studies, the observations from the current study suggest a potential role of DNA methylation-directed differential histone retention, (Fig. 7). The DMRs are proposed to assist in the guiding or directing of histone retention sites such that an increased number of sites appear transgenerationally. Therefore, the existence of DNA methylation-directed histone retention is proposed, and the observations support an integration of DMRs and DHRs transgenerationally. An interesting additional observation is the F1 and F2 generation DMRs that develop following direct exposure to toxicants are similar to the F3 generation DMRs, but that the DHRs did not form until the transgenerational F3 generation, (Figs. 3 and 6).

The current study findings help integrate the previous data obtained with ncRNA, DMRs, and DHRs [24, 25]. Potential roles of ncRNA-directed DMRs and DMR-directed DHRs are suggested. A percentage of the F1 generation DMRs are retained and conserved for subsequent F2 and F3 generations. The F1 generation ncRNA overlapped with the F2 and F3 generation DMRs, supporting the role for ncRNA-directed DNA methylation and formation of DMRs, (Fig. 7). The specific subtypes of sncRNA and lncRNA in this process will require further investigation. The potential for DMR-directed DHRs is suggested, but further information is required to elucidate the specific processes involved. Approximately half of the overlapping epimutations had associated known genes. Many of these genes are associated with previously identified pathologies, (Additional file 1: Figures S1 and S2), so support a mechanism for transgenerational pathology. The proposed model and integration of the transgenerational ncRNAs, DMRs and DHRs are presented in (Fig. 7). The current study observations suggest the integration of epigenetic processes in the epigenetic transgenerational phenomenon. Insights are provided into the development and generational transmission of these environmentally induced sperm epimutations that have previously been shown to associate with disease development and etiology. The potential use of these integrated epigenetic chromosomal sites as biomarkers to identify exposure and/or disease susceptibility suggests they could be used as diagnostics to facilitate preventative medicine in the future. Further investigation is needed to more thoroughly establish these mechanisms in the epigenetic transgenerational inheritance phenomenon, but the current study provides support and a framework for the integration of the various epigenetic processes.

Conclusions

The observations with the two different exposures of DDT or vinclozolin suggest the generational impacts and transgenerational integration of the ncRNA, DMRs, and DHRs are similar. Variation in the percent overlaps is observed, but the same trends and conclusions of integration of the various epimutations are similar for both DDT and vinclozolin exposure lineages. The colocalized epimutation sites for the different exposures demonstrate the same phenomenon, but independent sites are observed for each exposure. The two different models of environmentally induced epigenetic transgenerational inheritance support the general mechanism proposed for ncRNA-directed DNA methylation and DMR-directed DHR development. Although the current study identifies such colocalized and interacting epimutation sites, many of the specific ncRNAs, DMRs and DHRs are not colocalized [24, 25]. Therefore, independent actions of ncRNAs, DMRs and DHRs will also be important in the mechanism involved in environmentally induced epigenetic transgenerational inheritance. A combination of ncRNA, DMR, and DHR epimutations developed during gametogenesis allows for post fertilization embryonic impacts and suggests integration of ncRNA and DMR will be involved in the epigenetic inheritance. The proposed mechanism in (Fig. 7) helps elucidate the molecular mechanisms involved in the epigenetic transgenerational inheritance phenomenon.

Materials and methods summary

Animal studies and breeding

As previously described [24, 25] and expanded in the (Additional file 1: Supplemental Methods), outbred Sprague Dawley SD male and female rats were fed a standard diet with water ad lib and mated. Gestating female rats were exposed to DDT or vinclozolin, and offspring were bred within each lineage for three generations in the absence of exposure. The F3 generation was aged to 120 days for sperm isolation and molecular analysis, as described in the (Additional file 1: Supplemental

Methods). Sperm were isolated and used for epigenetic analysis, as described in the (Additional file 1: Supplemental Methods). All experimental protocols for the procedures with rats were pre-approved by the Washington State University Animal Care and Use Committee (protocol IACUC # 6252), and all methods were performed in accordance with the relevant guidelines and regulations.

Epigenetic analysis, statistics and bioinformatics

As previously described [44], DNA was isolated from sperm collected at the time of dissection. The DNA isolation protocol has been previously described [33, 34], (Additional file 1: Supplemental Methods). Methylated DNA immunoprecipitation (MeDIP), followed by next generation sequencing (MeDIP-Seq) was performed on the isolated DNA. MeDIP-Seq, sequencing libraries, next generation sequencing, and bioinformatics analysis were performed, as described previously [33, 34] and in the (Additional file 1: Supplemental Methods). All molecular data has been deposited into the public database at NCBI (GEO # GSE109775 and GSE106125), and R code computational tools are available at GitHub (https://github.com/skinnerlab/MeDIP-seq) and https://skinner.wsu.edu/genomic-data-and-r-code-files/.

Supplementary Information

The online version contains supplementary material available at https://doi.org/10.1186/s13072-020-00378-0.

Additional file 1: Figure S1. Vinclozolin lineage F3 generation conserved DMR in common with DHR and F1 generation ncRNA. **Figure S2.** DDT lineage F3 generation conserved DMR in common with DHR and F1 generation ncRNA. **Table S1.** Vinclozolin lineage F1 generation ncRNA & F1, F2 and F3 generation DMR overlap list. **Table S2.** DDT lineage F1 generation ncRNA & F1, F2 and F3 generation DMR overlap list. **Table S3.** F3 generation vinclozolin DMR & F3 generation DHR overlap list. **Table S4.** F3 generation DDT DMR & F3 generation DHR overlap list. **Table S5.** Vinclozolin lineage F1, F2, F3 generation DMR overlap list. **Table S6.** DDT lineage F1, F2, F3 generation DMR overlap list.

Acknowledgements

We thank Drs. Eric Nilsson and Jennifer L.M. Thorson for critical review of the manuscript. We acknowledge Ms. Amanda Quilty for editing and Ms. Heather Johnson for assistance in preparation of the manuscript. We thank the Genomics Core laboratory at WSU Spokane for sequencing data. This study was supported by John Templeton Foundation (50183and61174) (https://templeton.org/) grants to MKS and NIH (ES012974) (https://www.nih.gov/) grant to MKS. The funders had no role in study design, data collection and analysis, decision to publish, or preparation of the manuscript.

Authors' contributions

DB: bioinformatic analysis, data analysis, wrote and edited manuscript. MBM: molecular analysis, data analysis, edited manuscript. MKS: conceived, oversight, obtained funding, data analysis, wrote and edited manuscript. All authors read and approved the final manuscript.

Funding

This study was supported by John Templeton Foundation (50183and61174) (https://templeton.org/) grants to MKS and NIH (ES012974) (https://www.nih.gov/) grant to MKS. The funders had no role in study design, data collection and analysis, decision to publish, or preparation of the manuscript.

Availability of data and materials

All molecular data have been deposited into the public database at NCBI (GEO # GSE109775 and GSE106125, NCIB SRA accession numbers: PRJNA430483 largeRNA (control and DTT), PRJNA430740 smallRNA (control, vinclozolin and DTT)). The specific scripts used to perform the analysis can be accessed at github.com/skinnerlab and at www.skinner.wsu.edu/genomic-data-and-r-code-files.

Ethics approval and consent to participate

All experimental protocols for the procedures with rats were pre-approved by the Washington State University Animal Care and Use Committee (IACUC approval # 02568-39).

Consent for publication

Not applicable.

Competing interests

The authors declare that they have no competing interests.

Received: 30 September 2020 Accepted: 12 December 2020
Published online: 12 January 2021

References

1. Anway MD, Cupp AS, Uzumcu M, Skinner MK. Epigenetic transgenerational actions of endocrine disruptors and male fertility. Science. 2005;308(5727):1466–9.
2. Jirtle RL, Skinner MK. Environmental epigenomics and disease susceptibility. Nat Rev Genet. 2007;8(4):253–62.
3. Nilsson E, Sadler-Riggleman I, Skinner MK. Environmentally induced epigenetic transgenerational inheritance of disease. Environ Epigenetics. 2018;4(2):1–13.
4. Manikkam M, Guerrero-Bosagna C, Tracey R, Haque MM, Skinner MK. Transgenerational actions of environmental compounds on reproductive disease and identification of epigenetic biomarkers of ancestral exposures. PLoS ONE. 2012;7(2):1–12.
5. Chamorro-Garcia R, Sahu M, Abbey RJ, Laude J, Pham N, Blumberg B. Transgenerational inheritance of increased fat depot size, stem cell reprogramming, and hepatic steatosis elicited by prenatal exposure to the obesogen tributyltin in mice. Environ Health Perspect. 2013;121(3):359–66.
6. Gapp K, Jawaid A, Sarkies P, Bohacek J, Pelczar P, Prados J, et al. Implication of sperm RNAs in transgenerational inheritance of the effects of early trauma in mice. Nat Neurosci. 2014;17(5):667–9.
7. Jawaid A, Roszkowski M, Mansuy IM. Transgenerational Epigenetics of Traumatic Stress. Prog Mol Biol Transl Sci. 2018;158:273–98.
8. Yan W. Potential roles of noncoding RNAs in environmental epigenetic transgenerational inheritance. Mol Cell Endocrinol. 2014;398(1–2):24–30.
9. Burdge GC, Lillycrop KA, Jackson AA. Nutrition in early life, and risk of cancer and metabolic disease: alternative endings in an epigenetic tale? Br J Nutr. 2009;101(5):619–30.
10. Zheng X, Chen L, Li M, Lou Q, Xia H, Wang P, et al. Transgenerational variations in DNA methylation induced by drought stress in two rice varieties with distinguished difference to drought resistance. PLoS ONE. 2013;8(11):e80253.
11. Suter L, Widmer A. Environmental heat and salt stress induce transgenerational phenotypic changes in Arabidopsis thaliana. PLoS ONE. 2013;8(4):e60364.
12. Norouzitallab P, Baruah K, Vandegehuchte M, Van Stappen G, Catania F, Vanden Bussche J, et al. Environmental heat stress induces epigenetic transgenerational inheritance of robustness in parthenogenetic Artemia model. FASEB J. 2014;28(8):3552–63.
13. Waddington CH. Gene assimilation of an acquired character. Evolution. 1953;7:118–26.
14. Greer EL, Maures TJ, Ucar D, Hauswirth AG, Mancini E, Lim JP, et al. Transgenerational epigenetic inheritance of longevity in Caenorhabditis elegans. Nature. 2011;479(7373):365–71.

15. Carvan M, Kalluvila TA, Klingler RH, Larson JK, Pickens M, Mora-Zamorano FX, et al. Mercury-induced epigenetic transgenerational inheritance of abnormal neurobehavior is correlated with sperm epimutations in zebrafish. PLoS ONE. 2017;12(5):1–26.
16. Knecht AL, Truong L, Marvel SW, Reif DM, Garcia A, Lu C, et al. Transgenerational inheritance of neurobehavioral and physiological deficits from developmental exposure to benzo[a]pyrene in zebrafish. Toxicol Appl Pharmacol. 2017;329:148–57.
17. Bhandari RK, vom Saal FS, Tillitt DE. Transgenerational effects from early developmental exposures to bisphenol A or 17alpha-ethinylestradiol in medaka *Oryzias latipes*. Sci Rep. 2015;5:9303.
18. Leroux S, Gourichon D, Leterrier C, Labrune Y, Coustham V, Riviere S, et al. Embryonic environment and transgenerational effects in quail. Genet Sel Evol. 2017;49(1):14.
19. Brun JM, Bernadet MD, Cornuez A, Leroux S, Bodin L, Basso B, et al. Influence of grand-mother diet on offspring performances through the male line in Muscovy duck. BMC Genet. 2015;16(1):145.
20. Braunschweig M, Jagannathan V, Gutzwiller A, Bee G. Investigations on transgenerational epigenetic response down the male line in F2 pigs. PLoS ONE. 2012;7(2):e30583.
21. Bygren LO, Tinghog P, Carstensen J, Edvinsson S, Kaati G, Pembrey ME, et al. Change in paternal grandmothers' early food supply influenced cardiovascular mortality of the female grandchildren. BMC Genet. 2014;15:12.
22. Veenendaal MV, Painter RC, de Rooij SR, Bossuyt PM, van der Post JA, Gluckman PD, et al. Transgenerational effects of prenatal exposure to the 1944–45 Dutch famine. BJOG. 2013;120(5):548–53.
23. Skinner MK. Environmental epigenetics and a unified theory of the molecular aspects of evolution: a Neo-Lamarckian concept that facilitates Neo-Darwinian evolution. Genome Boil Evol . 2015;7(5):1296–302.
24. Ben Maamar M, Sadler-Riggleman I, Beck D, McBirney M, Nilsson E, Klukovich R, et al. Alterations in sperm DNA methylation, non-coding RNA expression, and histone retention mediate vinclozolin-induced epigenetic transgenerational inheritance of disease. Environ Epigenetics. 2018;4(2):1–19.
25. Skinner MK, Ben Maamar M, Sadler-Riggleman I, Beck D, Nilsson E, McBirney M, et al. Alterations in sperm DNA methylation, non-coding RNA and histone retention associate with DDT-induced epigenetic transgenerational inheritance of disease. Epigenetics Chromatin. 2018;11(1):8.
26. Cuerda-Gil D, Slotkin RK. Non-canonical RNA-directed DNA methylation. Nat Plants. 2016;2(11):16163.
27. Chow HT, Chakraborty T, Mosher RA. RNA-directed DNA Methylation and sexual reproduction: expanding beyond the seed. Curr Opin Plant Biol. 2019;54:11–7.
28. Matzke MA, Mosher RA. RNA-directed DNA methylation: an epigenetic pathway of increasing complexity. Nat Rev Genet. 2014;15(6):394–408.
29. Kouzarides T. Chromatin modifications and their function. Cell. 2007;128(4):693–705.
30. Jenkins TG, Carrell DT. The sperm epigenome and potential implications for the developing embryo. Reproduction. 2012;143(6):727–34.
31. Jenkins TG, Carrell DT. The paternal epigenome and embryogenesis: poising mechanisms for development. Asian J Androl. 2011;13(1):76–80.
32. Ben Maamar M, Sadler-Riggleman I, Beck D, Skinner MK. Epigenetic transgenerational inheritance of altered sperm histone retention sites. Sci Rep. 2018;8:5308.
33. King SE, McBirney M, Beck D, Sadler-Riggleman I, Nilsson E, Skinner MK. Sperm epimutation biomarkers of obesity and pathologies following DDT induced epigenetic transgenerational inheritance of disease. Environ Epigenetics. 2019;5(2):1–15.
34. Nilsson E, King SE, McBirney M, Kubsad D, Pappalardo M, Beck D, et al. Vinclozolin induced epigenetic transgenerational inheritance of pathologies and sperm epimutation biomarkers for specific diseases. PLoS ONE. 2018;13(8):1–29.
35. Saenen ND, Martens DS, Neven KY, Alfano R, Bove H, Janssen BG, et al. Air pollution-induced placental alterations: an interplay of oxidative stress, epigenetics, and the aging phenotype? Clinical epigenetics. 2019;11(1):124.
36. Kumar S, Kumari R, Sharma V, Sharma V. Roles, and establishment, maintenance and erasing of the epigenetic cytosine methylation marks in plants. J Genet. 2013;92(3):629–66.
37. Ooi SL, Henikoff S. Germline histone dynamics and epigenetics. Curr Opin Cell Biol. 2007;19(3):257–65.
38. van der Heijden GW, Derijck AA, Ramos L, Giele M, van der Vlag J, de Boer P. Transmission of modified nucleosomes from the mouse male germline to the zygote and subsequent remodeling of paternal chromatin. Developmental biology. 2006;298(2):458–69.
39. Meyer-Ficca ML, Lonchar JD, Ihara M, Meistrich ML, Austin CA, Meyer RG. Poly(ADP-ribose) polymerases PARP1 and PARP2 modulate topoisomerase II beta (TOP2B) function during chromatin condensation in mouse spermiogenesis. Biol Reprod. 2011;84(5):900–9.
40. Hammoud S, Liu L, Carrell DT. Protamine ratio and the level of histone retention in sperm selected from a density gradient preparation. Andrologia. 2009;41(2):88–94.
41. Berson A, Nativio R, Berger SL, Bonini NM. Epigenetic regulation in neurodegenerative diseases. Trends Neurosci. 2018;41(9):587–98.
42. Zhao M, Shirley CR, Yu YE, Mohapatra B, Zhang Y, Unni E, et al. Targeted disruption of the transition protein 2 gene affects sperm chromatin structure and reduces fertility in mice. Mol Cell Biol. 2001;21(21):7243–55.
43. Vymetalkova V, Vodicka P, Vodenkova S, Alonso S, Schneider-Stock R. DNA methylation and chromatin modifiers in colorectal cancer. Mol Aspects Med. 2019;69:73–92.
44. McBirney M, King SE, Pappalardo M, Houser E, Unkefer M, Nilsson E, et al. Atrazine induced epigenetic transgenerational inheritance of disease, lean phenotype and sperm epimutation pathology biomarkers. PLoS ONE. 2017;12(9):1–37.

Publisher's Note

Developmental Biology 445 (2019) 280–293

Contents lists available at ScienceDirect

Developmental Biology

journal homepage: www.elsevier.com/locate/developmentalbiology

Developmental origins of transgenerational sperm DNA methylation epimutations following ancestral DDT exposure

Millissia Ben Maamar[a], Eric Nilsson[a], Ingrid Sadler-Riggleman[a], Daniel Beck[a], John R. McCarrey[b], Michael K. Skinner[a,*]

[a] Center for Reproductive Biology, School of Biological Sciences, Washington State University, Pullman, WA 99164-4236, USA
[b] Department of Biology, University of Texas at San Antonio, San Antonio, TX 78249, USA

ARTICLE INFO

Keywords:
Epigenetic
Transgenerational
Primordial germ cells
Spermatogenesis
Sperm
Epimutation
DNA methylation
Testis

ABSTRACT

Epigenetic alterations in the germline can be triggered by a number of different environmental factors from diet to toxicants. These environmentally induced germline changes can promote the epigenetic transgenerational inheritance of disease and phenotypic variation. In previous studies, the pesticide DDT was shown to promote the transgenerational inheritance of sperm differential DNA methylation regions (DMRs), also called epimutations, which can in part mediate this epigenetic inheritance. In the current study, the developmental origins of the transgenerational DMRs during gametogenesis have been investigated. Male control and DDT lineage F3 generation rats were used to isolate embryonic day 16 (E16) prospermatogonia, postnatal day 10 (P10) spermatogonia, adult pachytene spermatocytes, round spermatids, caput epididymal spermatozoa, and caudal sperm. The DMRs between the control versus DDT lineage samples were determined at each developmental stage. The top 100 statistically significant DMRs at each stage were compared and the developmental origins of the caudal epididymal sperm DMRs were assessed. The chromosomal locations and genomic features of the different stage DMRs were analyzed. Although previous studies have demonstrated alterations in the DMRs of primordial germ cells (PGCs), the majority of the DMRs identified in the caudal sperm originated during the spermatogonia stages in the testis. Interestingly, a cascade of epigenetic alterations initiated in the PGCs is required to alter the epigenetic programming during spermatogenesis to obtain the sperm epigenetics involved in the epigenetic transgenerational inheritance phenomenon.

1. Introduction

Numerous environmental factors have been shown to promote the epigenetic transgenerational inheritance of disease such as the agricultural fungicide vinclozolin [1] and the pesticide DDT (dichlorodiphenyltrichloroethane) [2]. Caloric restriction, high fat diets, stress and a variety of different toxicants have also been linked to the transgenerational epigenetic inheritance phenomenon [3–5]. This non-genetic form of inheritance involves epigenetic modifications of the germline (sperm and egg) to pass an altered epigenome to the early embryo that can then impact the transcriptomes and epigenetics of all subsequently derived somatic cells [1,5]. Different epigenetic processes are involved in the transgenerational germline transmission where the environment can impact the health and evolution of species [3,4,6].

Epigenetics is defined as “molecular factors and processes around the DNA that regulate genome activity independent of DNA sequence and that are mitotically stable” [7]. Transgenerational epigenetic inheritance requires the germline transmission of epigenetic information. Different epigenetic processes have been shown to be involved in the transgenerational phenomenon such as DNA methylation [8–10], non-coding RNA [11,12], and histone modifications and retention [10,13,14]. Recently, concurrent alterations in all three of these processes have been observed in transgenerational sperm transmission after exposure to DDT and vinclozolin [15,16]. Most previous studies have been conducted in sperm due to the ability to isolate large numbers of cells and the inability to isolate large numbers of eggs, but experiments have shown that the female germline also has the capacity to transmit epigenetic inheritance [2,17]. The current study investigated the transgenerational sperm transmission of DNA methylation alterations after DDT exposure.

The primordial germ cells (PGCs), which give rise to spermatogenic (or oogenic) cells, develop and migrate down the genital ridge to colonize the indifferent gonad [18]. Upon sex determination and depending on the chromosomal sex, the PGCs differentiate into the

* Corresponding author.
E-mail address: skinner@wsu.edu (M.K. Skinner).

https://doi.org/10.1016/j.ydbio.2018.11.016
Received 5 September 2018; Received in revised form 1 November 2018; Accepted 26 November 2018
Available online 27 November 2018

male or female germline lineage [19]. In the rat gonad, the early developing testis germ cells will become prospermatogonia cells during the male gonadal sex determination period by embryonic day 16 (E16) [20,21]. By postnatal day 10 (P10) the germline develops into spermatogonia. Following the onset of puberty the initial wave of spermatogenesis begins in the testis where the spermatocytes, including the meiotic stage of pachytene spermatocytes, develop. After meiosis the round spermatid stage differentiates, then in the final spermatozoa stage the cells are released into the lumen of the seminiferous tubules [22], Fig. 1A. After entering the caput region of the epididymis the spermatozoa undergo further differentiation. During the transit in the epididymis the spermatozoa mature. When the spermatozoa reach the final caudal stage of the epididymis, the sperm have developed the capacity for motility and fertility [23,24]. Prior to ejaculation or degradation the mature caudal epididymal sperm will be stored in the vas deferens. In the current study we used several male germline developmental periods (E16 prospermatogonia, P10 spermatogonia, adult pachytene spermatocytes, round spermatids, caput epididymal spermatozoa, and caudal epididymal sperm), Fig. 1A, to investigate the developmental origins of the transgenerational sperm DMRs following DDT exposure in the F0 generation.

Epigenetic programming occurs during these male germline developmental periods. The migrating PGCs have an erasure of DNA methylation that then re-methylate during gonadal sex determination to create the male germline and prospermatogonia [25]. In the adult testis, during spermatogenesis some epigenetic programming events occur [26,27]. The first examples of this male germline epigenetic programming were observed with imprinted genes [28,29]. Imprinted genes can develop either early in the embryonic period or develop during spermatogenesis. Although previous studies have discussed the

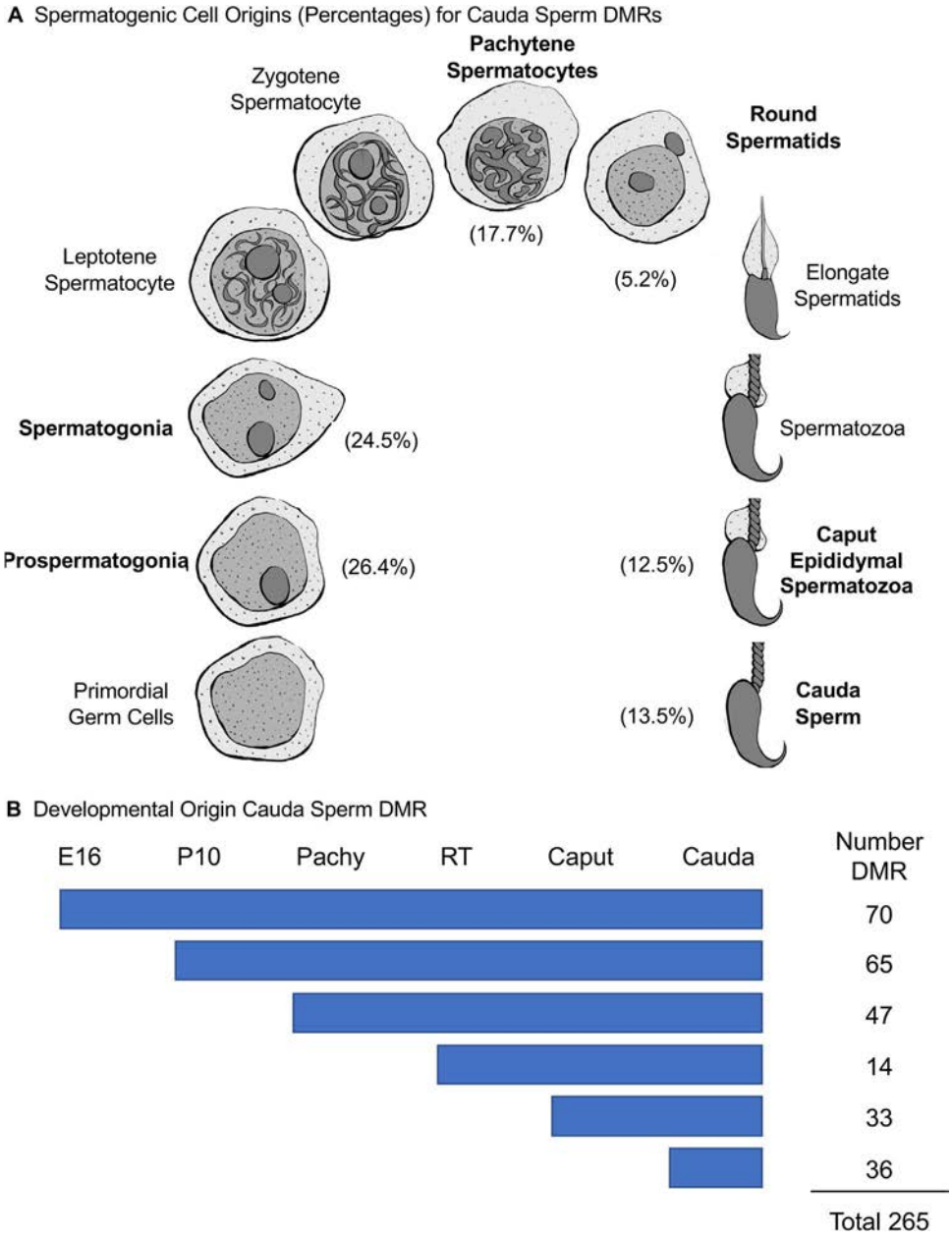

Fig. 1. Sperm DMR developmental origins. (A) Spermatogenic cell origin percentages for cauda sperm DMRs. The schematic of each developmental cell morphology listed during gametogenesis and spermatogenesis and epididymal maturation. The percentage DMR in brackets is presented for the developmental stages analyzed. (B) Developmental origins of cauda sperm DMRs for each stage of development with number DMRs at specific stages listed. The prospermatogonia (E16), spermatogonia (P10), pachytene spermatocytes (Pachy), round spermatids (RT), caput spermatozoa (Caput) and cauda sperm (Cauda) are presented.

germline developmental origins of epigenetic inheritance [5,30–34], none of these studies identified the developmental programming origins of the transgenerational epigenetic alterations observed in sperm.

The current study was designed to investigate the developmental origins of the DDT induced transgenerational sperm DMRs termed epimutations. The hypothesis tested is that a cascade of epigenetic changes occurs during development such that the majority of DMRs develop throughout gametogenesis and spermatogenic stages. It has been previously demonstrated that epigenetic alterations occur in the PGC [35]. However, due to this being the earliest stem cell stage of the germline, the PGCs DMRs were found to be different from the epimutations observed in sperm [35]. These observations suggest that the epimutations in sperm develop at later stages of epigenetic programming. The present study shows the majority of sperm DMRs originate during spermatogonia development and spermatogenesis, but some also do originate during epididymal maturation. This is one of the first genome-wide analyses of epigenetic programming during gametogenesis for transgenerational sperm epimutations [36].

2. Results

F3 generation control and DDT lineage male rats were used in this experimental design to isolate various germ cell stages for epigenetic analysis. The F0 generation gestating female rats at 90 days of age were transiently exposed to DDT or a vehicle control during gestational days 8–14. This stage of fetal development corresponds to when the PGCs migrate to colonize the indifferent gonad through the early stage of gonadal sex determination as previously described [18,25,35]. The F1 generation offspring were obtained and when they reached 90 days of age they were bred within the control and DDT lineages to generate the F2 generation (grand offspring) which were then bred at 90 days of age to obtain the transgenerational F3 generation for each control and DDT lineage. No cousin or sibling breedings were used to avoid any inbreeding artifacts. Only the F0 generation gestating females were exposed to DDT, which also directly exposed the F1 generation fetus and the germline within the F1 generation fetus that will generate the F2 generation. Therefore, the F3 generation is the first transgenerational generation not directly exposed [37] and was used to study the developmental origins of the transgenerational sperm epimutations. The F3 generation control and DDT lineage male rats were aged to the embryonic day 16 (E16) fetal stage for prospermatogonia cell isolation, to postnatal day 10 (P10) for spermatogonial cell isolation, and to 120 days of age for pachytene spermatocyte isolation, round spermatid isolation, caput spermatozoa isolation, and cauda epididymal sperm isolation. A gravity sedimentation StaPut protocol, as described in the Methods [38,39], was used to isolate the prospermatogonia, spermatogonia, pachytene spermatocytes and round spermatids cells. Three different pools each with different individual sets of animals from different litters were obtained with 5–6 males per pool for the E16 stage, 6–7 males per pool for the P10 stage, 3 adult males per pool for the adult stages. Therefore, 3–7 different males were used in the analysis within each of the three different pools analyzed for both the control and DDT lineages. Genomic DNA was isolated from each purified germ cell stage pool and from individual animals for epididymal caput spermatozoa and cauda sperm [8,13] and then three pools generated for subsequent epigenetic analysis.

The analysis of differential DNA methylation regions (DMRs) was performed with a methylated DNA immunoprecipitation (MeDIP) procedure followed by next generation sequencing for an MeDIP-Seq protocol described in the Methods [8]. The F3 generation control versus DDT lineage pools were compared to identify the DMRs at each developmental stage of the male germline. The DMRs at various p-value thresholds are presented at each developmental stage in Fig. 2. An EdgeR p-value of $p < 1e-05$ was selected at all stages for further analysis of the DMRs. This correlated with an FDR (false discovery rate) value of < 0.1 for all except the E16 prospermatogonia which was more variable. The All Windows is all DMRs with at least one 100 bp region (window) with statistical significance and the Multiple Windows being ≥2 significant 100 bp windows. The number of DMRs with multiple windows is also presented in Fig. 2. Most developmental stages showed approximately 100–300 DMRs. The epigenetic alterations were higher at the pachytene spermatocyte and round spermatid stages which showed more than 300 DMRs. The chromosomal locations of the DMRs at each developmental stage are presented in Fig. 3. The red arrowheads indicate the location of a DMR with the black boxes indicating clusters of DMRs. In most stages, all the chromosomes, except the Y and mitochondrial DNA (MT), were found to contain DMRs. The genomic features of the DMRs at each stage of development were investigated. The CpG density of the DMRs at all stages was 1–5 CpG per 100 bp with 1 CpG per 100 bp being predominant, Fig. 4. This is characteristic of a low density CpG desert [40] which has been observed with previous transgenerational DMRs. The length of the DMRs at all the developmental stages were between 1 and 4 kb with 1 kb length being predominant, Fig. 5. Therefore, the DMRs are generally 1 kb in size with around 10 CpGs as previously observed [40]. The overlap between the various developmental stage DMRs was investigated and is presented in Fig. 6A. The DMRs were found to be primarily stage specific with a very low number of DMRs overlapping between the stages with a $p < 1e-05$. The cauda sperm and the caput spermatozoa had the highest level of overlap with 88 DMRs, Fig. 6B and S7 Table, comprising over 45% of the caput epididymal spermatozoa DMRs. These observations suggest a cascade of epigenetic programming occurs throughout male germline development.

The DNA methylation alterations of the DMRs at each stage of development were investigated. For the developmental time-course the top 100 statistically significant DMRs at each stage of development were examined regarding the scaled mean read depth between the control versus DDT lineage DMR data. The scaled mean read depths at each DMR was separated into control greater than DDT data (i.e. decrease in DNA methylation) and DDT greater than control data (i.e. increase in DNA methylation) which is presented as a scaled mean read depth, Figs. 7 and 8. The E16 prospermatogonia DMRs had 28 DMR with a decrease in methylation and 72 DMR with an increase in methylation, Figs. 7A & 8A. For both data sets the DMR methylation alterations generally dropped by the P10 spermatogonia stage and became mixed with no distinct patterns in later stages. Although a few of both populations stayed elevated, the majority had an alteration in DNA methylation at later stages of development. The P10 spermatogonia DMRs had 38 DMRs with a decrease in methylation and 62 with an increase in methylation in regard to % mean read depth, Figs. 7B & 8B. A dramatic change in methylation between the prospermatogonia to spermatogonia stage and from the spermatogonia to later stages of development were observed. Therefore, the E16 prospermatogonia and P10 spermatogonia stage DMRs are for the most part unique at these stages of development. The pachytene spermatocyte DMRs had predominantly a decrease in methylation with 63 DMRs and 37 DMRs with an increase, Figs. 7C & 8C. Therefore, DNA methylation was primarily decreased in the pachytene spermatocyte DMRs. The round spermatid DMRs had a higher number of 72 DMR with an increase and 28 DMR with a decrease, Figs. 7D & 8D. The caput epididymal spermatozoa DMRs had 46 DMR with a decrease and 54 DMR with an increase in methylation, Figs. 7E & 8E. The cauda epididymal sperm DMRs had 49 DMR with a decrease and 51 DMR with an increase, Figs. 7F & 8F. The caput spermatozoa and cauda epididymal sperm have relatively consistent DNA methylation characteristics for both data sets. Therefore, the cauda sperm show more consistent DNA methylation profiles during spermatogenesis and epididymal sperm maturation, but are distinct in the spermatogonial stem cell stages.

Genes associated with the DMRs were identified and compared at each of the developmental stages. The DMRs that had a gene within 10 kb distance, so the promoter is considered, were identified and the

A Prospermatogonia (E16)

P-value	All Window	Multiple Window
0.001	4011	265
1e-04	522	25
1e-05	**94**	**11**
1e-06	27	5
1e-07	12	4

Number Windows	1	2	3	4	5
Number of DMR	83	7	2	1	1

B Spermatogonia (P10)

P-value	All Window	Multiple Window
0.001	4728	464
1e-04	722	107
1e-05	**195**	**47**
1e-06	86	32
1e-07	48	19

Number Windows	1	2	3	4	5	20
Number of DMR	148	35	4	5	2	1

C Pachytene Spermatocytes

P-value	All Window	Multiple Window
0.001	11776	891
1e-04	1917	78
1e-05	**340**	**13**
1e-06	71	5
1e-07	20	2

Number Windows	1	2	3
Number of DMR	327	9	4

D Round Spermatids

P-value	All Window	Multiple Window
0.001	11006	1276
1e-04	1816	131
1e-05	**323**	**17**
1e-06	60	0
1e-07	7	0

Number Windows	1	2
Number of DMR	306	17

E Caput Epididymal Spermatozoa

P-value	All Window	Multiple Window
0.001	6644	616
1e-04	1146	148
1e-05	**284**	**72**
1e-06	117	52
1e-07	74	38

Number Windows	1	2	3	4	≥5
Number of DMR	212	39	13	5	15

F Cauda Sperm

P-value	All Window	Multiple Window
0.001	4611	478
1e-04	809	143
1e-05	**265**	**82**
1e-06	140	55
1e-07	87	40

Number Windows	1	2	3	4	≥5
Number of DMR	183	39	20	10	13

Fig. 2. DMR identification and numbers. The number of DMRs found using different p-value cutoff thresholds. The All Window column shows all DMRs. The Multiple Window column shows the number of DMRs containing at least two significant windows (100 bp each). The number of DMRs with the number of significant windows (100 bp per window) at a p-value threshold of 1e-05 is presented. (A) E16 prospermatogoina. (B) P10 spermatogonia. (C) Pachytene spermatocytes. (D) Round Spermatids. (E) Caput Spermatozoa. (F) Cauda Sperm.

associated genes and gene functional categories determined, S1–S6 Tables. The DMRs with a p < 1e-05 were used in this analysis at all the developmental stages. The number of genes associated with specific gene functional categories is presented in Fig. 9A. Each of the developmental stages are presented to compare the major gene categories. The signaling, metabolism, transcription and receptor gene categories were the major categories present in the different developmental stages. Additional categories were cytoskeleton, development, transport and immune system, that were present in all the developmental stages, Fig. 9A. The DMR associated genes at each developmental stage were also used in a gene pathway analysis applying the KEGG pathway association as described in the Methods. The number of DMR associated genes involved with the major pathways is presented in Fig. 9B. The most predominant pathways present in at least two different developmental stages are shown. The E16 prospermatogonia, round spermatids, caput spermatozoa and cauda sperm had DMR associated genes in the metabolic pathways. The E16 prospermatogonia, P10 spermatogonia, pachytene spermatocytes had DMR associated genes in the pathways in cancer in common. Therefore, the only pathways that were present in nearly all the stages are metabolism and pathways in cancer. The caput epididymal spermatozoa and cauda sperm were more consistent than the others which were more distinct.

The final aspect of the study involved an investigation of the developmental origins of the cauda sperm DMRs, meaning when the differential DNA methylation alterations appeared within the developmental stages examined. In the cauda sperm there are 265 DMRs at p < 1e-05. For the analysis of developmental origins the 265 DMRs were examined individually with a reduced statistical stringency of p < 0.05 to see the first stage the DMR appears or originates. Fig. 1B demonstrates 70 DMRs were developed in the E16 prospermatogonia stage, 65 DMRs in the P10 spermatogonia stage, 47 DMRs in the spermatocyte stage, 14 DMRs in the round spermatid stage, 33 DMRs in the caput epididymal spermatozoa stage, and 36 DMRs in the cauda sperm stage, S8 Table. The cauda sperm had a total of 265 DMRs at p < 1e-05 with the majority of DMRs originating in the prospermatogonia and spermatogonia. Fewer were observed in the round spermatids and caput epididymal spermatozoa stages, Fig. 1B. The percentage of the total DMR origins and schematic of the different

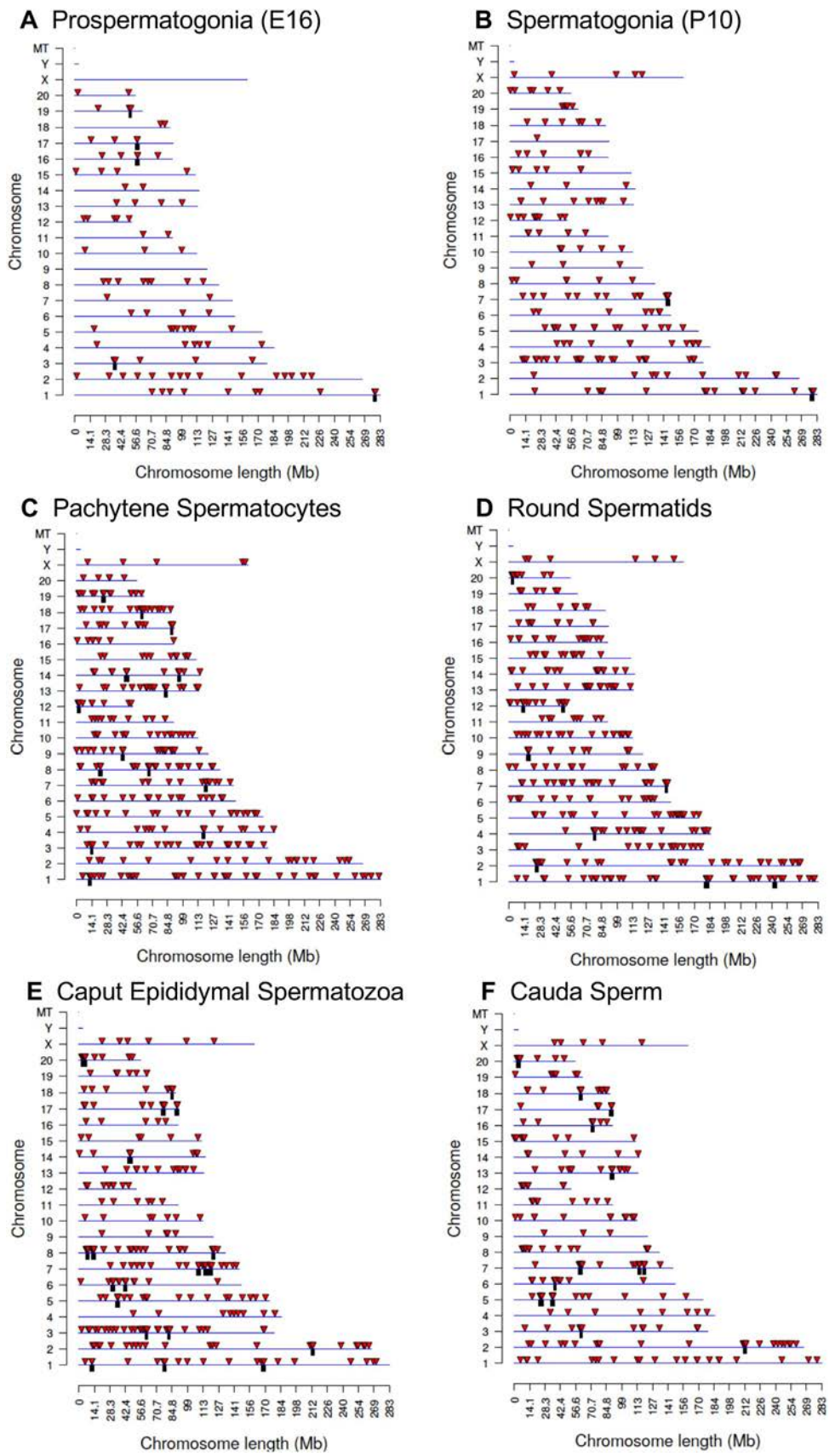

Fig. 3. DMR chromosomal locations. The DMR locations on the individual chromosomes is represented with an arrowhead and a cluster of DMRs with a black box. All DMRs containing at least one significant window at a p-value threshold of 1e-05 are shown. (A) E16 prospermatogoina. (B) P10 spermatogonia. (C) Pachytene spermatocytes. (D) Round Spermatids. (E) Caput Spermatozoa. (F) Cauda Sperm.

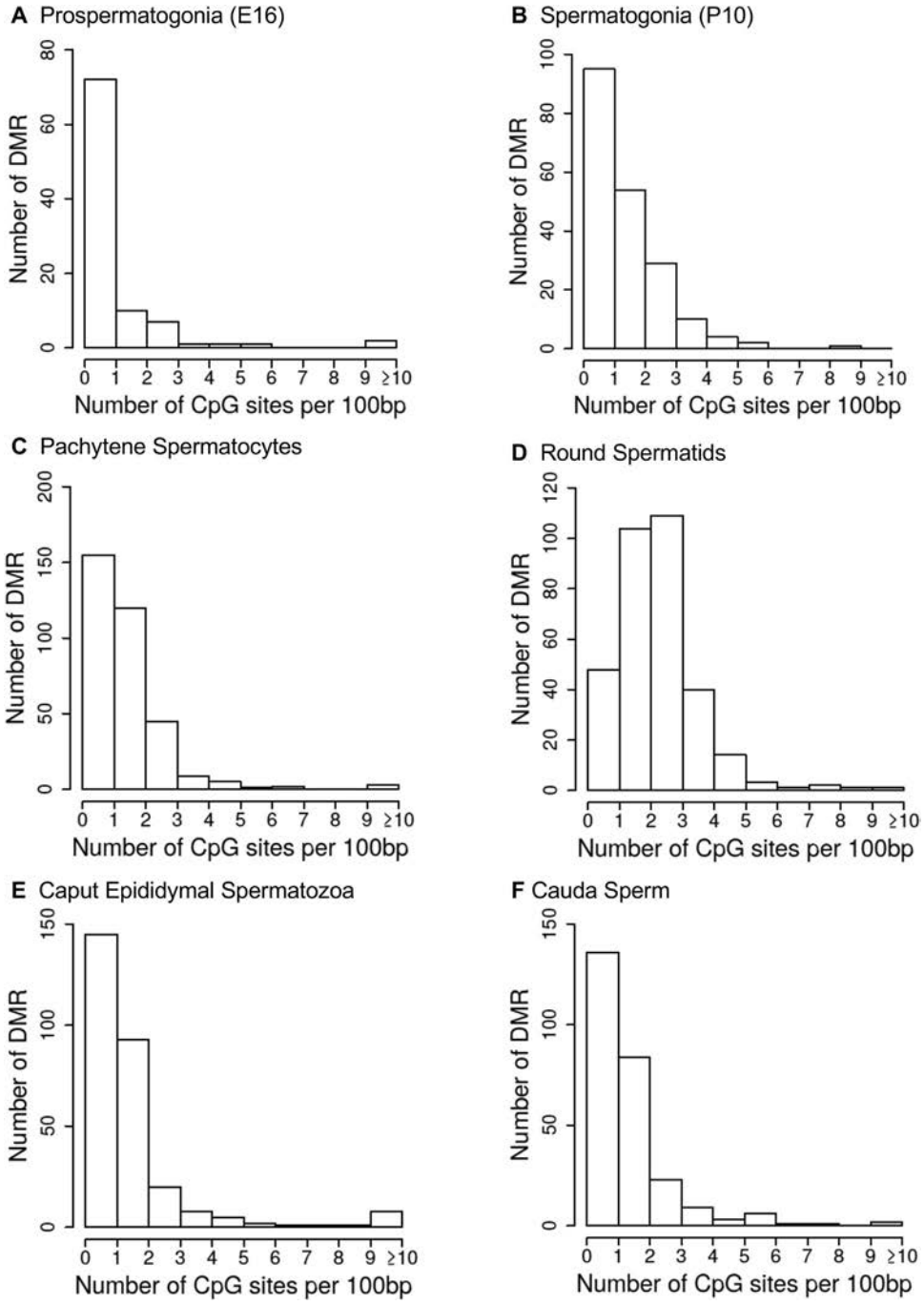

Fig. 4. DMR genomic features. The number of DMRs at different CpG densities. All DMRs at a p-value threshold of 1e-05 are shown. (A) E16 prospermatogoina. (B) P10 spermatogonia. (C) Pachytene spermatocytes. (D) Round Spermatids. (E) Caput Spermatozoa. (F) Cauda Sperm.

stage cells during development is presented in Fig. 1A. Therefore, the majority of the transgenerational sperm DMRs were developed during the prospermatogonia and spermatogonia stages with a small number developed in the epididymal maturation stages. This correlated to a cascade of epigenetic and transcriptome changes during these stages of male germline development to generate the transgenerational sperm epimutations, Fig. 1A.

3. Discussion

The aim of the current study was to identify the developmental origins of the cauda sperm transgenerational DMRs that transmit the epigenetic transgenerational inheritance of disease and phenotypic variation. During embryonic day 8–14 in the rat, when the primordial germ cells (PGCs) migrate to colonize the indifferent fetal gonad, the F0 generation gestating female exposure to DDT was performed [18,25,35]. Five different stages of male germ cell development were investigated: E16 prospermatogonia, P10 spermatogonia, and adult pachytene spermatocytes, round spermatids, caput epididymal spermatozoa and cauda sperm, Fig. 1A. The functional considerations of these cell populations involve the prospermatogonia precursor stem cell population, spermatogonia stem cell population in the testis, the meiotic pachytene spermatocyte cell population, the post-meiotic spermatid population and the spermatozoa present in the caput epididymis, and mature sperm in the cauda epididymis. The caput spermatozoa and cauda epididymal sperm were directly isolated as described in the Methods then sonicated and washed to remove any contaminating somatic cells, so are pure sperm cell preparations. For

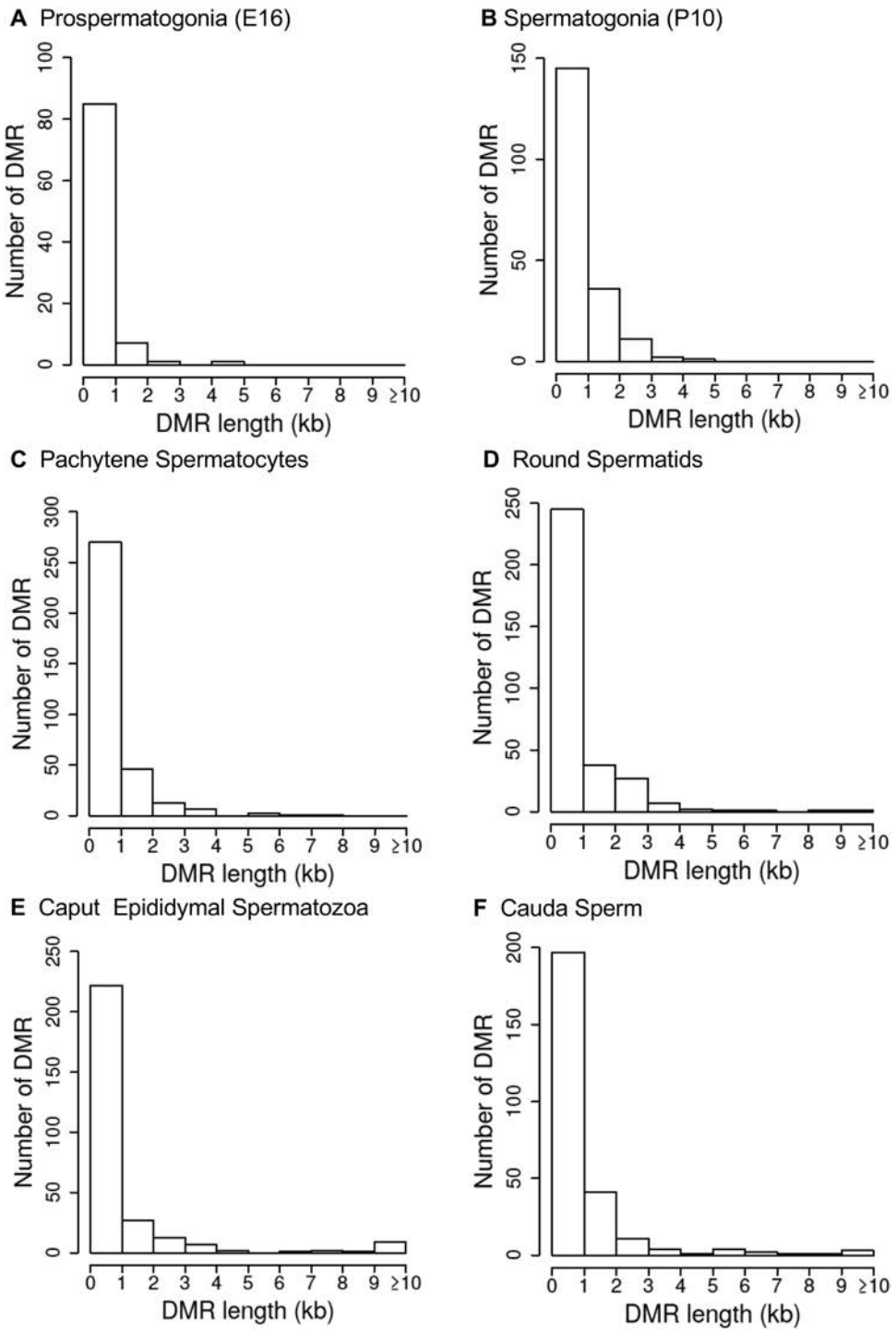

Fig. 5. DMR lengths. All DMRs at a p-value threshold of 1e-05 are shown. (A) E16 prospermatogoina. (B) P10 spermatogonia. (C) Pachytene spermatocytes. (D) Round Spermatids. (E) Caput Spermatozoa. (F) Cauda Sperm.

the other cell populations a gravity sedimentation on a StaPut apparatus procedure was used to isolate the specific cell populations as previously described [39,40]. The E16 prospermatogonia and P10 spermatogonia were found to have a greater than 85% purity. The pachytene spermatocytes were greater than 95% spermatocytes with two-thirds of these cells pachytene spermatocytes and one-third other spermatocyte stages. This is due to the longer developmental life span or developmental period of pachynema compared to the other stages of first meiotic prophase [41] and to the efficiency of the StaPut gradient protocol. For the isolated round spermatids 95% of them were spermatids with 90% of them being round spermatids and 10% being elongate spermatids and other spermatogenic cell stages [42]. Despite obtaining a high purity for these developmental stage male germline cell populations, cell purity needs to be considered in the data interpretations. The embryonic day 16 (E16) prospermatogonia were isolated from the fetal gonad, the postnatal day 10 (P10) from the early pubertal age, the pachytene spermatocytes, round spermatids, caput epididymal spermatozoa and cauda sperm were all isolated from postnatal day 120 (P120) age adult male rats. DDT has been previously shown to induce transgenerational inheritance of disease between 6 and 12 months of age [5]. Therefore, by choosing the postnatal day 120 or earlier with negligible disease present, no disease artifacts are

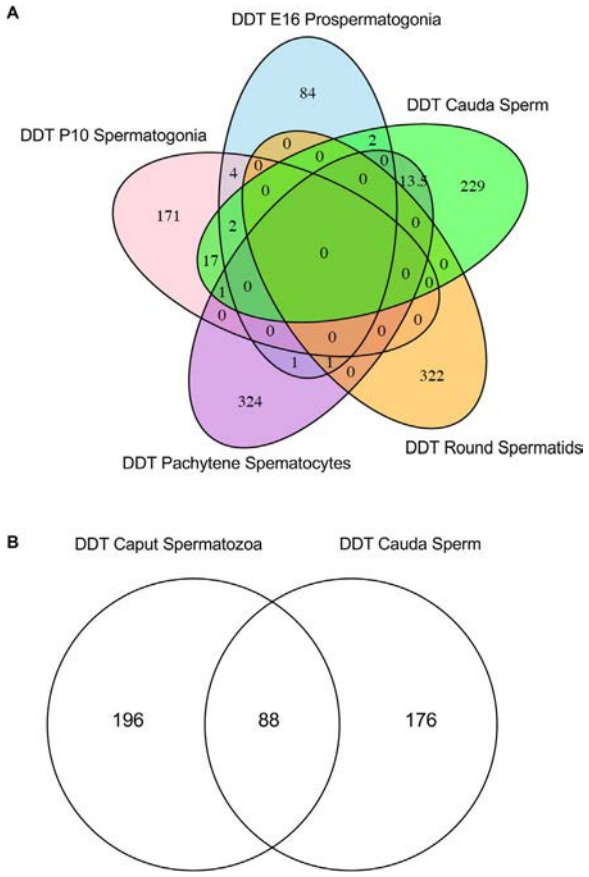

Fig. 6. Developmental stage DMR overlaps. (A) Different developmental stage DMRs overlap. (B) Epididymal caput spermatozoa and caudal sperm DMR overlap.

anticipated in the current study. This is consistent with the primary objective of the study to investigate the developmental origins of the sperm DMR, but future studies can now consider disease correlations.

The transgenerational F3 generation control and DDT lineage germline samples were compared at each of the developmental stages. The F1 and F2 generations have somatic cell and germline epigenetic alterations due to the F1 generation fetal direct exposure and F1 generation fetal germline direct exposure that will generate the F2 generation. Therefore, the F3 generation is the first transgenerational generation not having any direct exposures, so was the focus of the current study [37]. A comparison of the F1 generation direct exposure sperm DMR development with the transgenerational F3 generation observations will be an interesting future study to consider. All F3 generation developmental samples had differential DNA methylation regions (DMRs). Excluding the caput spermatozoa and cauda epididymal sperm with common DMRs, all the other stage DMRs were found to be primarily distinct from each other, Fig. 6. The majority of the epigenome was not altered (i.e. potentially millions of CpG regions) and the current study focused on the transgenerational alterations at each stage of development. The distinct DMRs at each stage indicate a cascade of epigenetic changes occur to program the sperm transgenerational epigenome.

A comparison of the different developmental stage germline populations was conducted in regard to DNA methylation alterations for the top 100 most statistically significant DMRs at each developmental stage separately. Analysis of these DNA methylation alterations for the different developmental stage DMRs revealed that the E16 prospermatogonia and P10 spermatogonia presented distinct patterns of DNA methylation compared to the other stages, Figs. 7 and 8. The statistically significant top 100 DMRs at both these developmental stages altered greatly with adjacent stages and often lost their statistical significance. In contrast, the pachytene spermatocytes, round spermatids, caput epididymal spermatozoa and caudal sperm were more consistent between each other regarding the DMRs maintaining similar DNA methylation alterations and statistical significance, Figs. 7 and 8. This suggests that the developing stem cells and spermatogonia have principally unique DNA methylation profiles associated with the cascade of epigenetic programming of the cells. When the spermatogonia initiate the spermatogenesis process there is a cascade of epigenetic programming and DNA methylation observed between the spermatogenic cell populations, as well as between spermatozoa undergoing epididymal maturation. Observations suggest a dynamic epigenetic programming of the male germline in the testis and epididymis. Epididymal maturation has been shown to promote structural and molecular alterations in the developing sperm, which also appear to be involved in the transgenerational sperm DMR programming [32].

Significant epigenetic reprogramming in the primordial germ cells (PGCs) has already been described. DNA methylation erasure during migration and colonization of the fetal gonad has been shown to occur [18]. This process enables the germline stem cell population to facilitate the generation of the male or female germ lines following gonadal sex determination [18,25]. A stable epigenetic cascade of events occurs to produce the spermatogonial stem cell population in the adult testis. Studies have shown that environmental toxicants have the ability to promote epigenetic DNA methylation alterations in the PGCs and prospermatogonia [35]. These transgenerational DMRs observed in the PGCs were found to be distinct from the caudal epididymal sperm DMRs [35]. The current study supports this observation and determines that sperm DMRs not only originate in the fetal period, but trigger a cascade of epigenetic alterations that eventually impact the mature sperm epigenome, Fig. 1B. Therefore, the developmental cascade of epigenetic programming initiated by fetal exposure induces a number of DMRs that are also maintained throughout development.

In the cauda sperm, the origins of the DMRs were identified. The majority of them originate throughout the development of prospermatogonia, spermatogonia and spermatocytes, Fig. 1B and S9 Table. A smaller number of DMRs also arose in the round spermatids and cauda epididymal sperm. The highest number of DMRs was observed in the prospermatogonia, the stage of development during which the initial F0 generation gestating female and F1 generation developing fetus were exposed. The DMRs in the cauda sperm originated in all the earlier developmental spermatogenic stages and through epididymal maturation. These observations correlated with the DNA methylation alteration data for DMRs between the different developmental stages shown in Figs. 7 and 8. Thus, the primary origin of the transgenerational sperm DMR epimutations/DMRs does not occur during early PGC development or in the embryonic stem cell population, but throughout development and spermatogenesis in the testis, as well as during epididymal maturation. Although the induction of a cascade of epigenetic programming in the PCGs is critical as previously suggested [7,35], there is a continual cascade of epigenetic alterations throughout spermatogenesis to give rise to the transgenerational sperm DMRs, Fig. 1A. Another recent study investigating vinclozolin induced sperm DMR origins found similar observations, but the highest level of DMRs were developed at the pachytene spermatocyte stage [36]. Therefore, an exposure specificity may exist in the developmental epigenetics observed.

The DMRs associated genes were identified for DMRs at $p < 1e\text{-}05$ at each stage of development. The analysis of associated gene functional categories identified signaling, transcription, metabolism and receptor as the major categories at all stages of development. The pathway analysis also identified a number of stage specific pathways with negligible overlap except in metabolism and pathways in cancer. Gene pathways more specific to testis development such as meiosis or the pyruvate pathway did not contain more than a few DMR associated

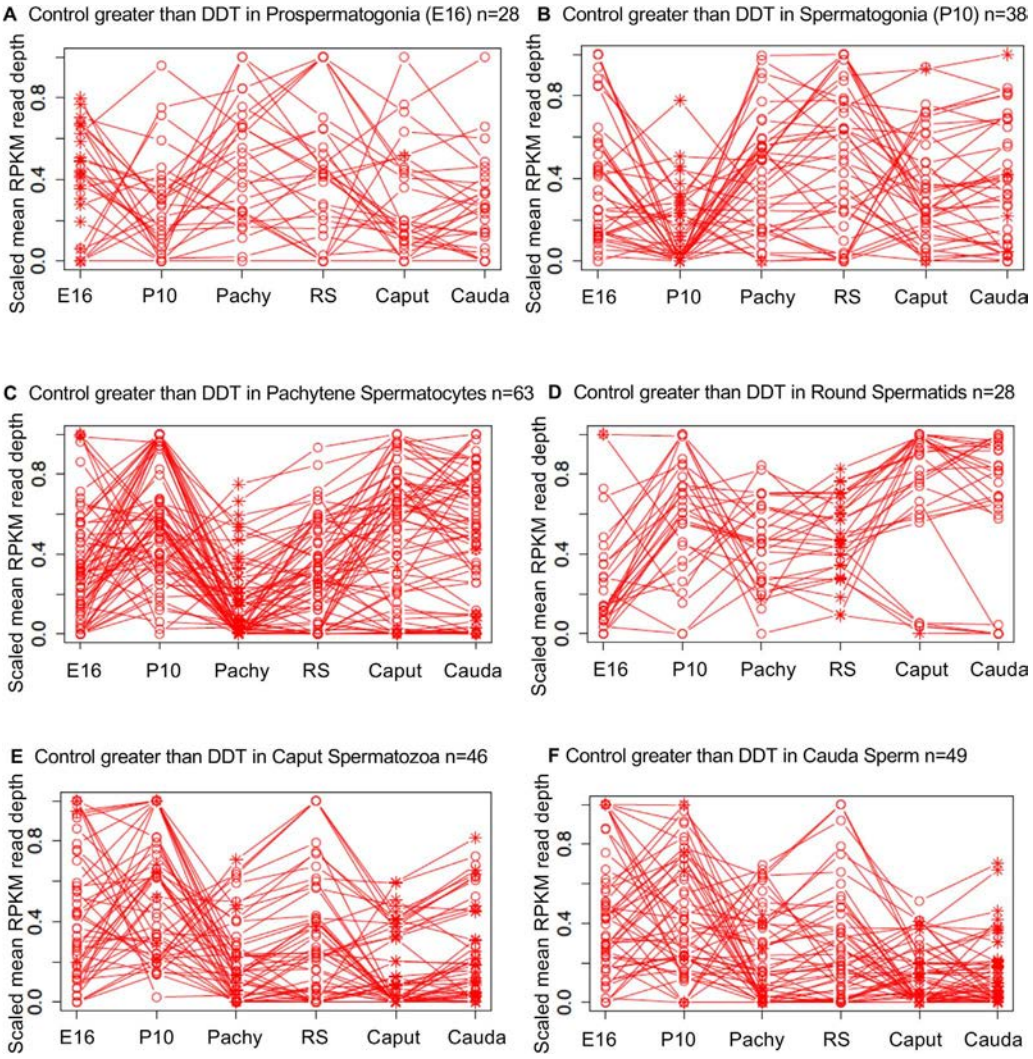

Fig. 7. Timeline DMR development. Top 100 statistically significant DMR developmental alterations for control greater than DDT in read depths (decrease in DNA methylation). Genomic windows with an edgeR p-value < 10^{-5} are indicated by astrisks and windows separated showing only those with an RPKM read depth elevated in the control. (A) E16 prospermatogoina. (B) P10 spermatogonia. (C) Pachytene spermatocytes. (D) Round spermatids. (E) Caput spermatozoa. (F) Cauda sperm.

genes. Therefore, for all the stages of development for the DMR-associated genes involved similar gene categories, but different pathways. Future studies are needed to correlate the DMRs with data identified from transcriptome and altered non-coding RNA expression to provide a better understanding as to how the DMRs may regulate genome activity.

The caput epididymal spermatozoa displayed unique DMRs and others that were in common with the cauda sperm. Interestingly, the cauda epididymal sperm did acquire DMRs that were not present in earlier stages of development. Even though the majority of the cauda epididymal sperm DMRs were obtained during prior developmental stages, 36 DMRs were acquired at the cauda epididymal sperm stage of maturation only, S7 and S8 Tables. Two studies have previously suggested that epididymal maturation (epididymosomes) may be involved with transgenerational sperm maturation regarding epigenetic alterations, but no direct data have been provided [43–45]. The current study supports a role for epididymal maturation altering sperm DMRs. However, the majority of DMRs originated during earlier developmental stages and spermatogenesis in the testis and not the epididymis, Fig. 1B. A combination of early development, spermatogenesis and epididymal mutation appears to be involved in the development of the transgenerational sperm epimutations. Further investigation is needed to elucidate the molecular mechanisms in the epididymis that alter sperm epigenetics.

4. Conclusions

The current study was designed to investigate the developmental origins of transgenerational sperm DMRs induced by the pesticide DDT. Results show that each stage of male germ cell development examined, including the E16 prospermatogonia, P10 spermatogonia, pachytene spermatocytes, round spermatids, caput epididymal spermatozoa and cauda sperm, has distinct and unique DMRs when the DDT lineage and control lineage F3 generation samples are compared. Both the prospermatogonia and spermatogonia display unique DNA methylation alterations in comparison with later stages that are more consistent. The origins of the cauda sperm DMRs developed throughout the earlier developmental stages with the highest number during prospermatogonia, spermatogonia and pachytene spermatocytes, and fewer originating during epididymal maturation. In conclusion, a developmental cascade of epigenetic programming occurs from the PGCs to the sperm with epimutations developing throughout the different stages of development, Fig. 1A. The initial speculation that the DMRs may develop in the PGCs is not the case, even though the developmental cascade initiated is important. Recently, sperm carrying transgenerational epimutations were found to have alterations in DNA methylation, ncRNAs and histone retention, such that all epigenetic factors are involved in the epigenetic transgenerational inheritance phenomenon [15,16]. Future studies will now need to investigate these

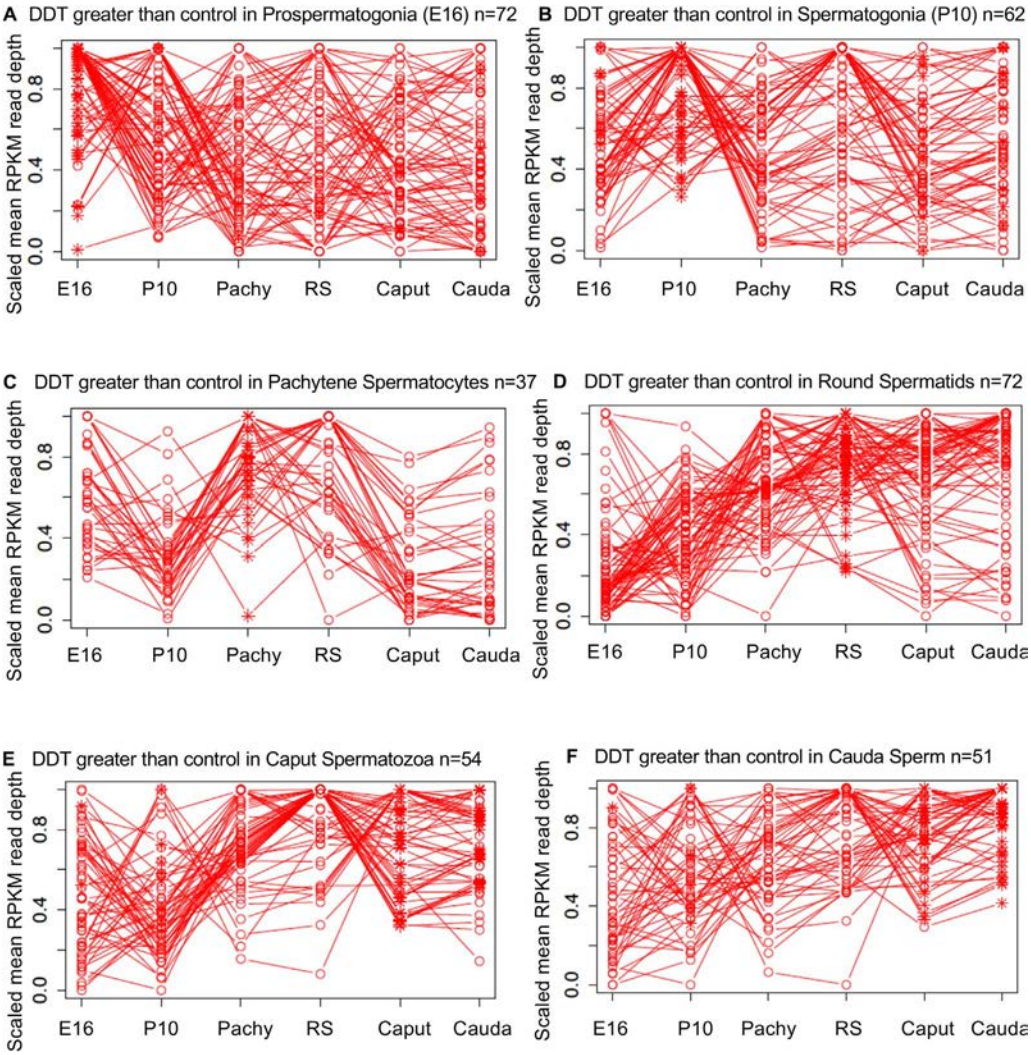

Fig. 8. Timeline DMR development. Top 100 statistically significant DMR developmental alterations for DDT greater than control in read depths (increase in DNA methylation). Genomic windows with an edgeR p-value < 10^{-5} are indicated by astrisks and windows separated showing only those with an RPKM read depth elevated in the DDT over control. (A) E16 prospermatogoina. (B) P10 spermatogonia. (C) Pachytene spermatocytes. (D) Round spermatids. (E) Caput spermatozoa. (F) Cauda sperm.

other epigenetic processes and correlated gene expression to develop a more systems biology assessment of the molecular mechanism involved.

5. Methods

5.1. Animal studies and breeding

Female and male rats of an outbred strain Hsd: Sprague Dawley®™SD®™ obtained from Harlan/Envigo (Indianapolis, IN) at about 70–100 days of age were maintained in ventilated (up to 50 air exchanges/hour) isolator cages (cages with dimensions of 10 ¾″ W×19 ¼″ D×10 ¾″ H, 143 square inch floor space, fitted in Micro-vent 36-cage rat racks; Allentown Inc., Allentown, NJ) containing Aspen Sani chips (pinewood shavings from Harlan) as bedding, and a 14 h light: 10 h dark regimen, at a temperature of 70 F and humidity of 25–35%. The mean light intensity in the animal rooms ranged from 22 to 26 ft-candles. Rats were fed ad lib with standard rat diet (8640 Teklad 22/5 Rodent Diet; Harlan) and ad lib tap water for drinking. To obtain time-pregnant females, the female rats in proestrus were pair-mated with male rats. The sperm-positive (i.e. sperm plug present) (day 0) rats were monitored for diestrus and body weight. On days 8 through 14 of gestation [46], the females received daily intraperitoneal injections of DDT (25 mg/kg body weight/day) or dimethyl sulfoxide (DMSO). The DDT (dichlorodiphenyltrichloroethane) was obtained from Chem Service Inc. (West Chester, PA) and reported to have a purity of 98.2%. DDT were dissolved and injected in DMSO vehicle as previously described [47]. Treatment lineages are designated 'control' or 'DDT' lineages. The treated gestating female rats were designated as the F0 generation. The offspring of the F0 generation rats were the F1 generation. Non-littermate females and males aged 70–90 days from the F1 generation of control or DDT lineages were bred to obtain F2 generation offspring. The F2 generation rats were bred to obtain F3 generation offspring. The F1–F3 generation offspring were not themselves treated directly with DDT. The control and DDT lineages were housed in the same room and racks with lighting, food and water as previously described [47–49]. All experimental protocols for the procedures with rats were pre-approved by the Washington State University Animal Care and Use Committee (IACUC approval # 6252).

5.2. Epididymal sperm collection and DNA isolation

Testis and epididymis were collected from 12 month old rats for germ cell collection. The epididymis was dissected free of connective tissue and divided into caput and cauda halves with a cut in the mid-corpus. A small cut made to the cauda and to the caput and each half was placed in 3 ml of PBS for up to 2 h at 4 °C. Caput and cauda epididymal tissue were each coarsely minced and the liquid with the

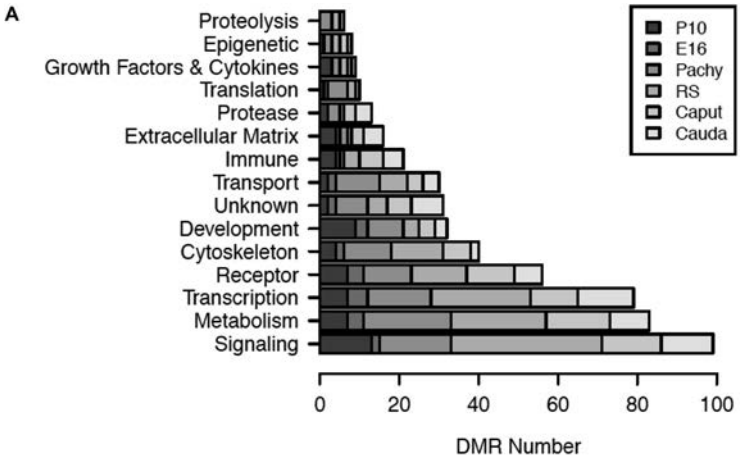

B DMR Gene Association Pathways

DDT Prospermatogonia E16
rno05160 Hepatitis C (2)
rno04913 Ovarian steroidogenesis (2)
rno04217 Necroptosis (2)
rno04976 Bile secretion (2)
rno01100 Metabolic pathways (2)

DDT Spermatogonia (P10)
rno05200 Pathways in cancer (6)
rno05224 Breast cancer (4)
rno05226 Gastric cancer (4)
rno04928 Parathyroid hormone synthesis, secretion and action (3)
rno04380 Osteoclast differentiation (3)

DDT Pachytene Spermatocytes
rno01100 Metabolic pathways (10)
rno04014 Ras signaling pathway (6)
rno05206 MicroRNAs in cancer (6)
rno05200 Pathways in cancer (6)
rno05165 Human papillomavirus infection (6)

DDT Round Spermatids
no01100 Metabolic pathways (11)
rno05200 Pathways in cancer (8)
rno04010 MAPK signaling pathway (7)
rno04360 Axon guidance (6)
rno04151 PI3K-Akt signaling pathway (6)
rno04144 Endocytosis (6)

DDT Caput Spermatozoa
rno05168 Herpes simplex infection (9)
rno04514 Cell adhesion molecules (CAMs) (9)
rno04612 Antigen processing and presentation (8)
rno05165 Human papillomavirus infection (8)
rno01100 Metabolic pathways (7)

DDT Cauda Sperm
rno01100 Metabolic pathways (5)
rno04514 Cell adhesion molecules (CAMs) (4)
rno04650 Natural killer cell mediated cytotoxicity (4)
rno04145 Phagosome (4)
rno04510 Focal adhesion (4)

Fig. 9. Sperm DMR associated gene categories and pathways. (A) DMR associated gene functional categories for each stage (color insert) versus DMR number. (B) DMR associated gene pathways for each stage of development with number of DMR associated genes in pathway in brackets. Bolded pathways show overlap in at least three developmental stages.

released sperm collected. For each sample the released sperm was centrifuged at 6000×*g*, then the supernatant removed, and the pellet resuspended in NIM buffer, to be stored at −80 °C until further use. One hundred µl of sperm suspension was sonicated to destroy somatic cells and tissue, spun down at 6000×*g*, the sperm pellet washed with 1x PBS once, and then combined with 820 µl DNA extraction buffer and 80 µl 0.1 M DTT. The sample was incubated at 65 °C for 15 min. Following this incubation 80 µl proteinase K (20 mg/ml) was added and the sample incubated at 55 °C for at least 2 h under constant rotation. Then 300 µl of protein precipitation solution (Promega, A7953) was added, the sample mixed thoroughly and incubated for 15 min on ice. The sample was centrifuged at 12,500×*g* for 30 min at 4 °C. One ml of the supernatant was transferred to a 2 ml tube and 2 µl of glycoblue and 1 ml of cold 100% isopropanol were added. The sample was mixed well by inverting the tube several times then left in −20 °C freezer for at least one hour. After precipitation the sample was centrifuged at 12,500×*g* for 20 min at 4 °C. The supernatant was taken off and discarded without disturbing the (blue) pellet. The pellet was washed with 70% cold ethanol by adding 500 µl of 70% ethanol to the pellet and returning the tube to the freezer for 20 min. After the incubation the tube was centrifuged for 10 min at 4 °C at 12,500×*g* and the supernatant discarded. The tube was spun again briefly to collect residual ethanol to bottom of tube and then as much liquid as possible was removed with gel loading tip. Pellet was air-dried at RT until it looked dry (about 5 min). Pellet was then resuspended in 100 µl of nuclease free water.

5.3. Developing germ cell stage isolation and DNA preparation

Harlan Sprague-Dawley rats (Harlan Inc., Indianapolis IN) were used for all experiments. The rats were kept in a temperature controlled environment and given food and water ad libitum. Estrous cycles of female rats were monitored by cellular morphology from vaginal smears. Rats in early estrus were paired with males overnight and mating confirmed by sperm-positive smears, denoted day 0 of pregnancy. Pregnant rats were euthanized at embryonic day 16 (E16) of gestation, and fetal gonads were collected for germ cell preparations. Sex was determined on the basis of gonadal morphology. Germ cells were isolated exclusively from males.

Purified populations of male PGCs type T1 prospermatogonia (at E16) were prepared using a mini StaPut gradient method as previously described [50,51]. Briefly, fetal testes were pooled and dissociated by incubation in 0.25% trypsin-EDTA (Sigma) with vigorous pipetting using a 1000 microliter pipette tip, and the resulting cell solution was filtered through 100 µm nylon mesh to yield a single cell suspension. This cell suspension was then loaded onto a 50 ml 2–4% bovine serum albumen (BSA) gradient prepared in KREBS buffer, and the cells were allowed to sediment at unit gravity at 4 °C for two hours as described [50,51]. The gradient was then fractionated and aliquots of the fractions were examined under phase optics to identify those enriched for the appropriate cell types on the basis of morphological characteristics. The enriched fractions were pooled to yield the final sample which was ≥85% pure for the desired male germ cell type in each case.

Three pools of prospermatogonia were prepared for each treatment group, with each pool derived from testes of 5–6 rats from different litters.

A similar mini StaPut gradient method [50,51] was used to isolate spermatogonia from testes of 10-day old rats, with the addition of incubation of the testes in 0.5 mg/ml collagenase (Sigma C1639) at 33 °C for 20 min with agitation to dissociate the seminiferous tubules. Three pools of spermatogonia from 10-day old rats were prepared for each treatment group, with each pool derived from testes of 6–7 rats from different litters.

To isolate pachytene spermatocytes and round spermatids, testes were collected from 12 month old rats suspended in F-12 culture medium (Gibco-Life Technologies, USA. Ref 11765-054) and shipped overnight on ice to Dr. John McCarrey. A StaPut gradient method was used to isolate the developing germ cell stages as previously described [50,51]. Three pools of cells of each cell type were prepared for each treatment group, with each pool derived from testes of three rats from different litters. DNA was isolated from prospermatogonia, spermatogonia, pachytene spermatocytes and round spermatids using the same procedure as was used for sperm, with the omission of sonication and DTT treatments.

5.4. Methylated DNA immunoprecipitation MeDIP

Methylated DNA Immunoprecipitation (MeDIP) with genomic DNA was performed as follows: rat DNA pools were generated using the appropriate amount of genomic DNA from each individual for 3 pools each of control and DDT lineage animals. Genomic DNA pools were sonicated using the Covaris M220 the following way: the pooled genomic DNA was diluted to 130 µl with TE buffer into the appropriate Covaris tube. Covaris was set to 300 bp program and the program was run for each tube in the experiment. 10 µl of each sonicated DNA was run on 1.5% agarose gel to verify fragment size. The sonicated DNA was transferred from the Covaris tube to a 1.7 ml microfuge tube and the volume measured. The sonicated DNA was then diluted with TE buffer (10 mM Tris HCl, pH7.5; 1 mM EDTA) to 400 µl, heat-denatured for 10 min at 95 °C, then immediately cooled on ice for 10 min. Then 100 µl of 5X IP buffer and 5 µg of antibody (monoclonal mouse anti 5-methyl cytidine; Diagenode #C15200006) were added to the denatured sonicated DNA. The DNA-antibody mixture was incubated overnight on a rotator at 4 °C.

The following day magnetic beads (Dynabeads M-280 Sheep anti-Mouse IgG; 11201D) were pre-washed as follows: The beads were resuspended in the vial, then the appropriate volume (50 µl per sample) was transferred to a microfuge tube. The same volume of Washing Buffer (at least 1 ml PBS with 0.1% BSA and 2 mM EDTA) was added and the bead sample was resuspended. Tube was then placed into a magnetic rack for 1–2 min and the supernatant discarded. The tube was removed from the magnetic rack and the beads washed once. The washed beads were resuspended in the same volume of IP buffer (50 mM sodium phosphate ph7.0, 700 mM NaCl, 0.25% TritonX-100) as the initial volume of beads. 50 µl of beads were added to the 500 µl of DNA-antibody mixture from the overnight incubation, then incubated for 2 h on a rotator at 4 °C.

After the incubation the bead-antibody-DNA complex was washed three times with IP buffer as follows: The tube was placed into magnetic rack for 1–2 min and the supernatant discarded, then washed with IP buffer 3 times. The washed bead-DNA solution is then resuspended in 250 µl digestion buffer with 3.5 µl Proteinase K (20 mg/ml). The sample was then incubated for 2–3 h on a rotator at 55 °C and then 250 µl of buffered Phenol-Chloroform-Isoamylalcohol solution was added to the supe and the tube vortexed for 30 s then centrifuged at 12,500×*g* for 5 min at room temperature. The aqueous supernatant was carefully removed and transferred to a fresh microfuge tube. Then 250 µl chloroform were added to the supernatant from the previous step, vortexed for 30 s and centrifuged at 12,500×*g* for 5 min at room temperature. The aqueous supernatant was removed and transferred to a fresh microfuge tube. To the supernatant 2 µl of glycoblue (20 mg/ml), 20 µl of 5 M NaCl and 500 µl ethanol were added and mixed well, then precipitated in −20 °C freezer for 1 h to overnight.

The precipitate was centrifuged at 12,500×*g* for 20 min at 4 °C and the supernatant removed, while not disturbing the pellet. The pellet was washed with 500 µl cold 70% ethanol in −20 °C freezer for 15 min then centrifuged again at 12,500×*g* for 5 min at 4 °C and the supernatant discarded. The tube was spun again briefly to collect residual ethanol to bottom of tube and as much liquid as possible was removed with gel loading tip. Pellet was air-dried at RT until it looked dry (about 5 min) then resuspended in 20 µl H2O or TE. DNA concentration was measured in Qubit (Life Technologies) with ssDNA kit (Molecular Probes Q10212).

5.5. MeDIP-Seq analysis

The MeDIP pools were used to create libraries for next generation sequencing (NGS) using the NEBNext® Ultra™ RNA Library Prep Kit for Illumina® (NEB, San Diego, CA) starting at step 1.4 of the manufacturer's protocol to generate double stranded DNA. After this step the manufacturer's protocol was followed. Each pool received a separate index primer. NGS was performed at WSU Spokane Genomics Core using the Illumina HiSeq. 2500 with a PE50 application, with a read size of approximately 50 bp and approximately 30 million reads per pool. Five to six libraries were run in one lane.

5.6. Statistics and bioinformatics

For the DMR analyses, the basic read quality was verified using summaries produced by the FastQC program http://www.bioinformatics.babraham.ac.uk/projects/fastqc/. The raw reads were trimmed and filtered using Trimmomatic. The reads for each MeDIP sample were mapped to the Rnor 6.0 rat genome using Bowtie2 [52] with default parameter options. The mapped read files were then converted to sorted BAM files using SAMtools [53]. To identify DMRs, the reference genome was broken into 100 bp windows. Genomic windows with no CpG or ambiguous base within 1000 bp were identified in the reference genome and used as control genes to perform RUVg normalization [54]. The MEDIPS [55] and edgeR [56] R packages were used to calculate differential coverage between control and exposure sample groups. The edgeR p-value was used to determine the relative difference between the two groups for each genomic window. Windows with an edgeR p-value less than 10–5 were considered DMRs. The FDR adjusted p-values were also calculated. The DMR edges were extended until no genomic window with an edgeR p-value < 0.1 remained within 1000 bp of the DMR. CpG density and other information was then calculated for the DMR based on the reference genome. DMRs were annotated using the biomaRt R package [57] to access the Ensembl database [58]. The genes that fell within 10kbp of the DMR edges were then input into the KEGG pathway search [59,60] to identify associated pathways. The associated genes were then sorted into functional groups by consulting information provided by the DAVID [61], Panther [62], and Uniprot databases incorporated into an internal curated database (www.skinner.wsu.edu under genomic data). All molecular data has been deposited into the public database at NCBI (GEO # GSE121585).

Acknowledgments

We acknowledge Ms. Margaux McBirney, Ms. Deepika Kubsad and Mr. Ryan Thompson for technical assistance and Ms. Heather Johnson for assistance in preparation of the manuscript. We thank Ms. Stephanie E. King for generating the germ cell schematics in Fig. 9. We thank the Genomics Core laboratory at WSU Spokane. This study was supported by a John Templeton Foundation, USA (50183)

(https://templeton.org/) grant to MKS and NIH, USA (ES012974) (https://www.nih.gov/) grant to MKS. The funders had no role in study design, data collection and analysis, decision to publish, or preparation of the manuscript

Declaration of interests

The authors declare no competing interests.

CRediT authorship contribution statement

Millissia Ben Maamar: Writing - original draft, Writing - review & editing, Formal analysis, Investigation, **Eric Nilsson:** Writing - review & editing, Formal analysis, Investigation, **Ingrid Sadler-Riggleman:** Writing - review & editing, Formal analysis, Investigation, Validation, **Daniel Beck:** Writing - review & editing, Data curation, Investigation, Validation, **John R. McCarrey:** Writing - review & editing, Investigation, Supervision, **Michael K. Skinner:** Writing - original draft, Writing - review & editing, Conceptualization, Funding acquisition, Investigation, Project administration, Supervision

Appendix A. Supporting information

Supplementary data associated with this article can be found in the online version at doi:10.1016/j.ydbio.2018.11.016.

References

Anway, M.D., Cupp, A.S., Uzumcu, M., Skinner, M.K., 2005]. Epigenetic transgenerational actions of endocrine disruptors and male fertility. Science 308 (5727), 1466–1469.

Skinner, M.K., Manikkam, M., Tracey, R., Guerrero-Bosagna, C., Haque, M.M., Nilsson, E., 2013]. Ancestral dichlorodiphenyltrichloroethane (DDT) exposure promotes epigenetic transgenerational inheritance of obesity. BMC Med. 11 (1–16), 228.

Soubry, A., 2015]. Epigenetic inheritance and evolution: a paternal perspective on dietary influences. Prog. Biophys. Mol. Biol. 118 (1–2), 79–85.

Vaiserman, A.M., Koliada, A.K., Jirtle, R.L., 2017]. Non-genomic transmission of longevity between generations: potential mechanisms and evidence across species. Epigenetics Chromatin 10 (1), 38.

Nilsson, E., Sadler-Riggleman, I., Skinner, M.K., 2018]. Environmentally induced epigenetic transgenerational inheritance of disease. Environ. Epigenetics 4 (2), 1–13, (dvy016).

Skinner, M.K., 2015]. Environmental epigenetics and a unified theory of the molecular aspects of evolution: a Neo-Lamarckian concept that facilitates Neo-Darwinian evolution. Genome Biol. Evol. 7 (5), 1296–1302.

Skinner, M.K., 2011]. Environmental epigenetic transgenerational inheritance and somatic epigenetic mitotic stability. Epigenetics 6 (7), 838–842.

Beck, D., Sadler-Riggleman, I., Skinner, M.K., 2017]. Generational comparisons (F1 versus F3) of vinclozolin induced epigenetic transgenerational inheritance of sperm differential DNA methylation regions (epimutations) using MeDIP-seq. Environ. Epigenetics 3 (3), 1–12, (dvx016).

Quadrana, L., Colot, V., 2016]. Plant transgenerational epigenetics. Annu. Rev. Genet. 50, 467–491.

Sharma, U., Rando, O.J., 2017]. Metabolic inputs into the epigenome. Cell Metab. 25 (3), 544–558.

Gapp, K., Jawaid, A., Sarkies, P., Bohacek, J., Pelczar, P., Prados, J., Farinelli, L., Miska, E., Mansuy, I.M., 2014]. Implication of sperm RNAs in transgenerational inheritance of the effects of early trauma in mice. Nat. Neurosci. 17 (5), 667–669.

Yan, W., 2014]. Potential roles of noncoding RNAs in environmental epigenetic transgenerational inheritance. Mol. Cell Endocrinol. 398 (1–2), 24–30.

Ben Maamar, M., Sadler-Riggleman, I., Beck, D., Skinner, M.K., 2018]. Epigenetic transgenerational inheritance of altered sperm histone retention sites. Sci. Rep. 8, 5308, (1-10).

Furuhashi, H., Kelly, W.G., 2010]. The epigenetics of germ-line immortality: lessons from an elegant model system. Dev. Growth Differ. 52 (6), 527–532.

Skinner, M.K., Ben Maamar, M., Sadler-Riggleman, I., Beck, D., Nilsson, E., McBirney, M., Klukovich, R., Xie, Y., Tang, C., Yan, W., 2018]. Alterations in sperm DNA methylation, non-coding RNA and histone retention associate with DDT-induced epigenetic transgenerational inheritance of disease. Epigenetics Chromatin 11 (1), 1–24, (8).

Ben Maamar, M., Sadler-Riggleman, I., Beck, D., McBirney, M., Nilsson, E., Klukovich, R., Xie, Y., Tang, C., Yan, W., Skinner, M.K., 2018]. Alterations in sperm DNA methylation, non-coding RNA expression, and histone retention mediate Vinclozolin induced epigenetic transgenerational inheritance of disease. Environ. Epigenetics 4 (2), 1–19, (dvy010).

Manikkam, M., Haque, M.M., Guerrero-Bosagna, C., Nilsson, E., Skinner, M.K., 2014]. Pesticide methoxychlor promotes the epigenetic transgenerational inheritance of adult onset disease through the female germline. PLoS One 9 (7), 1–19, (e102091).

Seisenberger, S., Andrews, S., Krueger, F., Arand, J., Walter, J., Santos, F., Popp, C., Thienpont, B., Dean, W., Reik, W., 2012]. The dynamics of genome-wide DNA methylation reprogramming in mouse primordial germ cells. Mol. Cell 48 (6), 849–862.

Jost, A., Vigier, B., Prepin, J., Perchellet, J.P., 1973]. Studies on sex differentiation in mammals. Recent Prog. Horm. Res. 29, 1–41.

McCarrey, J.R., 2013]. Toward a more precise and informative nomenclature describing fetal and neonatal male germ cells in rodents. Biol. Reprod. 89 (2), 47.

McCarrey, J.R., 2012]. The epigenome as a target for heritable environmental disruptions of cellular function. Mol. Cell Endocrinol. 354 (1–2), 9–15.

Dym, M., Fawcett, D.W., 1971]. Further observations on the numbers of spermatogonia, spermatocytes, and spermatids connected by intercellular bridges in the mammalian testis. Biol. Reprod. 4 (2), 195–215.

Orgebin-Crist, M.C., Danzo, B.J., Cooper, T.G., 1976]. Re-examination of the dependence of epididymal sperm viability on the epididymal environment. J. Reprod. Fertil. Suppl. 24 suppl, 115–128.

Cornwall, G.A., 2009]. New insights into epididymal biology and function. Hum. Reprod. Update 15 (2), 213–227.

Tang, W.W., Kobayashi, T., Irie, N., Dietmann, S., Surani, M.A., 2016]. Specification and epigenetic programming of the human germ line. Nat. Rev. Genet. 17 (10), 585–600.

Ku, H.Y., Gangaraju, V.K., Qi, H., Liu, N., Lin, H., 2016]. Tudor-SN interacts with Piwi antagonistically in regulating spermatogenesis but synergistically in silencing transposons in drosophila. PLoS Genet. 12 (1), e1005813.

La Salle, S., Oakes, C.C., Neaga, O.R., Bourc'his, D., Bestor, T.H., Trasler, J.M., 2007]. Loss of spermatogonia and wide-spread DNA methylation defects in newborn male mice deficient in DNMT3L. BMC Dev. Biol. 7, 104.

Mann, J.R., 2001]. Imprinting in the germ line. Stem Cells 19 (4), 287–294.

Barlow, D.P., Bartolomei, M.S., 2014]. Genomic imprinting in mammals. Cold Spring Harb. Perspect. Biol. 6 (2), 1–21.

Hanson, M.A., Skinner, M.K., 2016]. Developmental origins of epigenetic transgenerational inheritance. Environ. Epigenetics 2 (1), 1–9, (dvw002).

Soubry, A., Hoyo, C., Jirtle, R.L., Murphy, S.K., 2014]. A paternal environmental legacy: evidence for epigenetic inheritance through the male germ line. Bioessays 36 (4), 359–371.

Boskovic, A., Rando, O.J., 2018]. Transgenerational epigenetic inheritance. Annu. Rev. Genet. 52, (p. Epub ahead of print).

Soubry, A., Hoyo, C., Butt, C.M., Fieuws, S., Price, T.M., Murphy, S.K., Stapleton, H.M., 2017]. Human exposure to flame-retardants is associated with aberrant DNA methylation at imprinted genes in sperm. Environ. Epigenetics 3 (1), dvx003.

del Mazo, J., Prantera, G., Torres, M., Ferraro, M., 1994]. DNA methylation changes during mouse spermatogenesis. Chromosome Res. 2 (2), 147–152.

Skinner, M., Guerrero-Bosagna, C., Haque, M.M., Nilsson, E., Bhandari, R., McCarrey, J., 2013]. Environmentally induced transgenerational epigenetic reprogramming of primordial germ cells and subsequent germline. PLoS One 8 (7), 1–15, (e66318).

Skinner, M.K., Nilsson, E., Sadler-Riggleman, I., Beck, D., McCarrey, J.R., 2018]. Developmental origins of transgenerational sperm DNA methylation epimutations Following ancestral vinclozolin exposure. Pending.

Skinner, M.K., 2008]. What is an epigenetic transgenerational phenotype? F3 or F2. Reprod. Toxicol. 25 (1), 2–6.

Ariel, M., McCarrey, J., Cedar, H., 1991]. Methylation patterns of testis-specific genes. Proc. Natl. Acad. Sci. USA 88 (6), 2317–2321.

Hermann, B.P., Mutoji, K.N., Velte, E.K., Ko, D., Oatley, J.M., Geyer, C.B., McCarrey, J.R., 2015]. Transcriptional and translational heterogeneity among neonatal mouse spermatogonia. Biol. Reprod. 92 (2), 54.

Skinner, M.K., Guerrero-Bosagna, C., 2014]. Role of CpG deserts in the epigenetic transgenerational inheritance of differential DNA methylation regions. BMC Genom. 15 (1), 692.

Ventela, S., Ohta, H., Parvinen, M., Nishimune, Y., 2002]. Development of the stages of the cycle in mouse seminiferous epithelium after transplantation of green fluorescent protein-labeled spermatogonial stem cells. Biol. Reprod. 66 (5), 1422–1429.

Suresh, R., Aravindan, G.R., Moudgal, N.R., 1992]. Quantitation of spermatogenesis by DNA flow cytometry: comparative study among six species of mammals. J. Biosci. 17 (4), 413–419.

Sharma, U., Conine, C.C., Shea, J.M., Boskovic, A., Derr, A.G., Bing, X.Y., Belleannee, C., Kucukural, A., Serra, R.W., Sun, F., Song, L., Carone, B.R., Ricci, E.P., Li, X.Z., Fauquier, L., Moore, M.J., Sullivan, R., Mello, C.C., Garber, M., Rando, O.J., 2016]. Biogenesis and function of tRNA fragments during sperm maturation and fertilization in mammals. Science 351 (6271), 391–396.

Rompala, G.R., Mounier, A., Wolfe, C.M., Lin, Q., Lefterov, I., Homanics, G.E., 2018]. Heavy chronic intermittent ethanol exposure alters small noncoding RNAs in mouse sperm and epididymosomes. Front. Genet. 9, 32.

Ariel, M., Cedar, H., McCarrey, J., 1994]. Developmental changes in methylation of spermatogenesis-specific genes include reprogramming in the epididymis. Nat. Genet. 7 (1), 59–63.

Nilsson, E.E., Anway, M.D., Stanfield, J., Skinner, M.K., 2008]. Transgenerational epigenetic effects of the endocrine disruptor vinclozolin on pregnancies and female adult onset disease. Reproduction 135 (5), 713–721.

Manikkam, M., Guerrero-Bosagna, C., Tracey, R., Haque, M.M., Skinner, M.K., 2012]. Transgenerational actions of environmental compounds on reproductive disease and identification of epigenetic biomarkers of ancestral exposures. PLoS One 7 (2), 1–12, (e31901).

Skinner, M.K., Manikkam, M., Guerrero-Bosagna, C., 2010]. Epigenetic transgenerational actions of environmental factors in disease etiology. Trends Endocrinol. Metab. 21 (4), 214–222.

Anway, M.D., Leathers, C., Skinner, M.K., 2006]. Endocrine disruptor vinclozolin

induced epigenetic transgenerational adult-onset disease. Endocrinology 147 (12), 5515–5523.
McCarrey, J.R., Berg, W.M., Paragioudakis, S.J., Zhang, P.L., Dilworth, D.D., Arnold, B.L., Rossi, J.J., 1992]. Differential transcription of Pgk genes during spermatogenesis in the mouse. Dev. Biol. 154 (1), 160–168.
Kafri, T., Ariel, M., Brandeis, M., Shemer, R., Urven, L., McCarrey, J., Cedar, H., Razin, A., 1992]. Developmental pattern of gene-specific DNA methylation in the mouse embryo and germ line. Genes Dev. 6 (5), 705–714.
Bolger, A.M., Lohse, M., Usadel, B., 2014]. Trimmomatic: a flexible trimmer for Illumina sequence data. Bioinformatics 30 (15), 2114–2120.
Langmead, B., Salzberg, S.L., 2012]. Fast gapped-read alignment with Bowtie 2. Nat. Methods 9 (4), 357–359.
Risso, D., Ngai, J., Speed, T.P., Dudoit, S., 2014]. Normalization of RNA-seq data using factor analysis of control genes or samples. Nat. Biotechnol. 32 (9), 896–902.
Lienhard, M., Grimm, C., Morkel, M., Herwig, R., Chavez, L., 2014]. MEDIPS: genome-wide differential coverage analysis of sequencing data derived from DNA enrichment experiments. Bioinformatics 30 (2), 284–286.
Robinson, M.D., McCarthy, D.J., Smyth, G.K., 2010]. edgeR: a Bioconductor package for differential expression analysis of digital gene expression data. Bioinformatics 26 (1), 139–140.
Durinck, S., Spellman, P.T., Birney, E., Huber, W., 2009]. Mapping identifiers for the integration of genomic datasets with the R/Bioconductor package biomaRt. Nat. Protoc. 4 (8), 1184–1191.
Cunningham, F., Amode, M.R., Barrell, D., Beal, K., Billis, K., Brent, S., Carvalho-Silva, D., Clapham, P., Coates, G., Fitzgerald, S., Gil, L., Giron, C.G., Gordon, L., Hourlier, T., Hunt, S.E., Janacek, S.H., Johnson, N., Juettemann, T., Kahari, A.K., Keenan, S., Martin, F.J., Maurel, T., McLaren, W., Murphy, D.N., Nag, R., Overduin, B., Parker, A., Patricio, M., Perry, E., Pignatelli, M., Riat, H.S., Sheppard, D., Taylor, K., Thormann, A., Vullo, A., Wilder, S.P., Zadissa, A., Aken, B.L., Birney, E., Harrow, J., Kinsella, R., Muffato, M., Ruffier, M., Searle, S.M., Spudich, G., Trevanion, S.J., Yates, A., Zerbino, D.R., Flicek, P., 2015]. Ensembl 2015. Nucleic Acids Res. 43, D662–D669.
Kanehisa, M., Goto, S., 2000]. KEGG: kyoto encyclopedia of genes and genomes. Nucleic Acids Res. 28 (1), 27–30.
Kanehisa, M., Goto, S., Sato, Y., Kawashima, M., Furumichi, M., Tanabe, M., 2014]. Data, information, knowledge and principle: back to metabolism in KEGG. Nucleic Acids Res. 42, D199–D205.
Huang da, W., Sherman, B.T., Lempicki, R.A., 2009]. Systematic and integrative analysis of large gene lists using DAVID bioinformatics resources. Nat. Protoc. 4 (1), 44–57.
Mi, H., Muruganujan, A., Casagrande, J.T., Thomas, P.D., 2013]. Large-scale gene function analysis with the PANTHER classification system. Nat. Protoc. 8 (8), 1551–1566.